UCSF
UC San Francisco Electronic Theses and Dissertations

Title
Acinar plasticity and Kras dependent specification of pancreatic ductal adenocarcinoma precursors

Permalink
https://escholarship.org/uc/item/0b87k4k6

Author
Morris, John Pacheco

Publication Date
2011

Peer reviewed|Thesis/dissertation

eScholarship.org Powered by the California Digital Library
University of California

Acinar plasticity and Kras dependent specification of pancreatic ductal adenocarcinoma precursors

by

John P. Morris IV

DISSERTATION

Submitted in partial satisfaction of the requirements for the degree of

DOCTOR OF PHILOSOPHY

in

Biomedical Sciences

in the

GRADUATE DIVISION

of the

Dedicated to John W. Sheldon and John P. Morris Jr. You have no idea what a huge kick they would have got out of this. And yes, we're all named John.

Acknowledgements:

Telling stories is our quintessentially human attempt at interpreting the natural and social world. Creative types make fantastic stories out of what is real, the historical minded record stories of human action in an attempt to understand it, and scientists' stories try to develop a theoretical framework to rationalize infinitely complex systems. The next 100 odd pages of this thesis is a condensed narrative of the scientific story I've worked on for over 7 years. The next few paragraphs are my attempt at thanking the people who helped support the human element that wrote it.

There is science history, the accumulated knowledge of scientists past, and science present, the hypotheses of which depend on the work of those who came before. Graduate school is the start of a scientist living between these two worlds: exploring the data and interpretations of the past to build on, and more often than not, to challenge them. There is no more important person in helping graduate students rationalize this position than their thesis mentors. I would like to thank Dr. Matthias Hebrok for helping to guide me in developing my scientific personality. His guidance was critical in learning to balance reverence for the incredible insight of past and present colleagues with the need to view it with a critical eye. He is masterful at identifying where fields are lacking and filling these needs with elegant use of available tools. His ability to use the concepts of one field, for example developmental biology, as inspiration to better understand another, e.g. cancer biology, is the kind of anti-parochial thought that helps

scientists maintain perspective and use their knowledge to solve broader problems. It was an honor and a privilege to work in his group.

Furthermore, I would like to thank the other members of my close scientific family. Drs. Martin McMahon and Andrei Goga offered critical advice both scientific and career oriented that helped to resist my dogged propensity to blind myself to the need for advancement beyond the bench. Drs. Margaret Tempero, Kim Kirkwood, Eric Collisson, and Grace Kim all provided the opportunity for interaction with clinicians dealing with medical realities. They offered priceless opportunities for scientific discussion and collaboration that helped me maintain perspective about why we study pancreatic cancer, and to avoid the tunnel vision of being tantalized by “mouse-ology”.

Hebrok Lab members past and present became my second family. And every family needs a crazy uncle, a position I was more than happy to oblige. Without their guidance, friendship, and acceptance none of the work I accomplished would have been possible. The insight, knowledge, and training I received from senior members: especially Marina Pasca, David Cano, Shigeki Sekine, and Patrick Heiser, was invaluable. I am not surprised in the least by the subsequent success they have had in their new positions since leaving Matthias’ group. My contemporary lab colleagues were just as important. I’d like to thank Sam Wang, Renee Vanderlaan, Sapna Puri, Limor Landsman, Cecilia Austin, and most recently Guido Von Figura and Holger Russ. Science is a frustrating enterprise,

and their theoretical and technical help was absolutely critical. More important was their friendship and camaraderie. We created a very good team and a comfortable environment for asking great questions and dealing with the inevitable struggles of interpretation. It was exciting to see how different personalities meshed to drive discovery. I am indebted to the calming influences that made me realize that sound and fury are not proportional to elucidation. I look forward to seeing the Hebrok Lab evolve and continuing to work with all my former lab mates wherever we may end up in the coming years.

Finally, I'd like to acknowledge my family. My father grew up on a vegetable farm that he returned to as an adult and has run with my mother for over 30 years. Science and farming are uncannily similar ventures. Both require an entrepreneurial spirit, exquisite powers of adaptation, and the willingness to try and understand nature's unpredictability. People are surprised that the son of a corn farmer went into research. What they don't realize is that my life on the farm prepared me for everything science has been able to throw my way. Working the farm with my parents taught me the importance of using information and knowledge to stack the deck in your favor against the staggering uncertainty of nature. Reviewing my work as my graduate career comes to an end, I realize that my entire life has been one of experimentation, some involving cornfields and cow pastures and others cell culture and mouse genetics. Only time will tell which had more of an impact.

Contributions:

Chapters of this thesis indicated below contain published work with minimal formatting changes to fit UCSF Graduate Division requirements, e.g. margins. Chapter 3 is presently being prepared for submission. My non-first author contributions to other research papers as well as additional reviews are not reprinted in full, but are referenced appropriately.

Chapter 1, Introduction: Section, “Mutant Kras is a critical regulator of PDAC development”, reproduced from Morris IV, J.P., Wang, S.C., and Hebrok, M. 2010. KRAS, Hedgehog, Wnt and the twisted developmental biology of pancreatic ductal adenocarcinoma. *Nature Reviews Cancer* 10:683-695.

Chapter 2: Morris IV, J.P., Cano, D.A., Sekine, S., Wang, S.C., and Hebrok, M. 2010. Beta-catenin blocks Kras-dependent reprogramming of acini into pancreatic cancer precursor lesions in mice. *J Clin Invest* 120:508-520.

Chapter 3: Morris IV, J.P., Vanderlaan, R., Busch, A., Hertel, K., Kim, G., Russ, H.,Hebrok., M. 2011. miRNA processing constrains Kras driven acinar to ductal metaplasia, but is required for pancreatic ductal adenocarcinoma (PDA) formation in mice. *In preparation.*

Acinar plasticity and Kras dependent specification of pancreatic ductal adenocarcinoma precursors

John P. Morris IV

Pancreatic ductal adenocarcinoma (PDA) is characterized by near universal mutations in the Kras proto-oncogene. Targeting constitutively active Kras to the pancreas results in the development of preneoplastic lesions and malignant progression similar to that observed in human PDA. Here we explore the capacity of mutant Kras to initiate PDA by reprogramming pancreatic acinar cells into a lineage that resembles human pancreatic intraepithelial neoplasia (PanIN), believed to be the most common route to PDA in man. Chronic pancreatitis is a major risk factor for human PDA, and chemically induced pancreatitis provides a permissive environment for PanIN and PDA formation in mouse models driven by mutant Kras. We found that mutant Kras dramatically alters the plasticity of acinar cells, preventing regeneration at the expense of a normally restricted, persistently ductal cell fate capable of giving rise to PanINs. Unlike acinar regeneration, which is characterized by activation of Beta-catenin signaling, Beta-catenin signaling is inhibited during early stages of Kras driven metaplasia. Using gain and loss of function approaches, we found that Beta-catenin is required for acinar regeneration and that enforced stabilization of Beta-catenin antagonizes acinar to ductal reprogramming that can give rise to PanINs. Therefore, Kras dependent specification of acinar derived PanINs depends on critical temporal thresholds of Beta-catenin signaling. Continuing the theme of Kras altering pancreatic plasticity, we investigated the role of miRNA processing

in Kras driven PDA initiation. We found that deleting the critical miRNA biogenesis enzyme Dicer in the pancreas in the context of mutant Kras dramatically accelerates ductal metaplasia. However, this does not result in accelerated development of PanIN or PDA, and Dicer deficient cells do not contribute to PDA in mice. Dicer deficient acini display compromised expression of markers of acinar differentiation, which provides a permissive environment for Kras dependent ductal reprogramming. However, this differentiation state is unstable and displays considerable apoptosis, likely preventing the cells from contributing to PDA development. Therefore, we hypothesize that miRNA expression must be appropriately tuned to both permit preneoplastic differentiation and maintain cellular viability during Kras driven pancreatic transformation.

Table of Contents

List of Tables

List of Figures

Chapter 1: Introduction

Pancreatic Function, Development, and Plasticity

The adult pancreas is a complex organ composed of both exocrine and endocrine compartments. The exocrine compartment is comprised mainly of acinar cells, which produce and secrete digestive enzymes, and a system of duct cells that provide a link for these enzymes to the duodenum(1). A less understood cell type, centroacinar cells, are found at the junction between acini and the duct system, and are becoming better characterized as specific markers and increasingly sophisticated methods for their isolation are developed(2). The endocrine compartment is organized into the Islets of Langherhans, observed as groups of cells distributed throughout the exocrine tissue. Islets are composed of 5 different hormone-producing cells, predominantly insulin producing β-cells, that help regulate blood glucose homeostasis(3). Salient to the topic of this thesis, acinar, centroacinar, duct, and insulin producing cells have been proposed as cells of origin for pancreatic ductal adenocarcinoma (PDA)(reviewed in (4, 5). Although human PDA manifests ductal morphology and markers, mouse models targeting mutant Kras, one of the most common mutations in human PDA, to specific differentiated compartments in the adult mouse pancreas have mainly focused on the capacity of acinar cells to give rise to PDA precursors and in some cases PDA (reviewed in(5)). This may reflect the general paucity of tools specifically targeting the duct and centroacinar compartment, or differences in sensitivity to transformation by mutant Kras, a controversial issue that has yet to be resolved.

Embryonic pancreas development is a complex process that depends on tight control of the timing and signal strength of signaling pathways and transcriptional output. In the mouse, Pdx1 expressing multipotent pancreatic progenitors bud dorsally and ventrally from the gut tube around E8.5(1). These multipotent progenitors then develop through stages of waning plasticity until they reach fully differentiated status in young mice. Considerable effort has been applied to determining the developmental potency of pools of cells progressing through pancreatogenesis, which has resulted in a catalogue of markers and transcription factors marking different stages(6). Interestingly, most cell fate decisions in pancreas development are not binary, like the expression of the transcription factor neurogenin3 (Ngn3) that specifically drives cells to enter the endocrine lineage(7), but depend on signal pathway strength or level of transcription factor expression. For example high levels of Notch pathway activation block Ngn3 expression due to direct inhibition by the Notch effector Hes1(8). Therefore, cells experiencing Notch signaling levels that breach a threshold incompatible with Ngn3 expression trend towards an exocrine fate. However, during very early pancreatic development, Hes1 marks progenitors that can give rise to both endocrine and exocrine cells(9), and both elimination of Rbpj, a key Notch transcriptional effector(10), and uncontrolled levels of Notch signaling inhibit exocrine development(11). Therefore, dynamically tuned levels of Notch signaling are required for appropriate specification of the adult pancreatic lineages.

The role of β-catenin signaling in pancreatic development also highlights the importance of dynamic temporal regulation of signaling pathways in specification of adult pancreatic lineages. β-catenin signaling peaks between E11.5 and 13.5 in the developing pancreatic epithelium and is nearly inactive in differentiated cells at p0. Eliminating β-catenin in Pdx1 positive progenitors compromises the development and proliferation of acinar progenitors, and potentially endocrine precursors(12-14). Interestingly, instead of promoting exocrine differentiation as might be expected, enforcing uncontrolled β-catenin signaling in Pdx1 precursors around E9.0 inhibits normal pancreatic differentiation at the expense of aberrant duct like structures(15). However, stabilizing β-catenin at slightly later timepoints in Pdx1 and p48 positive progenitors not only permits normal development but also increases acinar cell proliferation(15, 16). Therefore, cells undergoing exocrine development pass through states that vary in their sensitivity and dependence on β-catenin levels to undergo appropriate cell fate decisions. Chapter 2 of this thesis describes a similar temporal role of β-catenin signaling in Kras dependent specification of a cell lineage capable of giving rise to PDA.

Following pancreatic development, transcription factors and signaling pathways that mark multipotent progenitors become restricted to specific differentiated cells(6). At the same time, differentiated cells appear to mainly lose the capacity to differentiate into other cell types, and homeostasis appears to depend mainly on the expansion of pre-existing cells rather than the proliferation of a dedicated

stem cell compartment(17-20). This understanding of pancreatic plasticity has come in large part from models of exocrine and endocrine regeneration.

Considerable effort has been applied to understanding β-cell regeneration to enhance techniques for generating cells for type-1 diabetes therapy. β-cell mass is gradually restored after selective β-cell killing. Lineage tracing of β-cells before and after conditional elimination reveals no significant reduction of previously marked cells, suggesting that β-cells mainly regenerate from the proliferation of existing β-cells(19). Acinar cells also appear to mainly regenerate from pre-existing cells, therefore possessing a facultative stem cell capacity(17, 18, 21).

Considerable insight into acinar cell regeneration and plasticity has come from models that depend on chemical induction of pancreatitis using the cholecystokinin analog caerulein. Supramaximal caerulein treatment hyperactivates the acinar secretory pathway, leading to precocious, intracellular enzyme activity and cell damage due to autodigestion(22). While a small percentage of acinar cells undergo cell death, remaining, damaged acinar cells assume a transiently de-differentiated state displaying expression of duct markers (eg CK19), stress associated markers (eg Clusterin), as well as elements of the pancreatic embryonic program (eg Sox9, Pdx1, Hes1, and others) not normally expressed in differentiated acinar cells(18, 21, 23-25). Despite significant changes in gene expression and differentiation, this damaged state rapidly regenerates into normally functioning acinar cells. Like β-cells, the

frequency of genetically labeled acinar cells before and after caerulein is not significantly decreased(18), indicating regeneration of acinar cells from mainly pre-existing cells. Furthermore, even though the regenerating acinar compartment widely expresses markers of ductal differentiation in response to acute pancreatitis, acinar cells do not undergo persistent ductal reprogramming and become fixed in a ductal lineage(21, 25). Acinar to ductal reprogramming in the absence of aberrant signaling (e.g. Kras mutation (reviewed in (5), TGF-α expression(26)) appears to be a fairly restricted cell fate, not even observed in regeneration from partial pancreatectomy(17). However, fixed acinar to ductal reprogramming of wildtype acinar cells has been observed in response to severe, persistent damage where regeneration does not take place, such as chronic caerulein administration or pancreatic duct ligation(17, 27). Indeed, near complete elimination of acinar cells by selective killing also appears to activate an alternative, non-acinar, pool of cells that can give rise to acinar cells(28). This suggests that while acinar cells represent the primary regenerative source for exocrine cells, and acinar cells do not generally take on other fates, the pancreas possesses “backup” routes for regeneration that are mobilized only in response to extreme levels of damage.

This current understanding of acinar plasticity provides a framework to begin to understand how mutant Kras alters exocrine plasticity to drive PDA initiation. As described below, genetic models have shown that mutant Kras can act as the primary driver of the PanIN/PDA lineage, and suggest that exocrine cells and

endocrine cells (again in the context of persistent inflammatory damage) can be reprogrammed into a cell lineage that can give rise to PDA.

Mutant Kras is a critical regulator of PDAC development

Significant effort has been applied to determining the molecular underpinnings of PDAC. While some (~2-10%) of PDAC appears associated with hereditary factors(29),(30), most disease is associated with high frequency somatic mutations in a subset of genes, including the small GTPase protein Kras(31), and the tumor suppressors p16/INK4a(32), p53(33, 34), and DPC4/SMAD4(35). Of these frequently observed alterations, it is key to note that Kras mutation is nearly universal (>95%) in human PDAC. The mutations catalogued in PDAC render the protein locked in a constitutively active state, unable to hydrolyze GTP, thus promoting persistent signaling to downstream effectors (as reviewed in(36)). Large-scale genomics studies are beginning to catalogue the landscape of mutations found in PDAC(37), but investigating the function of these ”classical” genes both in cell culture and animal modeling have significantly advanced insight into PDAC aetiology.

PDAC is associated with non-invasive, preneoplastic lesions that are believed to represent precursors to the disease(38)(Figure 1, originally Box1 in (5)). PanINs are the most common and most widely studied putative precursors. They are histologically classified into three stages of increasing cellular and nuclear atypia (Figure 2)(39). Molecular studies have shown that PanIN stage correlates with

increasing mutation frequency and variety(40). For example, PanIN1 lesions frequently possess Kras mutation (estimates suggest 15-40%(41)), but less often harbor mutations in p53 or SMAD4. PanIN3 lesions, on the other hand, display more frequent Kras mutation as well as more frequent loss of these tumor suppressors(42, 43).

Owing to its near universal frequency in PDAC, Kras mutation was hypothesized to represent an initiating genetic lesion in the disease. However, initial efforts to audit the sufficiency of mutant Kras to initiate PDAC progression were stymied by the limitations of transgenic approaches. Expression of mutant Kras under acinar and ductal promoters resulted in either ductal lesions reminiscent of PanINs and mixed acinar and ductal carcinomas(44), or peri-ductal inflammation(45), respectively. However, neither model resulted in PDAC nor a faithful recapitulation of the stepwise progression of precursor lesions. Although it is unclear why these models failed to recapitulate human disease progression, they may have been hampered by hyper-physiological Kras output, or activation of Kras in an inappropriate cell type or developmental stage. The ability of mutant Kras to drive PDAC was not successfully investigated until the development of a Cre inducible conditional allele (lox-stop-lox $Kras^{G12D}$ ($LSL\text{-}Kras^{G12D}$)) targeted to the endogenous Kras locus(46), thus permitting expression of constitutively active Kras under temporal and spatial control. This tool eliminated possible issues of confounding cellular response to overexpression as transcription of the mutant Kras allele depends on the activity of the endogenous promoter.

First, the *LSL-Kras^{G12D}* allele was mated against Cre driver lines in which the recombinase is expressed under the control of promoters of the key pancreatic progenitor genes Pdx1 and p48, thus targeting mutant Kras to most cells in the developing organ. Both *Pdx1-Cre; LSL-Kras^{G12D}* and *p48Cre; LSL-Kras^{G12D}* (Table 1) animals displayed development of PDAC in a small number of mice (~15%) over the course of more than a year(47). Furthermore, early stage PanINs were universally penetrant, and lesions resembling the entire human PanIN spectra were observed in an age dependent fashion.

Recently, these original models have been modified to begin to determine which pancreatic cell types are capable of being reprogrammed into PDAC under the control of mutant Kras. By utilizing inducible Cre strategies which allow activation of Kras in specific populations of adult cells, it has become evident that while PDAC displays ductal characteristics, it may not necessarily emanate from the duct compartment (Figure 1 and Box 2)(21, 48-53). Interestingly, considerable evidence has shown that acinar cells can give rise to the PanIN lineage, a reprogramming event that can be dramatically accelerated by inflammatory damage, namely pancreatitis. Therefore, mutant Kras is a critical determinant of the “PanIN/PDAC lineage”, capable of driving pancreatic cells from terminal differentiation into a duct like fate ultimately capable of giving rise to PDAC.

Additionally, Kras driven models have been combined with loss of function alleles of the most commonly inactivated tumor suppressors including *p16*, *p53,* and various components of the TGF-β signaling cascade (models are summarized in Table 1)(54-61), revealing that these pathways constrain Kras directed PDAC development. Interestingly, eliminating different tumor suppressors can dramatically alter the type of precursor lesion that develops and the ultimate differentiation state of the malignant disease. It is key to note that cells in these models are subjected to simultaneous activation of Kras and loss of tumor suppressor function. This is likely in contrast to human tumor progression in which Kras mutations appear to occur early in disease development, and cells subsequently undergo selection pressure and accumulate progressive tumor suppressor loss. The observation that compromising tumor suppressive pathways "out of order" changes the course of PDAC development suggests that the disease may depend on the sequential tuning of signaling pathways in a similar fashion to that seen in normal development.

The following 2 chapters explore the theme of mutant Kras altering acinar plasticity to drive the PanIN/PDA lineage, and the requirement of temporal control of developmental signaling pathways in order for acinar cells to be reprogrammed into the ductal, PanIN lineage. Important to both chapters is the permissive environment that damage and transient de-differentiation that acute chemical pancreatitis provides for ductal reprogramming and PanIN development. Chapter 2 shows that mutant Kras blocks acinar cell regeneration

at the expense of persistent ductal de-differentiation. Furthermore, while β-catenin signaling is activated during acinar regeneration, it is blocked during the early stages of Kras driven, acinar derived PanIN development, and stabilized β-catenin can block acinar to ductal reprogramming that can give rise to PanINs. Chapter 3 shows that miRNAs constrain acinar differentiation, and loss of miRNAs accelerates Kras driven acinar to ductal reprogramming similar to the early stages of Kras dependent acinar reprogramming following pancreatic damage. However, this de-differentiated state displays considerable apoptosis and Dicer deficient cells do not appear to be capable of giving rise to PDA. Therefore, miRNA processing must be appropriately tuned during Kras driven acinar to ductal reprogramming to permit the development of a viable, ductal fate that can give rise to PDA. Chapter 3 ends with a discussion of ongoing experiments to identify Dicer dependent factors that are important for Kras to drive acinar to ductal reprogramming that can give rise to PDA precursors.

References

1. Lau, J., Kawahira, H., and Hebrok, M. 2006. Hedgehog signaling in pancreas development and disease. *Cell Mol Life Sci* 63:642-652.
2. Rovira, M., Scott, S.G., Liss, A.S., Jensen, J., Thayer, S.P., and Leach, S.D. 2010. Isolation and characterization of centroacinar/terminal ductal progenitor cells in adult mouse pancreas. *Proceedings of the National Academy of Sciences of the United States of America* 107:75-80.
3. Guo, T., and Hebrok, M. 2009. Stem cells to pancreatic beta-cells: new sources for diabetes cell therapy. *Endocrine reviews* 30:214-227.
4. Morris, J.P.t., and Hebrok, M. 2009. It's a free for all--insulin-positive cells join the group of potential progenitors for pancreatic ductal adenocarcinoma. *Cancer Cell* 16:359-361.
5. Morris, J.P.t., Wang, S.C., and Hebrok, M. 2010. KRAS, Hedgehog, Wnt and the twisted developmental biology of pancreatic ductal adenocarcinoma. *Nature reviews. Cancer* 10:683-695.
6. Bonal, C., and Herrera, P.L. 2008. Genes controlling pancreas ontogeny. *The International journal of developmental biology* 52:823-835.
7. Gradwohl, G., Dierich, A., LeMeur, M., and Guillemot, F. 2000. neurogenin3 is required for the development of the four endocrine cell lineages of the pancreas. *Proceedings of the National Academy of Sciences of the United States of America* 97:1607-1611.
8. Lee, J.C., Smith, S.B., Watada, H., Lin, J., Scheel, D., Wang, J., Mirmira, R.G., and German, M.S. 2001. Regulation of the pancreatic pro-endocrine gene neurogenin3. *Diabetes* 50:928-936.
9. Kopinke, D., Brailsford, M., Shea, J.E., Leavitt, R., Scaife, C.L., and Murtaugh, L.C. 2011. Lineage tracing reveals the dynamic contribution of Hes1+ cells to the developing and adult pancreas. *Development* 138:431-441.
10. Apelqvist, A., Li, H., Sommer, L., Beatus, P., Anderson, D.J., Honjo, T., Hrabe de Angelis, M., Lendahl, U., and Edlund, H. 1999. Notch signalling controls pancreatic cell differentiation. *Nature* 400:877-881.
11. Murtaugh, L.C., Stanger, B.Z., Kwan, K.M., and Melton, D.A. 2003. Notch signaling controls multiple steps of pancreatic differentiation. *Proc Natl Acad Sci U S A* 100:14920-14925.
12. Murtaugh, L.C., Law, A.C., Dor, Y., and Melton, D.A. 2005. {beta}-Catenin is essential for pancreatic acinar but not islet development. *Development*.
13. Wells, J.M., Esni, F., Boivin, G.P., Aronow, B.J., Stuart, W., Combs, C., Sklenka, A., Leach, S.D., and Lowy, A.M. 2007. Wnt/beta-catenin signaling is required for development of the exocrine pancreas. *BMC Dev Biol* 7:4.
14. Dessimoz, J., Bonnard, C., Huelsken, J., and Grapin-Botton, A. 2005. Pancreas-Specific Deletion of beta-Catenin Reveals Wnt-Dependent and Wnt-Independent Functions during Development. *Curr Biol* 15:1677-1683.

15. Heiser, P.W., Lau, J., Taketo, M.M., Herrera, P.L., and Hebrok, M. 2006. Stabilization of beta-catenin impacts pancreas growth. *Development* 133:2023-2032.
16. Heiser, P.W., Cano, D.A., Kim, G., Kench, J.G., Taketo, M.M., Biankin, A.V., and Hebrok, M. 2008. Stabilization of beta-catenin induces pancreas tumor formation. *Gastroenterology* in press.
17. Desai, B.M., Oliver-Krasinski, J., De Leon, D.D., Farzad, C., Hong, N., Leach, S.D., and Stoffers, D.A. 2007. Preexisting pancreatic acinar cells contribute to acinar cell, but not islet beta cell, regeneration. *J Clin Invest* 117:971-977.
18. Fendrich, V., Esni, F., Garay, M.V., Feldmann, G., Habbe, N., Jensen, J.N., Dor, Y., Stoffers, D., Jensen, J., Leach, S.D., et al. 2008. Hedgehog Signaling Is Required for Effective Regeneration of Exocrine Pancreas. *Gastroenterology* 135:621-631.
19. Dor, Y., Brown, J., Martinez, O.I., and Melton, D.A. 2004. Adult pancreatic beta-cells are formed by self-duplication rather than stem-cell differentiation. *Nature* 429:41-46.
20. Strobel, O., Dor, Y., Stirman, A., Trainor, A., Fernandez-del Castillo, C., Warshaw, A.L., and Thayer, S.P. 2007. Beta cell transdifferentiation does not contribute to preneoplastic/metaplastic ductal lesions of the pancreas by genetic lineage tracing in vivo. *Proceedings of the National Academy of Sciences of the United States of America* 104:4419-4424.
21. Morris, J.P.t., Cano, D.A., Sekine, S., Wang, S.C., and Hebrok, M. 2010. Beta-catenin blocks Kras-dependent reprogramming of acini into pancreatic cancer precursor lesions in mice. *J Clin Invest* 120:508-520.
22. Halangk, W., Lerch, M.M., Brandt-Nedelev, B., Roth, W., Ruthenbuerger, M., Reinheckel, T., Domschke, W., Lippert, H., Peters, C., and Deussing, J. 2000. Role of cathepsin B in intracellular trypsinogen activation and the onset of acute pancreatitis. *The Journal of clinical investigation* 106:773-781.
23. Jensen, J.N., Cameron, E., Garay, M.V., Starkey, T.W., Gianani, R., and Jensen, J. 2005. Recapitulation of elements of embryonic development in adult mouse pancreatic regeneration. *Gastroenterology* 128:728-741.
24. Siveke, J.T., Lubeseder-Martellato, C., Lee, M., Mazur, P.K., Nakhai, H., Radtke, F., and Schmid, R.M. 2008. Notch signaling is required for exocrine regeneration after acute pancreatitis. *Gastroenterology* 134:544-555.
25. De La, O.J., and Murtaugh, L.C. 2009. Notch and Kras in pancreatic cancer: at the crossroads of mutation, differentiation and signaling. *Cell Cycle* 8:1860-1864.
26. Means, A.L., Meszoely, I.M., Suzuki, K., Miyamoto, Y., Rustgi, A.K., Coffey, R.J., Jr., Wright, C.V., Stoffers, D.A., and Leach, S.D. 2005. Pancreatic epithelial plasticity mediated by acinar cell transdifferentiation and generation of nestin-positive intermediates. *Development* 132:3767-3776.

27. Strobel, O., Dor, Y., Alsina, J., Stirman, A., Lauwers, G., Trainor, A., Castillo, C.F., Warshaw, A.L., and Thayer, S.P. 2007. In vivo lineage tracing defines the role of acinar-to-ductal transdifferentiation in inflammatory ductal metaplasia. *Gastroenterology* 133:1999-2009.
28. Criscimanna, A., Speicher, J.A., Houshmand, G., Shiota, C., Prasadan, K., Ji, B., Logsdon, C.D., Gittes, G.K., and Esni, F. 2011. Duct cells contribute to regeneration of endocrine and acinar cells following pancreatic damage in adult mice. *Gastroenterology* 141:1451-1462, 1462 e1451-1456.
29. Habbe, N., Langer, P., Sina-Frey, M., and Bartsch, D.K. 2006. Familial pancreatic cancer syndromes. *Endocrinology and metabolism clinics of North America* 35:417-430, xi.
30. Wescott, M.P., and Rustgi, A.K. 2008. Pancreatic cancer: translating lessons from mouse models and hereditary syndromes. *Cancer prevention research* 1:503-506.
31. Almoguera, C., Shibata, D., Forrester, K., Martin, J., Arnheim, N., and Perucho, M. 1988. Most human carcinomas of the exocrine pancreas contain mutant c-K-ras genes. *Cell* 53:549-554.
32. Caldas, C., Hahn, S.A., Hruban, R.H., Redston, M.S., Yeo, C.J., and Kern, S.E. 1994. Detection of K-ras mutations in the stool of patients with pancreatic adenocarcinoma and pancreatic ductal hyperplasia. *Cancer research* 54:3568-3573.
33. Ruggeri, B., Zhang, S.Y., Caamano, J., DiRado, M., Flynn, S.D., and Klein-Szanto, A.J. 1992. Human pancreatic carcinomas and cell lines reveal frequent and multiple alterations in the p53 and Rb-1 tumor-suppressor genes. *Oncogene* 7:1503-1511.
34. Scarpa, A., Capelli, P., Mukai, K., Zamboni, G., Oda, T., Iacono, C., and Hirohashi, S. 1993. Pancreatic adenocarcinomas frequently show p53 gene mutations. *The American journal of pathology* 142:1534-1543.
35. Schutte, M., Hruban, R.H., Hedrick, L., Cho, K.R., Nadasdy, G.M., Weinstein, C.L., Bova, G.S., Isaacs, W.B., Cairns, P., Nawroz, H., et al. 1996. DPC4 gene in various tumor types. *Cancer research* 56:2527-2530.
36. Rodriguez-Viciana, P., Tetsu, O., Oda, K., Okada, J., Rauen, K., and McCormick, F. 2005. Cancer targets in the Ras pathway. *Cold Spring Harbor symposia on quantitative biology* 70:461-467.
37. Jones, S., Zhang, X., Parsons, D.W., Lin, J.C., Leary, R.J., Angenendt, P., Mankoo, P., Carter, H., Kamiyama, H., Jimeno, A., et al. 2008. Core signaling pathways in human pancreatic cancers revealed by global genomic analyses. *Science* 321:1801-1806.
38. Hruban, R.H., Maitra, A., Kern, S.E., and Goggins, M. 2007. Precursors to pancreatic cancer. *Gastroenterology clinics of North America* 36:831-849, vi.
39. Hruban, R.H., Takaori, K., Klimstra, D.S., Adsay, N.V., Albores-Saavedra, J., Biankin, A.V., Biankin, S.A., Compton, C., Fukushima, N., Furukawa, T., et al. 2004. An illustrated consensus on the classification of pancreatic intraepithelial neoplasia and intraductal papillary mucinous neoplasms. *Am J Surg Pathol* 28:977-987.

40. Feldmann, G., Beaty, R., Hruban, R.H., and Maitra, A. 2007. Molecular genetics of pancreatic intraepithelial neoplasia. *Journal of hepato-biliary-pancreatic surgery* 14:224-232.
41. Lohr, M., Kloppel, G., Maisonneuve, P., Lowenfels, A.B., and Luttges, J. 2005. Frequency of K-ras mutations in pancreatic intraductal neoplasias associated with pancreatic ductal adenocarcinoma and chronic pancreatitis: a meta-analysis. *Neoplasia* 7:17-23.
42. Maitra, A., Adsay, N.V., Argani, P., Iacobuzio-Donahue, C., De Marzo, A., Cameron, J.L., Yeo, C.J., and Hruban, R.H. 2003. Multicomponent analysis of the pancreatic adenocarcinoma progression model using a pancreatic intraepithelial neoplasia tissue microarray. *Mod Pathol* 16:902-912.
43. Wilentz, R.E., Iacobuzio-Donahue, C.A., Argani, P., McCarthy, D.M., Parsons, J.L., Yeo, C.J., Kern, S.E., and Hruban, R.H. 2000. Loss of expression of Dpc4 in pancreatic intraepithelial neoplasia: evidence that DPC4 inactivation occurs late in neoplastic progression. *Cancer Res* 60:2002-2006.
44. Grippo, P.J., Nowlin, P.S., Demeure, M.J., Longnecker, D.S., and Sandgren, E.P. 2003. Preinvasive pancreatic neoplasia of ductal phenotype induced by acinar cell targeting of mutant Kras in transgenic mice. *Cancer research* 63:2016-2019.
45. Brembeck, F.H., Schreiber, F.S., Deramaudt, T.B., Craig, L., Rhoades, B., Swain, G., Grippo, P., Stoffers, D.A., Silberg, D.G., and Rustgi, A.K. 2003. The mutant K-ras oncogene causes pancreatic periductal lymphocytic infiltration and gastric mucous neck cell hyperplasia in transgenic mice. *Cancer Res* 63:2005-2009.
46. Tuveson, D.A., Shaw, A.T., Willis, N.A., Silver, D.P., Jackson, E.L., Chang, S., Mercer, K.L., Grochow, R., Hock, H., Crowley, D., et al. 2004. Endogenous oncogenic K-ras(G12D) stimulates proliferation and widespread neoplastic and developmental defects. *Cancer cell* 5:375-387.
47. Hingorani, S.R., Petricoin, E.F., Maitra, A., Rajapakse, V., King, C., Jacobetz, M.A., Ross, S., Conrads, T.P., Veenstra, T.D., Hitt, B.A., et al. 2003. Preinvasive and invasive ductal pancreatic cancer and its early detection in the mouse. *Cancer Cell* 4:437-450.
48. Guerra, C., Schuhmacher, A.J., Canamero, M., Grippo, P.J., Verdaguer, L., Perez-Gallego, L., Dubus, P., Sandgren, E.P., and Barbacid, M. 2007. Chronic pancreatitis is essential for induction of pancreatic ductal adenocarcinoma by K-Ras oncogenes in adult mice. *Cancer Cell* 11:291-302.
49. Habbe, N., Shi, G., Meguid, R.A., Fendrich, V., Esni, F., Chen, H., Feldmann, G., Stoffers, D.A., Konieczny, S.F., Leach, S.D., et al. 2008. Spontaneous induction of murine pancreatic intraepithelial neoplasia (mPanIN) by acinar cell targeting of oncogenic Kras in adult mice. *Proc Natl Acad Sci U S A* 105:18913-18918.
50. De La, O.J., Emerson, L.L., Goodman, J.L., Froebe, S.C., Illum, B.E., Curtis, A.B., and Murtaugh, L.C. 2008. Notch and Kras reprogram

pancreatic acinar cells to ductal intraepithelial neoplasia. *Proc Natl Acad Sci U S A*.
51. Shi, G., Zhu, L., Sun, Y., Bettencourt, R., Damsz, B., Hruban, R.H., and Konieczny, S.F. 2009. Loss of the acinar-restricted transcription factor Mist1 accelerates Kras-induced pancreatic intraepithelial neoplasia. *Gastroenterology* 136:1368-1378.
52. Ji, B., Tsou, L., Wang, H., Gaiser, S., Chang, D.Z., Daniluk, J., Bi, Y., Grote, T., Longnecker, D.S., and Logsdon, C.D. 2009. Ras activity levels control the development of pancreatic diseases. *Gastroenterology* 137:1072-1082, 1082 e1071-1076.
53. Gidekel Friedlander, S.Y., Chu, G.C., Snyder, E.L., Girnius, N., Dibelius, G., Crowley, D., Vasile, E., DePinho, R.A., and Jacks, T. 2009. Context-dependent transformation of adult pancreatic cells by oncogenic K-Ras. *Cancer cell* 16:379-389.
54. Aguirre, A.J., Bardeesy, N., Sinha, M., Lopez, L., Tuveson, D.A., Horner, J., Redston, M.S., and DePinho, R.A. 2003. Activated Kras and Ink4a/Arf deficiency cooperate to produce metastatic pancreatic ductal adenocarcinoma. *Genes Dev* 17:3112-3126.
55. Bardeesy, N., Aguirre, A.J., Chu, G.C., Cheng, K.H., Lopez, L.V., Hezel, A.F., Feng, B., Brennan, C., Weissleder, R., Mahmood, U., et al. 2006. Both p16(Ink4a) and the p19(Arf)-p53 pathway constrain progression of pancreatic adenocarcinoma in the mouse. *Proc Natl Acad Sci U S A* 103:5947-5952.
56. Hingorani, S.R., Wang, L., Multani, A.S., Combs, C., Deramaudt, T.B., Hruban, R.H., Rustgi, A.K., Chang, S., and Tuveson, D.A. 2005. Trp53R172H and KrasG12D cooperate to promote chromosomal instability and widely metastatic pancreatic ductal adenocarcinoma in mice. *Cancer Cell* 7:469-483.
57. Bardeesy, N., Cheng, K.H., Berger, J.H., Chu, G.C., Pahler, J., Olson, P., Hezel, A.F., Horner, J., Lauwers, G.Y., Hanahan, D., et al. 2006. Smad4 is dispensable for normal pancreas development yet critical in progression and tumor biology of pancreas cancer. *Genes Dev* 20:3130-3146.
58. Ijichi, H., Chytil, A., Gorska, A.E., Aakre, M.E., Fujitani, Y., Fujitani, S., Wright, C.V., and Moses, H.L. 2006. Aggressive pancreatic ductal adenocarcinoma in mice caused by pancreas-specific blockade of transforming growth factor-beta signaling in cooperation with active Kras expression. *Genes Dev* 20:3147-3160.
59. Izeradjene, K., Combs, C., Best, M., Gopinathan, A., Wagner, A., Grady, W.M., Deng, C.X., Hruban, R.H., Adsay, N.V., Tuveson, D.A., et al. 2007. Kras(G12D) and Smad4/Dpc4 haploinsufficiency cooperate to induce mucinous cystic neoplasms and invasive adenocarcinoma of the pancreas. *Cancer Cell* 11:229-243.
60. Kojima, K., Vickers, S.M., Adsay, N.V., Jhala, N.C., Kim, H.G., Schoeb, T.R., Grizzle, W.E., and Klug, C.A. 2007. Inactivation of Smad4 accelerates Kras(G12D)-mediated pancreatic neoplasia. *Cancer research* 67:8121-8130.

61. Vincent, D.F., Yan, K.P., Treilleux, I., Gay, F., Arfi, V., Kaniewski, B., Marie, J.C., Lepinasse, F., Martel, S., Goddard-Leon, S., et al. 2009. Inactivation of TIF1gamma cooperates with Kras to induce cystic tumors of the pancreas. *PLoS genetics* 5:e1000575.

Figure Legend

Figure 1. Kras is a master regulator of pancreatic ductal adenocarcinoma initiation and progression.

Constitutively active Kras ($Kras^{G12D}$, or $Kras^{G12V}$) is sufficient to initiate the development of pancreatic intraepithelial neoplasia (PanINs) and pancreatic ductal adenocarcinoma (PDAC). PanINs are classified into three stages of increasing cellular atypia and in humans have been found to possess increasing numbers of mutations (common mutations are indicated). In mouse models the human PanIN spectrum followed by progression to PDAC has been recapitulated by activating mutant Kras in embryonic pancreatic progenitors. Eliminating tumor suppressors commonly inactivated in the human disease dramatically decreases PDAC latency. Mouse models in which Kras is activated specifically in some adult cell types have shown that both acini and insulin positive cells can give rise to PanINs and in some cases PDAC depending on tissue damage and tumor suppressor inactivation. For these cell types, reprogramming into a "ductal" cell type is required to assume the PanIN–PDAC lineage. Question marks are shown for centroacinar and duct cells as they have not been specifically audited for their ability to be reprogrammed into a lineage capable of becoming PDAC under the control of Kras. However, until specific targeting has been achieved they cannot be ruled out as sources of the "precursor-PDAC" lineage. Note: line drawing modified from Hruban and colleagues (*Clin Cancer Res* 6, 2969-72 (2000)).

Figure 1

Box 1 | **KRAS necessity and sufficiency in the stepwise progression to pancreatic ductal adenocarcinoma**

Mucinous cystic neoplasm (MCN), intraductal papillary mucinous neoplasm (IPMN) and pancreatic intraepithelial neoplasia (PanIN)[1] are thought to represent precursor stages for pancreatic ductal adenocarcinoma (PDAC). This view is supported by KRAS-driven mouse models in which such preneoplastic lesions precede the development of PDAC (TABLE 1). Indeed, in models that develop PanINs (the most commonly observed putative precursor lesion in humans) and PDAC, PanIN lesions increase in severity and PDAC becomes more prevalent as mice age. Therefore, in this Review, we refer to this cell fate as the PanIN–PDAC lineage (indicated as precursor–PDAC lineage in the figure below). However, other mouse models suggest that IPMNs and MCNs could be parallel routes to PDAC development. All three lesions share expression of ductal markers and therefore would require reprogramming into a ductal lineage if they emerge from non-ductal compartments, such as acini, centroacinar cells or endocrine cells.

Even though mutant KRAS is sufficient to initiate the PanIN–PDAC lineage in mice, there is some evidence that it may not be necessary. Although frequently observed, KRAS mutation is not universal in early human PanINs. Furthermore, in mice, lesions resembling early-stage PanINs can develop owing to Hedgehog ligand overexpression during pancreatic development[57] and chronic inflammation[120]. KRAS mutation becomes increasingly frequent in advanced PanINs and PDAC, leading to an important but unresolved question as to when deregulated KRAS activity becomes necessary for disease progression.

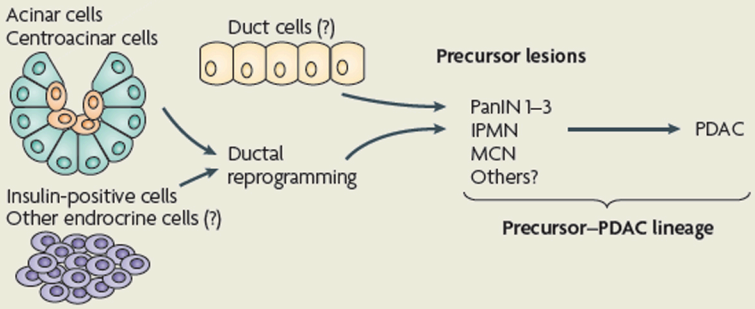

Figure 2

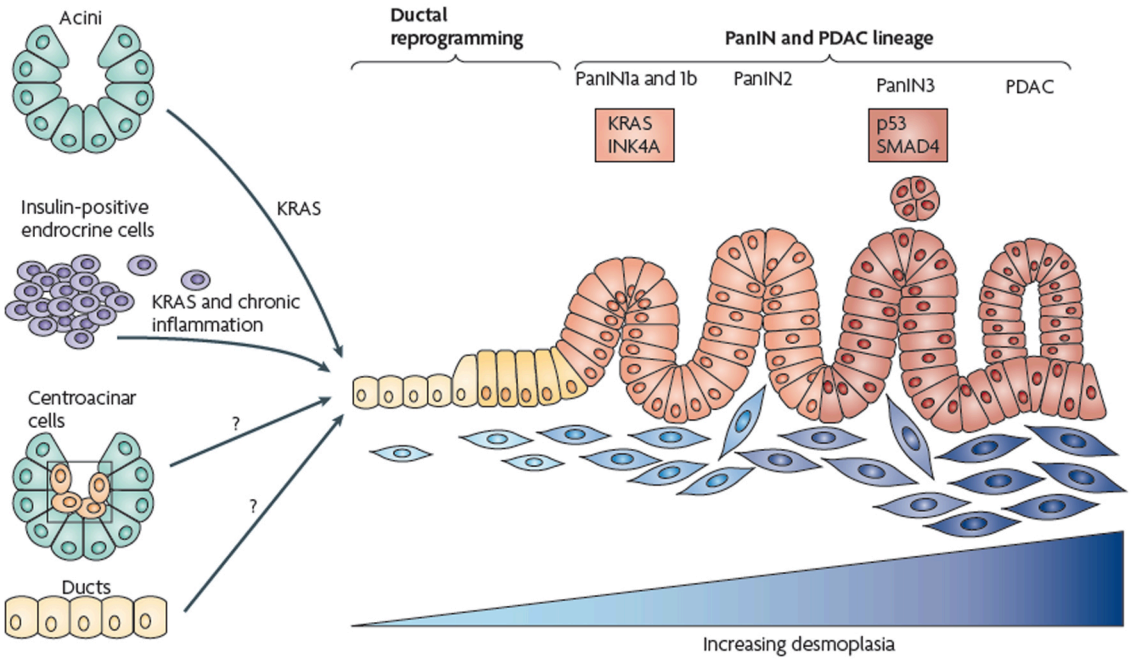
Acini
Ductal reprogramming
PanIN and PDAC lineage
PanIN1a and 1b
PanIN2
PanIN3
PDAC
KRAS
INK4A
p53
SMAD4
Insulin-positive endrocrine cells
KRAS
KRAS and chronic inflammation
Centroacinar cells
?
?
Ducts
Increasing desmoplasia

Chapter 2:

β-catenin blocks Kras dependent reprogramming of acini into pancreatic cancer precursors in mice.

This work appeared in published form as:

Morris IV, J.P., Cano, D.A., Sekine, S., Wang, S.C., and Hebrok, M. 2010. Beta-catenin blocks Kras-dependent reprogramming of acini into pancreatic cancer precursor lesions in mice. *J Clin Invest* 120:508-520.

β-catenin blocks Kras dependent reprogramming of acini into pancreatic cancer precursors in mice.

John P. Morris IV[1], David A. Cano[1, 2], Shigeki Sekine[1, 3], Sam C. Wang[1], Matthias Hebrok[1, *]

[1] Diabetes Center, Department of Medicine, University of California, San Francisco, CA 94143, USA.

[2] Present address: Instituto de Biomedicina de Sevilla, Servicio de Endocrinología y Nutrición, Hospitales Universitarios Virgen del Rocío, Sevilla 41013, Spain

[3] Present address: Pathology Division, National Cancer Center Research Institute, Tokyo, Japan

Conflict of interest statement: The authors have declared that no conflict of interest exists.

Nonstandard abbreviations used: Acinar to ductal metaplasia (ADM), Immunohistochemistry (IHC), Pancreatic intraepithelial neoplasia (PanIN), Pancreatic ductal adenocarcinoma (PDA), Tubular complex (TC)

Corresponding author: Matthias Hebrok, Diabetes Center, Department of Medicine, HSW1119, 513 Parnassus Avenue, University of California, San Francisco, CA 94143. Phone: 415-514-0820; Fax: 415-564-5813: Email: mhebrok@diabetes.ucsf.edu.

Abstract:

Cellular plasticity in adult organs is involved in both regeneration and carcinogenesis. In response to injury that mimics acute pancreatitis, wild type mouse pancreatic acinar cells have been shown to rapidly regenerate through intermediates that re-activate elements of embryonic pancreatic development. In contrast, such injury promotes the development of pancreatic ductal adenocarcinoma (PDA) precursor lesions in mice in which constitutively active Kras is targeted to the exocrine pancreas. At present, the molecular environment that mediates acinar regeneration versus the development of PDA precursors is poorly understood. Here, we use genetically engineered mice to demonstrate that mutant Kras promotes acinar to ductal metaplasia (ADM) and pancreatic cancer precursor lesion formation by blocking acinar regeneration following acute pancreatitis. Our results show that temporary activation of ß-catenin signaling, an embryonic signaling pathway known to regulate development of acinar cells during organogenesis, is critical for acinar cell regeneration. Importantly, we find that this transient increase in ß-catenin signaling is not observed during the initiation of Kras induced acinar to ductal reprogramming. Furthermore, stabilized ß-catenin signaling antagonizes the ability of Kras to reprogram acini into PDA pre-neoplastic precursors. Therefore, our study highlights β-catenin as a critical determinant of acinar regeneration versus Kras induced fate decisions during the specification of PDA precursors. More broadly, it points to the importance of temporal regulation of embryonic signaling pathways in the development of neoplastic cell fates.

Introduction

Pancreatic ductal adenocarcinoma (PDA) is the fourth leading cause of cancer death in the United States (1). Analysis of patient samples and genetically engineered mouse models suggest that it likely develops from pre-neoplastic ductal lesions, including pancreatic intraepithelial neoplasias (PanINs) (2). Understanding how signaling pathways interact in the pancreatic epithelium to elicit PanINs therefore represents a key step in the possible development of tools for early PDA detection and treatment. While PanINs express markers of ductal differentiation, many recent studies suggest that they can arise from pancreatic acinar cells that are reprogrammed into a preneoplastic state by undergoing acinar to ductal metaplasia (ADM) (3-7)

Activating mutations in the KRAS gene are nearly universal in human PDA (8) and targeting of mutated Kras to mouse pancreatic progenitors recapitulates the human PanIN to PDA progression sequence (9). While ADM is observed in these models (6), and Kras can spontaneously induce ADM and PanIN formation when activated in adult acini (3, 4, 7), expression of mutant Kras in acinar cells does not guarantee ductal reprogramming. Acini expressing mutant Kras during embryogenesis appear grossly unaffected (9) and some normal acinar tissue is maintained in the context of PanIN and PDA progression as mice age (9,10). Therefore, additional events must occur to enable a cellular environment permissive for Kras to drive ADM/PanIN formation.

Recently, environmental insults that result in exocrine damage and inflammation have been shown to represent one such permissive environment. For example, Guerra and colleagues (5) and Carriere and colleagues (11) have demonstrated that chronic and acute chemical pancreatitis, respectively, induced by the cholecystikinin receptor agonist caerulein, accelerate development of ADM/PanIN and PDA progression when mutant Kras is expressed in the acinar/centroacinar compartment. These findings, particularly that of Guerra and colleagues (5), support clinical data showing that chronic pancreatitis represents a potent risk factor for PDA (12, 13). However, the exact manner by which active Kras co-opts exocrine damage to initiate the PanIN to PDA sequence is unclear.

In response to caerulein induced acute pancreatitis, wild type mouse acinar cells decrease expression of acinar markers and re-activate factors expressed during pancreatic development (14, 15). These cells may also assume a transient duct-like morphology (16, 17). Lineage tracing has revealed that it is mainly pre-existing acini, rather than a dedicated acinar stem cell, which rapidly re-differentiate and repopulate the acinar compartment following caerulein pancreatitis (16, 17). Thus, this transient de-differentiation of acini into duct-like cells during regeneration differs from ADM, where ductal differentiation becomes fixed. Nonetheless, acini undergoing ADM both *in vitro* due to EGF ligand signaling (18, 19) and *in vivo* in the context of mutant Kras share expression of some embryonic markers of regenerating wild type acinar cells, such as Nestin and Notch pathway activation (14, 16). Since expression of many of these

reactivated embryonic factors are also maintained throughout PanIN and PDA development, such as Notch signaling (20), achieving a less-differentiated expression profile that resembles pancreatic development may play a role in PanIN initiation. Furthermore, some factors reactivated during acinar regeneration have also been shown to promote ADM. For example, while the transcription factor Pdx1 is transiently up-regulated during acinar regeneration (14), enforced exocrine expression induces ADM (21). This suggests that reactivation of developmental signaling pathways must be tightly regulated to permit acinar regeneration but prevent persistent ductal reprogramming.

Given the ability of mutant Kras to spontaneously induce ADM and PanINs, which share molecular similarity to regenerating acini, we set out to investigate the effects of mutant Kras on differentiation and regeneration-associated signaling pathways immediately following acinar damage. Using acute caerulein pancreatitis as a model, we find that mutant Kras blocks acinar regeneration and promotes persistently de-differentiated ADM/PanIN. Probing for the molecular mechanisms underlying this switch we find that regeneration-associated β-catenin signaling is inhibited during Kras induced acinar to ductal reprogramming and that β-catenin is required for efficient acinar regeneration. Finally, we show that stabilized β-catenin signaling antagonizes Kras induced ADM and prevents the formation of acinar derived PanINs. Thus, we conclude that β-catenin signaling is a key modulator of acinar plasticity, and represents a critical

molecular modulator of acinar regeneration versus Kras induced reprogramming of acini into PDA precursors.

Results

Mutant Kras blocks acinar regeneration in favor of ADM/PanIN formation

To determine how mutant Kras affects acinar regeneration we generated mice in which a constitutively active form of Kras, *LSL-Kras*^{G12D} (9), is induced via Cre recombinase expressed in all pancreatic progenitors by the *Pdx1* promoter, *Pdx1-Cre*^{Early} (22). At six weeks of age the pancreas in these mice is comprised mostly of morphologically normal acini with few ductal PanIN lesions despite efficient recombination at the conditional Kras locus (asterisk Figure 1E, M). We induced acute caerulein pancreatitis using the 'staggered' protocol described in the Methods section, and compared regeneration in control *Pdx1-Cre*^{Early} and *Pdx1-Cre*^{Early}*; LSL-Kras*^{G12D} mice. The exocrine compartments of both cohorts responded comparably 2 days after caerulein treatment, displaying de-granulated acinar cells (Figure 1B, F), decreased amylase expression (Figure 1J, N), and duct like structures consistent with acute pancreatitis (Figure 1B, F and insets). These structures were morphologically similar to the transient ductal intermediates reported by other groups during wild type acinar regeneration (16, 17). In *Pdx1-Cre*^{Early} control mice these structures also weakly co-expressed the duct marker CK19, while CK19 was strongly expressed in comparable structures in *Pdx1-Cre*^{Early}*; LSL-Kras*^{G12D} animals (compare Figure 1 J, N and insets). By seven days following caerulein treatment regeneration of the acinar compartment of *Pdx1-Cre*^{Early} control animals was nearly complete, as amylase and CK19 expression was redistributed in similar fashion to PBS treatment (Figure 1C, K).

Similarly, pancreata at 21 days following caerulein were indistinguishable from PBS treated animals (Figure 1D, L).

In stark contract, acinar regeneration was blocked in *Pdx1-Cre^{Early}; LSL-Kras^{G12D}* mice, resulting in replacement of the normal exocrine compartment with ductal structures. Seven days following treatment, *Pdx1-Cre^{Early}; LSL-Kras^{G12D}* pancreata were comprised mainly of CK-19 positive duct structures embedded in an expanded stromal compartment (Figure 1G, O). Morphologically normal, amylase expressing acinar cells were rare, with some amylase positive cells found in duct structures (Figure 1O, arrowheads). By 21 days following treatment, the exocrine compartment was predominately composed of CK-19 positive, mucinous ductal lesions resembling low grade PanINs (Figure 1H, P). As observed in other reports of spontaneous mouse PanINs (9), these lesions frequently stained for Alcian Blue, a marker of mucin accumulation in human PanINs (Supplemental Figure 1B). Consistent with histological features at both time points and a progression in severity of the observed defects, Alcian Blue positive structures were more common at day 21 following caerulein than seven days after treatment (compare Supplemental Figure 1A, 1B).

To further test whether acinar reprogramming is a source of the abnormal ducts and PanINs resulting from inhibited acinar regeneration we also performed this analysis using transgenic mice that have Kras activation in a more restricted set of cells during embryogenesis (*Pdx1-Cre^{Late}; LSL-Kras^{G12D}*) as well as mice in

which Kras acitivity is restricted to adult acinar cells (*Elastase-Cre^{ERT2}*; *LSL-Kras^{G12D}*). We have previously shown that in the *Pdx1-Cre^{Late}* driver line, Cre activity is found in acinar cells but notably absent from ducts (22). Caerulein treatment in these mice displayed a similar time course of subverted regeneration and accelerated ADM/PanIN development as *Pdx1-Cre^{Early}; LSL-Kras^{G12D}* mice (Supplemental Figure 1C-F), supporting acinar reprogramming as a source of the observed duct structures and PanINs.

To more rigorously test if acini serve as the cell of origin for ADM/PanIN following inhibited acinar regeneration, we also performed these experiments with *Elastase-Cre^{ERT2}* driven mouse models. This line was chosen as it permits tamoxifen inducible Cre activation restricted to adult acini (23). To trace cells where Cre was active we also included a *R26R-EYFP* reporter line in our matings, which possesses a Cre inducible lox-stop-lox-EYFP cassette targeted to the Rosa26 locus (24). *Elastase-Cre^{ERT2}*; *R26R-EYFP* and *Elastase-Cre^{ERT2}*; *LSL-Kras^{G12D}; R26R-EYFP* mice were generated and stimulated with tamoxifen (see Methods) at four weeks of age. Two weeks later, mice were treated with PBS or the staggered caerulein protocol as described above. As expected, YFP expression was limited to amylase positive acinar cells and absent from CK19 positive duct cells in tamoxifen stimulated, PBS treated *Elastase-Cre^{ERT2}*; *R26R-YFP* mice (Supplemental Figure 1G). Two days following caerulein however, we observed CK19/YFP double positive cells in duct like structures (Supplemental Figure 1H) similar to those observed in *Pdx1-Cre^{Early}* control mice (Figure 1F, J),

supporting a transient ductal state during acinar regeneration. These CK19/YFP double positive cells may be similar to the acinar derived type 1 Tubular Complexes (TC1) duct like structures described by Strobel and colleagues (17). They also resemble double amylase/CK19 positive structures observed during regeneration following partial pancreatectomy in rats (25). Of note, we also found CK19 positive acinar structures that were YFP negative. Due to the mosaic nature of CreERT2 activation we cannot rule out that these are cells in which YFP was not activated. Alternatively, they may represent non-acinar derived TC2 structures as described previously (17). As expected, upon regeneration seven and 21 days after caerulein treatment, YFP expression was again limited to acinar cells (Supplemental Figure 1I,J).

Tamoxifen stimulated *Elastase-Cre^{ERT2}*; *LSL-Kras^{G12D}*, and *Elastase-Cre^{ERT2}*; *LSL-Kras^{G12D}; R26R-EYFP* mice treated with PBS possessed grossly normal pancreata (Supplemental Figure 1K) that rarely demonstrated ADM/PanIN (one of six mice, four to five weeks following tamoxifen). Except such rare lesions in *Elastase-Cre^{ERT2}*; *LSL-Kras^{G12D}; R26R-EYFP* mice, YFP expression was limited to acinar cells and excluded from CK19 positive ducts (Figure 1Q). Two days following caerulein *Elastase-Cre^{ERT2}*; *LSL-Kras^{G12D}; R26R-EYFP* mice developed duct like structures similar to those observed in other genotypes (Supplemental Figure 1L) which were composed of acinar derived, double CK19/YFP positive cells (Figure 1R). In contrast to *Elastase-Cre^{ERT2}*; *R26R-EYFP* control mice, acinar derived CK19/YFP double positive ducts persisted 7 days following

caerulein (Figure 1S; Supplemental Figure 1M,). Due to the acinar origin of these structures, they may represent persistent TC1 type structures. 21 days following caerulein we observed frequent CK19/YFP double positive, acinar derived PanIN lesions (Figure 1T, Supplemental Figure 1N,). Therefore, mutant Kras subverts the regenerative capacity of otherwise morphologically normal acini following acute pancreatitis, and instead promotes a fixed ductal fate that is permissive for ADM/PanIN formation.

Mutant Kras alters acinar regeneration by maintaining a persistently de-differentiated state

Since mutant Kras subverts acinar cell fate decisions following damage, we next asked if mutant Kras effects the reactivation of embryonic signaling pathways during normal acinar regeneration. Two days following caerulein, the exocrine compartment in both *Pdx1-Cre*^{Early} and *Pdx1-Cre*^{Early}*; LSL-Kras*^{G12D} mice displayed re-activation of elements of embryonic development or markers of immature acini, frequently in duct like structures, including Clusterin (Figure 2B ,F) (15), Sox9 (Figure 2J, N) (26), Pdx1 (Supplemental Figure 2B, F) (14), and the Notch target gene Hes1 (Supplemental Figure 2J, N) (14). This suggests that exocrine cells possessing mutant Kras assume progenitor like properties in response to acinar damage similar to wild type exocrine cells. The adult expression pattern of these embryonic factors before injury was re-established seven and 21 days following caerulein administration in *Pdx1-Cre*^{Early} control mice, (Figure 2C, D, K, L, Supplemental Figure 2C, D, K, L). In stark contrast,

expression of all tested embryonic factors persisted in ductal metaplasia and in PanINs observed in *Pdx1-Cre^{Early}; LSL-Kras^{G12D}* (Figure 2G, H, O, P), similar to spontaneous PanINs found in age-matched PBS treated mice (Figure 2E, M, Supplemental Figure 2E, M).

Next, we directly compared acinar differentiation during regeneration and ADM/PanIN formation in *Elastase-Cre^{ERT2}*; *R26R-EYFP* and *Elastase-Cre^{ERT2}*; *LSL-Kras^{G12D}; R26R-EYFP* mice. Consistent with our observations in *Pdx1-Cre^{Early}* and *Pdx1-Cre^{Early}; LSL-Kras^{G12D}* mice, we observed acinar derived (YFP positive) cells in both tamoxifen stimulated *ElastaseCre^{ERT2}; R26R-EYFP* and *Elastase-Cre^{ERT2}*; *LSL-Kras^{G12D}; R26R-EYFP* mice that expressed Clusterin (Supplemental Figure 3B), Sox9 (Supplemental Figure 3J), and Pdx1 (data not shown) two days following caerulein. As expected, strong expression of Clusterin, Sox9, and Pdx1 was absent from acini in *ElastaseCre^{ERT2}; R26R-EYFP* when regeneration was complete (Supplemental Figure 3 C, D, K, L, and data not shown). In contrast, acinar derived metaplastic ducts and PanINs in *Elastase-Cre^{ERT2}*; *LSL-Kras^{G12D}; R26R-EYFP* mice maintained strong expression of these embryonic factors (Supplemental Figure 3G, H, O, P, data not shown). Therefore, mutant Kras not only diverts regeneration towards a ductal fate, but also promotes a persistently de-differentiated state (Figure 2Q).

We also asked if maintenance of a de-differentiated ductal state corresponded with persistent activation of Kras effector pathways. As assessed by

phosphorylation of both p42 and p44 (ERK1/2), which are readouts for the activity of the MAP Kinase (MAPK) pathway downstream of Kras signaling, we found that the pattern of Kras activity matched that of the persistently active embryonic factors. While spontaneous ADM/PanIN in PBS treated *Pdx1-Cre*^{Early}*; LSL-Kras*^{G12D} displayed phospho-ERK1/2 reactivity, it was mainly absent in morphologically normal acini (Supplemental Figure 4E). However, phospho-ERK1/2 staining was frequently observed in cells assuming a ductal morphology two days following caerulein (Supplemental Figure 4F) and was maintained in subsequent metaplastic ducts and PanINs (seven and 21 days following caerulein, Supplemental Figure 4G, H). In the regenerating exocrine compartment of control *Pdx1-Cre*^{Early} mice, phospho-ERK1/2 was observed in a subset of cells two days following caerulein (Supplemental Figure 4B), but was not found in acini in PBS treated animals (Supplemental Figure 4A) or in acini following regeneration (Supplemental Figure 4C, D). Summarily, these data suggest that the regenerative environment produced by acute pancreatic damage not only promotes cell fate changes permissive for Kras induced ADM/PanIN formation, but may also provide a permissive environment for sustained Kras effector function.

Regeneration associated ß-catenin signaling is inhibited during Kras induced acinar to ductal reprogramming

Since ductal metaplasia is synchronized and widespread in caerulein treated *Pdx1-Cre*^{Early}*; LSL-Kras*^{G12D} mice, this model provides an opportunity to identify

key signaling pathways that are inappropriately modulated in the presence of mutant Kras to prevent regeneration and promote ADM/PanIN. One candidate pathway is ß-catenin signaling. ß-catenin is the prime transcriptional activator of canonical Wnt signaling, and has been implicated in regeneration of many organs including the liver, lung, and limbs (for review see (27)). During pancreatic development, ß-catenin is critical for acinar specification (28, 29) and has been implicated in endocrine development (30). Furthermore, ß-catenin has been shown to accumulate in regenerating wild type acini following caerulein pancreatitis (14), although a role for ß-catenin signaling activity has not been investigated during pancreas regeneration. Thus, we compared ß-catenin accumulation and signaling during acinar regeneration and Kras induced ADM/PanIN formation.

In PBS treated *Pdx1-Cre*^{Early} mice, weak ß-catenin signal was apparent at the membrane of acinar cells and ducts (Figure 3A and data not shown). While spontaneous PanINs in PBS treated *Pdx1-Cre*^{Early}*; LSL-Kras*^{G12D} mice frequently displayed strong membranous and cytoplasmic ß-catenin staining, morphologically normal acini presented with weak membranous labeling comparable to that of PBS treated *Pdx1-Cre*^{Early} acini (Figure 3E). Two days after caerulein treatment, cells in the regenerating exocrine compartment of *Pdx1-Cre*^{Early} mice displayed accumulation of ß-catenin, predominately at the cell periphery and in the cytoplasm (Figure 3B). Like other embryonic factors, ß-catenin distribution reverted to the pattern of PBS treated mice at seven and 21

days after treatment (Figure 3C, D). In contrast to other reactivated developmental signaling factors, the damaged exocrine compartment in *Pdx1-Cre^{Early}; LSL-Kras^{G12D}* mice displayed weaker overall ß-catenin levels as well as less frequent cytoplasmic accumulation two days following caerulein treatment compared to cells in similarly treated *Pdx1-Cre^{Early}* control mice (Figure 3F). Western blot for ß-catenin protein confirmed these immunostaining results (Figure 3I, quantification of Western blot results shown in Figure 3J). In metaplastic ducts seven days following treatment, overall ß-catenin accumulation was still weaker than that observed during the regenerative phase in *Pdx1-Cre^{Early}* mice (Figure 3G). Only after 3 weeks did ß-catenin frequently accumulate in the cytoplasm of PanIN lesions (Figure 3H).

Quantitative PCR analysis of the canonical Wnt signaling/ß-catenin target genes *Axin2* and *Lef1* revealed a pattern of ß-catenin transcriptional activation corresponding with the observed pattern of ß-catenin accumulation. In *Pdx1-Cre^{Early}* mice, expression of both genes increased two days following caerulein treatment and returned to PBS treated levels by 21 days (Figure 3K, L). We detected no increase in *Axin2* and *Lef1* expression during ADM 2 and 7 days following caerulein treatment of *Pdx1-Cre^{Early}; LSL-Kras^{G12D}*, while both genes were significantly up-regulated when PanINs predominated after 21 days (Figure 3K, L). Therefore, a distinction between transiently de-differentiated, regenerating wild type acini and acini possessing mutant Kras undergoing the initial stages of ductal reprogramming is the inability of the latter to normally

reactivate Wnt/ß-catenin signaling. We also tested if previously reported regeneration associated accumulation of E-cadherin (14, 31), which binds to ß-catenin at adherens junctions, was similarly inhibited during Kras induced ADM. We observed accumulation of E-cadherin two days after caerulein treatment in both *Pdx1-Cre*^{Early} and *Pdx1-Cre*^{Early}*; LSL-Kras*^{G12D} mice, (Supplemental Figure 5B, F), suggesting that Kras induced ADM is not associated with a gross decrease in E-cadherin accumulation.

ß-catenin is required for efficient acinar cell regeneration

Next we tested if ß-catenin inhibition is an important component of Kras driven ADM and PanIN formation. First, we asked whether ß-catenin plays a functional role in acinar regeneration. To address this question, we set out to subject acinar cells lacking ß-catenin to caerulein pancreatitis and gauge their regenerative ability. ß-catenin is required for acinar development (28-30), but not adult acinar cell viability or differentiation (28) as shown by conditional inactivation of a Cre-dependent, floxed ß-catenin allele (*ß-catenin*^{F}). We have previously demonstrated that Cre recombinase driven by the *Ptf1a* (*p48*) promoter induces recombination in both acini and a subset of ductal progenitors (32). Although its expression occurs during the early stages of pancreas development, we have found that using it to conditionally manipulate the ß-catenin pathway avoids developmental phenotypes induced by earlier acting Cre drivers, such as the *Pdx1-Cre*^{Early} strain (22). We generated *p48-Cre; ß-catenin*$^{F/F}$ mice, which were viable and born at the expected Mendelian ratio, and

tested if they possessed ß-catenin negative acinar cells at 6 weeks of age. Similar to previous results investigating β-catenin deletion during pancreas development, the number of acinar cells was severely reduced in *p48-Cre; ß-catenin$^{F/F}$* mice (representing ~35% of the area of controls, Figure 4M) and pancreata displayed accumulation of fat (Figure 4D). However, the remaining pancreas was composed of ß-catenin-null, amylase-positive acinar cells (Figure 4J) along with a mixture of β-catenin negative and positive ducts and islets. Therefore, although p48 positive acinar progenitors develop far less efficiently without ß-catenin than wildtype counterparts, *p48Cre; ß-catenin$^{flox/flox}$* mice were tractable for testing the ability of ß-catenin null acinar cells to regenerate.

Next, we compared acinar regeneration following caerulein pancreatitis in control *p48-Cre; ß-catenin$^{F/+}$* and *p48-Cre; ß-catenin$^{F/F}$* mice. We induced pancreatitis using the method of Jensen and colleagues (14) in which mice are subjected to consecutive days of caerulein treatment. We employed this particular regimen as it has been frequently used to test genetic modifiers of acinar regeneration. Previous studies have shown that in response to this caerulein protocol, acinar cells both assume a duct like morphology (16) and reactivate similar embryonic signaling factors (14, 15) to those we observed in mice treated with the staggered caerulein regimen that we used in our ADM/PanIN studies (See Figure 1, 2). Therefore, similar regenerative pathways are likely induced by both caerulein techniques. As expected, three days after caerulein treatment, *p48-Cre; ß-catenin$^{F/+}$* control mice displayed a significant decrease in acinar area,

approximately 50-60% of PBS treated control (Figure 4M), possessed regenerating acini, including duct-like cells (Figure 4B), and displayed increased ß-catenin accumulation compared to acini in PBS treated mice (compare Figure 4G, H). By five days following treatment, acinar regeneration in *p48-Cre; ß-catenin$^{F/+}$* mice had significantly progressed, as nearly 75% of acinar area was re-established (Figure 4M). In contrast, at both three and five days following caerulein, *p48-Cre; ß-catenin$^{F/F}$* mutant mice displayed a persistent decrease in ß-catenin-negative, amylase-positive cells. Quantitative analysis revealed a reduction of greater than 90% of acinar area when compared to PBS treated *p48-Cre; ß-catenin$^{F/+}$* mice and ~10 fold reduction (Figure 4M) when compared to PBS treated *p48-Cre; ß-catenin$^{F/F}$* mice (Figure 4E, K and F, L, respectively). The remaining epithelium consisted predominately of both ß-catenin-negative and CK19 positive duct cells as well as ß-catenin-negative and positive endocrine cells remaining in morphologically distinct islet clusters (Figure 4K, L and insets). This data suggests that ß-catenin deficient acinar cells regenerate far less efficiently than wildtype acini and supports a role for ß-catenin as a key node in acinar regeneration.

Stabilized ß-catenin signaling antagonizes Kras driven ADM/PanIN

Since ß-catenin is important in acinar regeneration and a block in its reactivation correlates with Kras induced ductal reprogramming we asked next whether increased ß-catenin signaling could antagonize the ability of Kras to reprogram

acini into ADM/PanIN. To answer this question, we used a gain of function strategy to enforce ß-catenin signaling in acini possessing mutant Kras.

To induce stabilized ß-catenin in acini co-expressing mutant Kras we utilized a Cre induced conditional transgenic allele of ß-catenin that lacks exon 3 (*ß-catenin^{exon3}*), a region required for proteosomal turnover (33), in combination with the *LSL-Kras^{G12D}* allele. We have previously shown that one copy of this allele increases ß-catenin signaling in pancreatic epithelium (22, 32). We analyzed the effect of simultaneous Kras and ß-catenin activation on ductal reprogramming in mice in which both pathways were activated in the developing exocrine compartment and specifically in adult acini. For studies of embryonic activation we again used the *p48-Cre* driver to activate the conditional ß-catenin allele rather than the *Pdx1-Cre^{Early}* allele employed earlier in this study to avoid previously reported developmental defects and perinatal lethality (22).

First, we compared pancreata of PBS injected, six week old *p48-Cre; LSL-Kras^{G12D}* and compound *p48-Cre; ß-catenin$^{exon3/+}$; LSL-Kras^{G12D}* mice. As expected, *p48-Cre; LSL-Kras^{G12D}* pancreas displayed morphologically normal acinar cells with few PanIN lesions (Supplemental Figure 6A). *p48-Cre; ß-catenin$^{exon3/+}$; LSL-Kras^{G12D}* mice presented with a mixture of abnormal duct cells and amylase positive cells with acinar morphology, representing ~25% of the acinar area of *p48-Cre; LSL-Kras^{G12D}* animals (Figure 5 A, B, M). Strikingly, PanIN lesions were not observed under these conditions. Therefore, even at this

early time point and in the absence of a damaging insult that accelerates Kras induced PanIN formation, the propensity of mutant Kras to drive PanIN development is inhibited by stabilized ß-catenin. In support of this notion, we have previously shown that *p48-Cre; ß-catenin$^{exon3/+}$; LSL-Kras^{G12D}* mice develop tumors resembling human intraductal tubular tumors (ITT) as they age but show evidence of neither PanIN lesions nor PDA (32).

Next, we compared acinar replacement in *p48-Cre; LSL-Kras^{G12D}* and compound *p48-Cre; ß-catenin$^{exon3/+}$; LSL-Kras^{G12D}* mice seven days following caerulein treatment. As expected, caerulein treatment in *p48-Cre; LSL-Kras^{G12D}* mice resulted in a significant replacement of acinar cells with metaplastic ducts, leading to a decrease of amylase area to less than 10% of PBS treated mice (Figure 5F, M). As observed in *Pdx1-Cre^{Early}; LSL-Kras^{G12D}* mice, metaplastic ducts (Figure 5E) strongly expressed embryonic factors (Sox9, Figure 5G, Clusterin 5H, Hes1 Supplemental Figure 7A) and displayed phospho-ERK1/2 labeling (Supplemental Figure 7B). In stark contrast, cells with acinar morphology were maintained with a similar distribution seven days following caerulein treatment in *p48-Cre; ß-catenin$^{exon3/+}$; LSL-Kras^{G12D}* animals as compared to mice treated with PBS (Figure 5J, M). Even two days after treatment, at the height of caerulein induced de-differentiation, the distribution of acini and ductal cells in *p48-Cre; ß-catenin$^{exon3/+}$; LSL- Kras^{G12D}* mice was similar to that observed in PBS treated mice (Supplemental Figure 6G, H). Furthermore, Sox9 (Figure 5K), Clusterin (Figure 5L), Hes1 (Supplemental Figure 7E), and

phospho-ERK1/2 (Supplemental Figure 7F), were rarely present in cells with acinar morphology in *p48-Cre; ß-catenin$^{exon3/+}$; LSL-Kras^{G12D}* mice (Figure 5K, L) regardless of caerulein treatment. Immunoflouresence for ß-catenin displayed widespread accumulation in all epithelial cell types in *p48-Cre; ß-catenin$^{exon3/+}$; LSL-Kras^{G12D}* pancreas compared to *p48-Cre; LSL-Kras^{G12D}* mice, confirming transgenic ß-Catenin stabilization (Compare Supplemental Figure 7D, H). ß-catenin activation was also confirmed by quantitative PCR for target genes *Axin2* and *Lef1*, which displayed significant increase in *p48-Cre*; *ß-catenin$^{exon3/+}$; LSL-Kras^{G12D}* versus *p48-Cre; LSL-Kras^{G12D}* pancreas (data not shown). Taken together, this data suggests that when activated simultaneously during pancreatic development, ß-catenin signaling antagonizes the normal course of Kras induced acinar reprogramming.

We have previously established that *p48-Cre*; *ß-catenin$^{exon3/+}$; LSL-Kras^{G12D}* mice do not develop PanIN lesions (32). However, in this model Cre activation is not limited to acini and mice develop significant abnormalities, including fibrosis, that may exert non-cell autonomous effects on acinar reprogramming. Therefore, to more rigorously interrogate the ability of ß-catenin signaling to antagonize Kras induced ADM/PanIN originating from adult acini we compared tamoxifen stimulated, caerulein treated *Elastase-Cre^{ERT2}*; *LSL-Kras^{G12D}* and *Elastase-Cre^{ERT2}; β-catenin$^{exon3/+}$; LSL-Kras^{G12D}* mice two and three weeks following pancreatitis. Unlike *p48-Cre*; *ß-catenin$^{exon3/+}$; LSL-Kras^{G12D}* mice, tamoxifen stimulated *Elastase-Cre^{ERT2}; β-catenin$^{exon3/+}$; LSL-Kras^{G12D}* animals showed no

gross structural defects when treated either with PBS or with caerulein (Figure 6A). Furthermore, cellular defects, in the form of abnormal ductal structures, were rare in PBS treated *Elastase-Cre^{ERT2}; β-catenin$^{exon3/+}$; LSL-Kras^{G12D};* mice (such ducts were observed in one of seven mice, four to five weeks after tamoxifen treatment). This frequency matched that of spontaneous PanINs observed in similarly treated *Elastase-Cre^{ERT2}; LSL-Kras^{G12D}* mice (Figure 1 and Supplemental Figure 1). Therefore, without caerulein treatment, the effects of activating Kras alone or both Kras and β-catenin simultaneously were minimal, presenting an opportunity to determine the ability of stabilized β-catenin signaling to affect Kras induced ADM/PanIN in the absence of pre-existing structural defects.

Two and three weeks following caerulein treatment, all *Elastase-Cre^{ERT2}*; *LSL-Kras^{G12D}* mice tested (n=4, n=3) displayed frequent CK19, Alcian Blue positive PanINs (Figure 6E, F). However, PanIN formation was blocked in *Elastase-Cre^{ERT2}; β-catenin$^{exon3/+}$; LSL-Kras^{G12D}* mice as we observed no structures that morphologically resembled PanINs at either time point (n=4, n=3). While we did observe CK19 positive abnormal duct structures in all caerulein treated *Elastase-Cre^{ERT2}; β-catenin$^{exon3/+}$; LSL-Kras^{G12D}* mice, cells comprising the ducts maintained a cuboidal rather than columnar morphology and generally possessed weak CK19 expression (Figure 6I,J). Furthermore, in contrast to PanINs observed in *Elastase-Cre^{ERT2}*; *LSL-Kras^{G12D}* mice, Alcian Blue staining was exceedingly infrequent in these structures (two of seven mice possessed

one to two structures that displayed patchy or weakly Alcian Blue positive cells) (Figure 6J, and data not shown). Interestingly, we found that distinct patterns of ß-catenin accumulation correlated with the development of PanINs or abnormal duct structures. PanINs in *Elastase-Cre*^{ERT2}; *LSL-Kras*^{G12D} mice possessed strong membranous and cytoplasmic ß-catenin accumulation, while ß-catenin was frequently localized to the nucleus in the abnormal ducts observed in *Elastase-Cre*^{ERT2}*; β-catenin*$^{exon3/+}$*; LSL-Kras*^{G12D} mice (Compare Figure 6G, K). However, both structures displayed phospho-ERK1/2 staining (Figure 6H, L). Therefore, while a Kras effector pathway is active in both cell types, abnormal ducts in *ElaCre*^{ERT2}*; LSL-Kras*^{G12D}*; β-catenin*$^{exon3/+}$ mice are likely subjected to a higher level of ß-catenin signaling than cells comprising PanINs. Taken together, this data suggests that while uncontrolled ß-catenin and Kras signaling can change acinar fate, levels of ß-catenin signaling that exceed a critical threshold block the ability of Kras to reprogram acini into a ductal PanIN lineage.

Discussion

Regeneration is a key process in maintaining tissue homeostasis. Interestingly, regenerative processes often involve reactivation of developmental signaling pathways that may contribute to tumorigenesis when aberrantly active in adult tissue. This balance between regeneration and neoplasia appears to be pertinent in the pancreas as both acute pancreatitis, an insult that produces a regenerative response in pancreatic acini (14, 15, 16), and chronic pancreatitis accelerate Kras driven ADM/PanIN and PDA in mice (11, 5, respectively). These studies support clinical observations suggesting a link between chronic pancreatitis and PDA in humans (12, 13). However, how Kras co-opts the permissive environment provided by pancreatitis to initiate reprogramming of acini into ductal PanINs is unclear. Here, we show that one route by which Kras drives ADM and PanIN formation is by subverting acinar regeneration. Our results demonstrate that acini possessing an activating mutation in Kras are biologically distinct from normal acini. As schematized in figure 2Q, while possessing normal morphology and expressing markers of acinar differentiation, acinar cells carrying constitutively active Kras cannot activate a wild type regenerative program. Instead these cells undergo ductal reprogramming when damaged, a state characterized by persistent, rather than transient, progenitor factor expression, permissive for the development of PanINs that are molecularly similar to spontaneous lesions. As progenitor factor expression is maintained from the outset of ADM/PanIN following damage, our data suggests that de-

differentiation may be a key rate-limiting step in initiating Kras transformation of acini into PanIN precursors.

While mutant Kras is sufficient to reprogram acini into ductal PanINs, this process occurs gradually and stochastically. Both tissue damage (i.e. pancreatitis (this study, 5, 11), inflammation induced by metabolic stress (34), and additional oncogene activation such as activated Gli (35), Notch (3), and Tgf-α signaling (36) significantly accelerate ADM/PanIN. Therefore, expression of mutant Kras is not optimally efficient to reprogram acini into PanINs without additional molecular events. During Kras induced ADM/PanIN following damage we find not only persistent activation of regeneration associated embryonic signaling factors, but that the activity of the MAPK Kras effector pathway is widely and persistently maintained. This is in contrast to morphologically normal acini in age matched, control treated mice where MAPK activity is infrequently observed. These data suggest that this de-differentiated state is not only plastic for ADM and PanIN formation but may permit increased signaling output by Kras effectors. Recently, Ji and colleagues (37) reported a relationship between increasing levels of acinar Kras activity and the development of chronic pancreatitis or ADM/PanIN with the capacity to give rise to PDA. Interestingly, Duan and colleagues (38) have shown that cholecystikinin, which caerulein mimics functionally, can increase Ras activity. Therefore, although we did not directly assay Kras activity levels in our studies, caerulein treatment itself may be involved in breaching a threshold of Ras activity critical to initiating ADM/PanIN.

Even so, the question remains if de-differentiation is a consequence of Kras activity, or whether it is required for Kras activation to occur. Combining the ability to titrate Kras activity in acini with genetic techniques that target the reactivated embryonic signaling pathways observed during ADM/PanIN may make an epistatic relationship between differentiation and Kras signaling more clear. Another critical future direction is to determine what molecular roadblocks prevent Kras from becoming fully active in unstressed acini and how they are subverted under conditions of damage or spontaneously to allow ADM/PanIN. Identification of such factors might supply diagnostic or therapeutic targets that are aimed at the specification of PDA precursors.

The accelerated and synchronous ADM induced in response to acute pancreatic damage in our models of embryonic Kras activation allowed us to isolate β-catenin as an essential player in acinar regeneration and Kras mediated reprogramming of PDA precursors. β-catenin is critical for acinar development (28-30) but does not seem to be required for the viability of unstressed adult acini (28). We find that β-catenin is essential for acinar regeneration. β-catenin has significant effects on both gene expression and on cell to cell adhesion as a part of complexes at the membrane. Since target genes are upregulated during acinar regeneration, our data suggest that β-catenin dependent transcription may be involved in establishing a regenerative program. Further experiments detailing how specific β-catenin target genes direct regeneration and if β-catenin

dependent adhesion is critical to the process are key to better understanding this aspect of acinar plasticity.

Since β-catenin is key for acinar development, we expected it to share the expression pattern of other reactivated embryonic factors and remain persistently reactivated during Kras induced ADM. Surprisingly, we found that while β-catenin signaling was activated during normal acinar regeneration, such transient activation was not observed during early stages of Kras induced ADM/PanIN. Instead, we found that β-catenin signaling did not increase until PanIN lesions began to predominate in the pancreatic epithelium. Our gain of function studies suggest that this balance between active Kras signaling and low levels of β-catenin signaling is key to specifying a duct-like lineage capable of forming PanINs. In response to damage, acini expressing mutant Kras and stabilized β-catenin throughout development do not undergo ADM as readily as acini expressing mutant Kras alone. Cells maintaining acinar morphology rarely express the reactivated elements of embryonic development or phospho-MAPK as seen persistently in acini undergoing Kras induced ADM/PanIN. Also, stabilized β-catenin signaling prevents Kras induced reprogramming of adult acini into PanIN lesions. Therefore, high levels of β-catenin signaling are incompatible with the molecular environment permissive for Kras to specify a ductal lineage with the capacity to develop into PDA. Interestingly, this interaction may be similar to the antagonism of *β*-catenin target genes by Hras signaling that is observed in the zonation of periportal verus pericentral hepatocytes in the liver

(39, 40), although the mechanism of inhibition in this context is unclear. Understanding how β-catenin levels and signaling is controlled during the initiation of ADM/PanIN, if Kras directly inhibits β-catenin, and which β-catenin targets must be blocked for Kras to take advantage of an otherwise permissive differentiation state also may merit new insight into the development of PDA precursors as well as an important developmental signaling interaction.

Our findings elucidate seemingly contradictory data regarding Kras and *β*-catenin signaling in PDA initiation and maintenance. It is well established that ß-catenin and Kras signaling synergize to drive tumorigenesis in other organs, including the colon and prostate (41, 42). Our group has previously shown that while Kras and *β*-catenin do ultimately synergize to induce tumor formation in aged *p48-Cre; ß-catenin*$^{exon3/+}$*; LSL-Kras*^{G12D} mice, the ITT-like disease caused by simultaneous Kras activation and ß-catenin stabilization throughout acinar cell development is molecularly and morphologically distinct from the Kras induced PanIN-PDA sequelae (32). These results suggest that PDA cannot form in the context of simultaneous, constitutive activation of Kras and ß-catenin signaling. However, *β*-catenin signaling is elevated in human PDA and in PanINs and PDA of Kras-driven mouse models (43, 44). Indeed, our results support this notion since we observed Wnt-target gene upregulation in Kras mice 21 days after caerulein treatment, a time point in which PanIN formation is widespread. Furthermore, ß-catenin knockdown in human PDA cell lines possessing activating Kras mutations compromises cell growth (43). Our study presents a

possible explanation for the temporal dissonance in the relationship between Kras and β-catenin in PDA. As schematized in Figure 7, we propose that β-catenin signaling is a gatekeeper for Kras induced reprogramming of acini and must be kept below a critical threshold in order for Kras to drive cells into forming a metaplastic lineage with the potential to develop into PanIN/PDA. Once this state is achieved, cells fated for PDA can evolve a requirement for β-catenin signaling, possibly through stimulating effects supplied by other signaling pathways, including Hedgehog/Gli signaling (43).

Recently, concomitant activation of Notch and Kras in adult acinar cells has been shown to greatly accelerate ADM/PanIN formation (3). Notch signaling plays critical roles in pancreatic development (45), and must be inactivated in pancreatic progenitors in order to permit differentiation of exocrine and endocrine cells (46). We show that the Notch target gene Hes1, normally reactivated transiently during acinar regeneration, is persistently up-regulated during ADM/PanIN formation. Siveke and colleagues have shown that Notch signaling is not only important in exocrine regeneration but that Notch also inhibits ß-catenin in acinar cells (15). Taken together, this may suggest that persistently active Notch signaling may be part of the mechanism preventing ß-catenin re-activation during Kras reprogramming of acini into the PanIN lineage.

In conclusion, this study shows that acinar regeneration provides a permissive environment for Kras to induce early events in PDA initiation, promoting

ADM/PanIN. Reactivation of ß-catenin signaling, required for efficient acinar regeneration, is blocked during Kras induced ductal reprogramming and unless a critical level of ß-catenin activity is maintained, Kras induced acinar to ductal reprogramming into a PanIN lineage is inhibited. Therefore our study underlines the likelihood that not only must mutations be acquired in a specific sequence in order to develop PDA, but levels of developmental signaling pathways must be tightly regulated to alter normal cellular plasticity and drive neoplastic cell fates.

Methods:

Mouse lines:

Experimental animals were generated by crossing *Pdx-Cre^{Early}* (gift of Doug Melton, Harvard University, Cambridge, MA, USA); *Pdx-Cre^{Late}* (gift of Pedro Herrera, University of Geneva Medical School, Geneva, Switzerland); *p48-Cre* mice (gift of Chris Wright, Vanderbilt University, Nashville, TN, USA); or *Elastase-Cre^{ERT2}* (gift of Doris Stoffers, University of Pennsylvania, Pennsylvania, USA) with *LSL-Kras^{G12D}* (gift of Dave Tuveson, Cancer Research UK Cambridge Research Institute, Cambridge, UK), *β-catenin$^{F/F}$* (47), and/or *β-catenin$^{exon3/exon3}$* (gift of Mark Taketo, Kyoto University School of Medicine, Kyoto, Japan) and R26R-EYFP (24). All mouse experiments were performed under the approval of the UCSF Institutional Care and Use of Animals Committee (IACUC). Littermate heterozygote conditional or Cre only animals were used as controls.

Tamoxifen treatment

Cre activity in *Elastase-Cre^{ERT2}*; *R26R-EYFP, Elastase-Cre^{ERT2}*; *LSL-Kras^{G12D}; R26R-EYFP, Elastase-Cre^{ERT2}*; *LSL-Kras^{G12D}* and *Elastase-Cre^{ERT2}; β-catenin$^{exon3/+}$; LSL-Kras^{G12D}* mice was induced in 4 week old mice by 5 consecutive daily treatments of 1mg of tamoxifen (Sigma) dissolved in corn oil (to a concentration of 10mg/ml, Sigma).

Caerulein treatment

Acute pancreatitis was induced at 6 weeks of age in *Pdx1-Cre^{Early}; LSL-Kras^{G12D}*, *Pdx1-Cre^{Late}; LSL-Kras^{G12D}*, *p48-Cre; LSL-Kras^{G12D}*, *p48-Cre; β-catenin^{exon3}*, *p48-Cre; LSL-Kras^{G12D}; β-catenin$^{exon3l+}$,* and tamoxifen induced *Elastase-Cre^{ERT2}*; *R26R-EYFP, Elastase-Cre^{ERT2}*; *LSL-Kras^{G12D}; R26R-EYFP, Elastase-Cre^{ERT2}*; *LSL-Kras^{G12D} and Elastase-Cre^{ERT2}; β-catenin$^{exon3/+}$; LSL-Kras^{G12D}* mice by 2 sets of 6 hourly i.p. caerulein injections (Sigma, 50μg/kg) on alternating days separated by 24 hours (48). This protocol is referred to as the 'staggered' protocol in the text. For the regeneration study in *p48-Cre; β-catenin^{F}* mice, pancreatitis was induced as described by Jensen and colleagues(14) by 8 hourly caerulein injections (2ug/injection) on two consecutive days. This protocol is referred to as the 'consecutive' protocol in the text. Mouse weight ranged from 22-25 grams. For both protocols, the final day of caerulein injection was considered day 0.

Immunohistochemistry and Immunofluorescence

Pancreata were fixed overnight in zinc-containing neutral-buffered formalin (Anatech LTD), embedded in paraffin, cut into 5-μm-thick sections, and placed on Superfrost Plus slides (Fisher Scientific). Sections were subjected to hematoxylin and eosin (H&E), immunohistochemical, and immunofluorescent staining as described (22, 35). The following primary antibodies were used: rabbit anti-amylase (1:300; Sigma), rat anti-CK19 (TROMAIII, 1:200 dilution; developed by Dr. Rolf Kemler [Max-Planck Institute of Immunobiology, Freiburg, Germany] and

obtained from the Hybridoma Bank at the University of Iowa), guinea pig anti-Pdx1 (1:1000; generous gift from Michael German, University of California, San Francisco), rabbit anti-Hes1 (1:500 dilution; generous gift from Dr. Tetsuo Sudo, Toray Industries, Inc., Kamakura, Japan), goat anti-clusterin (1:200; Santa Cruz), rabbit anti-Sox9 (1:1000; Chemicon), mouse anti-β-catenin (1:200; Becton and Dickinson), chicken anti-GFP (1:200; Abcam), and anti phospho-p42/p44 (1:200; Cell Signaling Technologies). For immunohistochemistry, biotinylated anti-rabbit (Vector Laboratories), and anti-goat and anti-rat (Jackson Immunoresearch) antibodies were used as secondary antibodies at a 1:200 dilution. 3-3′-Diaminobenzidine tetrahydrochloride (Vector Labs) was used as a chromogen. Bright-field images were acquired using a Zeiss Axio Imager D1 scope. For immunofluorescence, Alexafluor donkey anti goat 555, donkey anti rabbit 488, goat anti-chicken 488, goat anti mouse 633, goat anti-rabbit 488, goat anti rat 633, and goat anti-rat 555 (Invitrogen Molecular Probes) were used as secondary antibodies at a 1:200 dilution. Confocal images were collected on a Leica SP2 microscope at consistent gain and offset settings.

Western Blotting

Immunoblotting was performed by homogenizing tissue samples in RIPA buffer, electrophoresing on 10% SDS-PAGE Gels, incubating with primary antibodies overnight at 4°C, and detecting primary antibodies using HRP-conjugated secondary antibodies (Santa Cruz, 1:5000 dilution) and ECL (Amersham Biosciences) as described (35). The primary antibodies used were anti mouse β-

catenin (1:1000;Becton and Dickinson and anti-rabbit GAPDH (1:1000, Santa Cruz). Western blots were quantified by calculating an integrated density value (IDV) for each band using ADOBE Photoshop CS2 and normalizing to the IDV of GAPDH.

Evaluation of amylase area

To calculate relative amylase area in the *p48-Cre; β-catenin$^{F/F}$* regeneration experiment, six random, non-overlapping, 400x fluorescent images, separated by a depth of 100uM were collected from 3 mice per condition. For each image, ADOBE Photoshop CS2 was used to calculate positive amylase pixel number, which was normalized to number of DAPI positive nuclei (scored by the "analyze particle" in NIH ImageJ). To quantify relative amylase area in the *p48-Cre; LSL-Kras^{G12D}; β-catenin$^{3/+}$* acinar replacement experiment, eight random, non-overlapping, 100x IHC images, 2 each at consecutive tissue level, separated by a depth of 100uM were collected from 3 mice per condition. For each image, ADOBE Photoshop CS2 was used to calculate positive amylase pixel number, which was normalized to pancreas tissue area.

Quantitative PCR

Pancreas tissue was preserved in RNALater (Ambion) overnight at 4°C and stored at -80°C. Total RNA was extracted by tissue dissociation in TRIZOL reagent (Invitrogen) and purification of chloroform extracted aqueous phase using RNAeasy columns (Qiagen). On column DNAse treatment was performed

according to manufacturer's instructions. RNA quality was audited using and Agilent Bioanalyzer and RNA Nano Chip Kit (Agilent Technologies). cDNA was synthesized from 1ug of total RNA using Superscript II Reverse Transcriptase (Invitrogen). Taqman QPCR was performed using inventoried probes for mouse *Axin2* (Mm01265783_m1, Applied Biosystems) and *Lef1* (Mm00550265_m1, Applied Biosystems). Expression levels were normalized using a custom primer/probe set for *Gapdh* (generously provided by the Genome Analysis Core at the UCSF Helen Diller Family Comprehensive Cancer Center, sequences listed in Supplemental Table 1).

Statistical methods:

Comparison of means was performed using unpaired T-Tests, calculated using Prism for Macintosh version 4. Statistical significance was assumed when $P<0.05$, P-values below 0.05 are noted in figure legends. Results are represented as mean ± SD or SEM where noted. All mouse tissue data represents at least 3 mice unless otherwise noted and represents at least 10 5μM sections unless noted.

Acknowledgements:

The authors would like to thank Renee VanderLaan and Limor Landsman for critical reading of the manuscript and Cecilia Austin for histology assistance. Also, we thank the following for providing us with the indicated mouse lines: Douglas Melton—*Pdx1-Cre*^{Early}, Pedro Herrera--*Pdx-Cre* ^{Late}, Chris Wright--*p48-Cre*, Doris Stoffers--*Elastase-Cre*^{ERT2}, Dave Tuveson--*LSL-Kras*^{G12D}, and Mark Taketo--*ß-catenin*^{exon3}. Work in M.H.'s laboratory is supported by a grant from the Pancreatic Cancer Action Network (PanCAN) and the NIH (CA112537). S. W. is supported by the National Institutes of Health under Ruth L. Kirschstein National Research Service Award F32 from the National Cancer Institute and the American College of Surgeons Resident Research Scholarship. Imaging experiments were supported by resources from the UCSF Diabetes and Endocrinology Research Center (DERC).

References

1. Jemal, A., Siegel, R., Ward, E., Hao, Y., Xu, J., Murray, T., and Thun, M.J. 2008. Cancer statistics, 2008. *CA Cancer J Clin* 58:71-96.
2. Feldmann, G., Beaty, R., Hruban, R.H., and Maitra, A. 2007. Molecular genetics of pancreatic intraepithelial neoplasia. *J Hepatobiliary Pancreat Surg* 14:224-232.
3. De La, O.J., Emerson, L.L., Goodman, J.L., Froebe, S.C., Illum, B.E., Curtis, A.B., and Murtaugh, L.C. 2008. Notch and Kras reprogram pancreatic acinar cells to ductal intraepithelial neoplasia. *Proc Natl Acad Sci U S A* 105:18907-18912.
4. Habbe, N., Shi, G., Meguid, R.A., Fendrich, V., Esni, F., Chen, H., Feldmann, G., Stoffers, D.A., Konieczny, S.F., Leach, S.D., et al. 2008. Spontaneous induction of murine pancreatic intraepithelial neoplasia (mPanIN) by acinar cell targeting of oncogenic Kras in adult mice. *Proc Natl Acad Sci U S A* 105:18913-18918.
5. Guerra, C., Schuhmacher, A.J., Canamero, M., Grippo, P.J., Verdaguer, L., Perez-Gallego, L., Dubus, P., Sandgren, E.P., and Barbacid, M. 2007. Chronic pancreatitis is essential for induction of pancreatic ductal adenocarcinoma by K-Ras oncogenes in adult mice. *Cancer Cell* 11:291-302.
6. Zhu, L., Shi, G., Schmidt, C.M., Hruban, R.H., and Konieczny, S.F. 2007. Acinar cells contribute to the molecular heterogeneity of pancreatic intraepithelial neoplasia. *Am J Pathol* 171:263-273.
7. Shi, G., Zhu, L., Sun, Y., Bettencourt, R., Damsz, B., Hruban, R.H., and Konieczny, S.F. 2009. Loss of the acinar-restricted transcription factor Mist1 accelerates Kras-induced pancreatic intraepithelial neoplasia. *Gastroenterology* 136:1368-1378.
8. Almoguera, C., Shibata, D., Forrester, K., Martin, J., Arnheim, N., and Perucho, M. 1988. Most human carcinomas of the exocrine pancreas contain mutant c-K-ras genes. *Cell* 53:549-554.
9. Hingorani, S.R., Petricoin, E.F., Maitra, A., Rajapakse, V., King, C., Jacobetz, M.A., Ross, S., Conrads, T.P., Veenstra, T.D., Hitt, B.A., et al. 2003. Preinvasive and invasive ductal pancreatic cancer and its early detection in the mouse. *Cancer Cell* 4:437-450.
10. Hingorani, S.R., Wang, L., Multani, A.S., Combs, C., Deramaudt, T.B., Hruban, R.H., Rustgi, A.K., Chang, S., and Tuveson, D.A. 2005. Trp53R172H and KrasG12D cooperate to promote chromosomal instability and widely metastatic pancreatic ductal adenocarcinoma in mice. *Cancer Cell* 7:469-483.
11. Carriere, C., Young, A.L., Gunn, J.R., Longnecker, D.S., and Korc, M. 2009. Acute pancreatitis markedly accelerates pancreatic cancer progression in mice expressing oncogenic Kras. *Biochem Biophys Res Commun* 382:561-565.
12. Lowenfels, A.B., Maisonneuve, P., Cavallini, G., Ammann, R.W., Lankisch, P.G., Andersen, J.R., Dimagno, E.P., Andren-Sandberg, A., and

Domellof, L. 1993. Pancreatitis and the risk of pancreatic cancer. International Pancreatitis Study Group. *N Engl J Med* 328:1433-1437.

13. Malka, D., Hammel, P., Maire, F., Rufat, P., Madeira, I., Pessione, F., Levy, P., and Ruszniewski, P. 2002. Risk of pancreatic adenocarcinoma in chronic pancreatitis. *Gut* 51:849-852.
14. Jensen, J.N., Cameron, E., Garay, M.V., Starkey, T.W., Gianani, R., and Jensen, J. 2005. Recapitulation of elements of embryonic development in adult mouse pancreatic regeneration. *Gastroenterology* 128:728-741.
15. Siveke, J.T., Lubeseder-Martellato, C., Lee, M., Mazur, P.K., Nakhai, H., Radtke, F., and Schmid, R.M. 2008. Notch signaling is required for exocrine regeneration after acute pancreatitis. *Gastroenterology* 134:544-555.
16. Fendrich, V., Esni, F., Garay, M.V., Feldmann, G., Habbe, N., Jensen, J.N., Dor, Y., Stoffers, D., Jensen, J., Leach, S.D., et al. 2008. Hedgehog Signaling Is Required for Effective Regeneration of Exocrine Pancreas. *Gastroenterology* 135:621-631.
17. Strobel, O., Dor, Y., Alsina, J., Stirman, A., Lauwers, G., Trainor, A., Castillo, C.F., Warshaw, A.L., and Thayer, S.P. 2007. In vivo lineage tracing defines the role of acinar-to-ductal transdifferentiation in inflammatory ductal metaplasia. *Gastroenterology* 133:1999-2009.
18. Means, A.L., Meszoely, I.M., Suzuki, K., Miyamoto, Y., Rustgi, A.K., Coffey, R.J., Jr., Wright, C.V., Stoffers, D.A., and Leach, S.D. 2005. Pancreatic epithelial plasticity mediated by acinar cell transdifferentiation and generation of nestin-positive intermediates. *Development* 132:3767-3776.
19. Sawey, E.T., Johnson, J.A., and Crawford, H.C. 2007. Matrix metalloproteinase 7 controls pancreatic acinar cell transdifferentiation by activating the Notch signaling pathway. *Proc Natl Acad Sci U S A* 104:19327-19332.
20. Miyamoto, Y., Maitra, A., Ghosh, B., Zechner, U., Argani, P., Iacobuzio-Donahue, C.A., Sriuranpong, V., Iso, T., Meszoely, I.M., Wolfe, M.S., et al. 2003. Notch mediates TGF alpha-induced changes in epithelial differentiation during pancreatic tumorigenesis. *Cancer Cell* 3:565-576.
21. Miyatsuka, T., Kaneto, H., Shiraiwa, T., Matsuoka, T.A., Yamamoto, K., Kato, K., Nakamura, Y., Akira, S., Takeda, K., Kajimoto, Y., et al. 2006. Persistent expression of PDX-1 in the pancreas causes acinar-to-ductal metaplasia through Stat3 activation. *Genes Dev* 20:1435-1440.
22. Heiser, P.W., Lau, J., Taketo, M.M., Herrera, P.L., and Hebrok, M. 2006. Stabilization of beta-catenin impacts pancreas growth. *Development* 133:2023-2032.
23. Desai, B.M., Oliver-Krasinski, J., De Leon, D.D., Farzad, C., Hong, N., Leach, S.D., and Stoffers, D.A. 2007. Preexisting pancreatic acinar cells contribute to acinar cell, but not islet beta cell, regeneration. *J Clin Invest* 117:971-977.

24. Srinivas, S., Watanabe, T., Lin, C.S., William, C.M., Tanabe, Y., Jessell, T.M., and Costantini, F. 2001. Cre reporter strains produced by targeted insertion of EYFP and ECFP into the ROSA26 locus. *BMC Dev Biol* 1:4.
25. Tokoro, T., Tezel, E., Nagasaka, T., Kaneko, T., and Nakao, A. 2003. Differentiation of acinar cells into acinoductular cells in regenerating rat pancreas. *Pancreatology* 3:487-496.
26. Yoshida, T., Shiraki, N., Baba, H., Goto, M., Fujiwara, S., Kume, K., and Kume, S. 2008. Expression patterns of epiplakin1 in pancreas, pancreatic cancer and regenerating pancreas. *Genes Cells* 13:667-678.
27. Stoick-Cooper, C.L., Moon, R.T., and Weidinger, G. 2007. Advances in signaling in vertebrate regeneration as a prelude to regenerative medicine. *Genes Dev* 21:1292-1315.
28. Murtaugh, L.C., Law, A.C., Dor, Y., and Melton, D.A. 2005. Beta-catenin is essential for pancreatic acinar but not islet development. *Development* 132:4663-4674.
29. Wells, J.M., Esni, F., Boivin, G.P., Aronow, B.J., Stuart, W., Combs, C., Sklenka, A., Leach, S.D., and Lowy, A.M. 2007. Wnt/beta-catenin signaling is required for development of the exocrine pancreas. *BMC Dev Biol* 7:4.
30. Dessimoz, J., Bonnard, C., Huelsken, J., and Grapin-Botton, A. 2005. Pancreas-Specific Deletion of beta-catenin Reveals Wnt-Dependent and Wnt-Independent Functions during Development. *Curr Biol* 15:1677-1683.
31. Lerch, M.M., Lutz, M.P., Weidenbach, H., Muller-Pillasch, F., Gress, T.M., Leser, J., and Adler, G. 1997. Dissociation and reassembly of adherens junctions during experimental acute pancreatitis. *Gastroenterology* 113:1355-1366.
32. Heiser, P.W., Cano, D.A., Landsman, L., Kim, G.E., Kench, J.G., Klimstra, D.S., Taketo, M.M., Biankin, A.V., and Hebrok, M. 2008. Stabilization of beta-catenin induces pancreas tumor formation. *Gastroenterology* 135:1288-1300.
33. Kemler, R., Hierholzer, A., Kanzler, B., Kuppig, S., Hansen, K., Taketo, M.M., de Vries, W.N., Knowles, B.B., and Solter, D. 2004. Stabilization of beta-catenin in the mouse zygote leads to premature epithelial-mesenchymal transition in the epiblast. *Development* 131:5817-5824.
34. Khasawneh, J., Schulz, M.D., Walch, A., Rozman, J., Hrabe de Angelis, M., Klingenspor, M., Buck, A., Schwaiger, M., Saur, D., Schmid, R.M., et al. 2009. Inflammation and mitochondrial fatty acid beta-oxidation link obesity to early tumor promotion. *Proc Natl Acad Sci U S A* 106:3354-3359.
35. Pasca di Magliano, M., Sekine, S., Ermilov, A., Ferris, J., Dlugosz, A.A., and Hebrok, M. 2006. Hedgehog/Ras interactions regulate early stages of pancreatic cancer. *Genes Dev* 20:3161-3173.
36. Siveke, J.T., Einwachter, H., Sipos, B., Lubeseder-Martellato, C., Kloppel, G., and Schmid, R.M. 2007. Concomitant pancreatic activation of Kras(G12D) and Tgfa results in cystic papillary neoplasms reminiscent of human IPMN. *Cancer Cell* 12:266-279.

37. Ji, B., Tsou, L., Wang, H., Gaiser, S., Chang, D.Z., Daniluk, J., Bi, Y., Grote, T., Longnecker, D.S., and Logsdon, C.D. 2009. Ras activity levels control the development of pancreatic diseases. *Gastroenterology* 137:1072-1082, 1082 e1071-1076.
38. Duan, R.D., Zheng, C.F., Guan, K.L., and Williams, J.A. 1995. Activation of MAP kinase kinase (MEK) and Ras by cholecystokinin in rat pancreatic acini. *Am J Physiol* 268:G1060-1065.
39. Hailfinger, S., Jaworski, M., Braeuning, A., Buchmann, A., and Schwarz, M. 2006. Zonal gene expression in murine liver: lessons from tumors. *Hepatology* 43:407-414.
40. Braeuning, A., Ittrich, C., Kohle, C., Buchmann, A., and Schwarz, M. 2007. Zonal gene expression in mouse liver resembles expression patterns of Ha-ras and beta-catenin mutated hepatomas. *Drug Metab Dispos* 35:503-507.
41. Janssen, K.P., Alberici, P., Fsihi, H., Gaspar, C., Breukel, C., Franken, P., Rosty, C., Abal, M., El Marjou, F., Smits, R., et al. 2006. APC and oncogenic KRAS are synergistic in enhancing Wnt signaling in intestinal tumor formation and progression. *Gastroenterology* 131:1096-1109.
42. Pearson, H.B., Phesse, T.J., and Clarke, A.R. 2009. K-ras and Wnt signaling synergize to accelerate prostate tumorigenesis in the mouse. *Cancer Res* 69:94-101.
43. Pasca di Magliano, M., Biankin, A.V., Heiser, P.W., Cano, D.A., Gutierrez, P.J., Deramaudt, T., Segara, D., Dawson, A.C., Kench, J.G., Henshall, S.M., et al. 2007. Common activation of canonical wnt signaling in pancreatic adenocarcinoma. *PLoS ONE* 2:e1155.
44. Wang, L., Heidt, D.G., Lee, C.J., Yang, H., Logsdon, C.D., Zhang, L., Fearon, E.R., Ljungman, M., and Simeone, D.M. 2009. Oncogenic function of ATDC in pancreatic cancer through Wnt pathway activation and beta-catenin stabilization. *Cancer Cell* 15:207-219.
45. Apelqvist, A., Li, H., Sommer, L., Beatus, P., Anderson, D.J., Honjo, T., Hrabe de Angelis, M., Lendahl, U., and Edlund, H. 1999. Notch signalling controls pancreatic cell differentiation. *Nature* 400:877-881.
46. Esni, F., Ghosh, B., Biankin, A.V., Lin, J.W., Albert, M.A., Yu, X., MacDonald, R.J., Civin, C.I., Real, F.X., Pack, M.A., et al. 2004. Notch inhibits Ptf1 function and acinar cell differentiation in developing mouse and zebrafish pancreas. *Development* 131:4213-4224.
47. Brault, V., Moore, R., Kutsch, S., Ishibashi, M., Rowitch, D.H., McMahon, A.P., Sommer, L., Boussadia, O., and Kemler, R. 2001. Inactivation of the beta-catenin gene by Wnt1-Cre-mediated deletion results in dramatic brain malformation and failure of craniofacial development. *Development* 128:1253-1264.
48. Nagashio, Y., Ueno, H., Imamura, M., Asaumi, H., Watanabe, S., Yamaguchi, T., Taguchi, M., Tashiro, M., and Otsuki, M. 2004. Inhibition of transforming growth factor beta decreases pancreatic fibrosis and protects the pancreas against chronic injury in mice. *Lab Invest* 84:1610-1618.

Figure Legends

Figure 1. Mutant Kras blocks acinar regeneration and promotes ADM/PanIN formation.

(A-H) Hematoxylin and Eosin (H&E) staining of regeneration timecourse in *Pdx1-Cre^{Early}* (A-D) and *Pdx1-Cre^{Early}; LSL-Kras^{G12D}* (E-H) mice. (E, M) Asterisks indicate spontaneous PanIN lesions in PBS treated *Pdx1-Cre^{Early}; LSL-Kras^{G12D}* animals. Insets (B, F) show morphologically similar duct like cells 2 days after induction of acute pancreatitis. **(I-P)** Amylase (red)/CK19 (green) immunofluorescent labeling. Note CK19 expression in spontaneous PanIN lesions in *Pdx1-Cre^{Early}; LSL-Kras^{G12D}* mice (asterisk, M). (J, N) Amylase is downregulated and CK19 is weakly expressed in transient duct like cells in *Pdx1-Cre^{Early}* mice (inset J), while strongly expressed in duct like cells in *Pdx1-Cre^{Early}; LSL-Kras^{G12D}* mice (inset N). Rare amylase positive cells are found in metaplastic epithelium (arrowheads, O). **(Q-T)** Amylase (red), CK19 (blue) YFP (green) immunofluorescent labeling in *Elastase-Cre^{ERT}*; *LSL-Kras^{G12D}; R26R-EYFP* mice. Without caerulein treatment, YFP expression is restricted to amylase positive cells and restricted from CK19 positive cells. Arrowheads indicate autofluorescent erythrocytes (Q). CK19/YFP double positive cells (cyan, indicating blue/green overlap) persist following caerulein (R-T). (A-P, X400) (insets, original magnification x400) (Q-T, scale bars=50μm).

Figure 2. Mutant Kras blocks blocks acinar regeneration in favor of a persistently de-differentiated state.

(A-H) Clusterin and Sox9 **(I-P)** expression during regeneration and Kras induced ADM. (A, I) Clusterin expression is limited to some normal ducts in PBS treated *Pdx1-Cre^{Early}* mice, while Sox9 is restricted to ducts and centroacinar cells (arrowheads). (E, M) Acini in PBS treated *Pdx1-Cre^{Early}; LSL-Kras^{G12D}* mice are negative for Clusterin and Sox9, while normal ducts and spontaneous PanINs are positive (asterisk). (B, F; J, N) Damaged duct like cells of both genotypes display clusterin and Sox9 positive cells (insets). (C, D; K, L) Clusterin and Sox9 are mainly restricted to duct cells (arrowheads) following regeneration in *Pdx1-Cre^{Early}* pancreata. Rare clusterin positive cells were observed 7 days following caerulein (arrow, C). (G, H; O, P) Clusterin and Sox9 remain strongly expressed in ADM and PanINs in *Pdx1-Cre^{Early}; LSL-Kras^{G12D}* mice. **(Q)** Schematic of failed regeneration of acini possessing mutant Kras (Acini*) versus wild type (WT). Wild type acini transiently de-differentiate and rapidly regenerate, while acini possessing mutant Kras are sensitized to persistent de-differentiation and ADM/PanIN formation. (A-P, X400) (insets, original magnification X400).

Figure 3. Regeneration associated re-activation of β-catenin signaling is inhibited during Kras induced ductal reprogramming.

(A-H) β-catenin (above dashed line, gray; below dashed line, green) and amylase (above dashed line, not shown; below dashed line, blue) immunofluorescent staining. (A-D) *Pdx1-Cre^{Early}* mice; (E-H) *Pdx1-Cre^{Early}; LSL-*

Kras^{G12D} mice. Asterisk in E marks spontaneous PanIN lesions. **(I, J)** Western blot analysis of β-catenin 2 days following caerulein. Intensity, normalized to GAPDH, is quantified in J (Bars represent mean ± SD). **(K, L)** Quantitative PCR for β-catenin target genes during WT acinar regeneration (blue bars) and ADM/PanIN (red bars). Values are relative to PBS treated *Pdx1-Cre*^{Early} mice and are presented as mean ± SD (n=3). P = PBS treatment; 2, 7, 21 indicate days after caerulein treatment (*P<0.05, ***P<0.001). (A-H, X600).

Figure 4. β-catenin is required for efficient acinar regeneration

(A-F) H&E staining of regenerating control (*p48-Cre; β-catenin*$^{F/+}$) versus *p48-Cre; β-catenin*$^{F/F}$ pancreas following caerulein treatment. 'f', fat accumulation (D-F). Rare acini following caerulein treatment are marked with arrowheads (E, F). **(G-L)** β-catenin (green), Amylase (blue), and CK19 (red) immunofluorescent labeling. Acini in *p48-Cre; β-catenin*$^{F/F}$ mice lack membrane β-catenin staining (compare insets in G, J). Arrowheads mark rare acini (K, L). Both β-catenin negative (arrow) and positive (#) CK-19 labeled ducts are observed. "i", islets. **(M)** Quantfication of relative amylase area in control (blue bars) and *p48-Cre; β-catenin*$^{F/F}$ (red bars) following caerulein pancreatitis. Bars represent mean ± SD. *: P<0.05, **: P<0.01, ***: P<0.001 (A-L, x400) (insets, original magnification X400).

Figure 5. Stabilized β-catenin antagonizes Kras induced ADM.

(A-L) Characterization of 6 week old, PBS and caerulein treated *p48Cre; β-catenin$^{exon3/+}$; LSL-Kras^{G12D}* mice and caerulein treated *p48Cre; LSL-Kras^{G12D}* mice. (A, E, I) H&E staining. Yellow lines separate areas of cells with acinar morphology (a), and ductal morphology (d). (B, F, J) Amylase staining. (C, G, K) Sox9 staining. (D, H, L) Clusterin staining. **(M)** Quantification of relative amylase area 7 days following caerulein in *p48Cre; β-catenin$^{Exon3/+}$; LSL-Kras^{G12D}* (red bars) and control *p48Cre; LSL-Kras^{G12D}* (blue bars) mice. Bars represent mean ± SD. *: P<0.05, **:P<0.01, ***: P<0.001, NS: not significant. (A-L, original magnification X400).

Figure 6. β-catenin signaling inhibits Kras induced reprogramming of acini into PanINs.

(A, E, I) H&E staining of tamoxifen stimulated, Caerulein or PBS treated, *ElaCre^{ERT}; β-catenin$^{exon3/+}$*; *LSL-Kras^{G12D}* or *ElaCre^{ERT}; LSL-Kras^{G12D}* mice. **(B, F, J)** CK19/Alcian Blue staining. Note that normal ducts in PBS treated *ElaCre^{ERT}; β-catenin$^{exon3/+}$*; *LSL-Kras^{G12D}* mice are strongly CK19 positive, but Alcian Blue negative (B). **(C, G, K)** β-catenin (green), DAPI (blue) immunofluorescent labeling. β-catenin accumulation is rare in PBS treated *ElaCre^{ERT}; β-catenin$^{exon3/+}$*; *LSL-Kras^{G12D}* mice (asterisk, C). Nuclear localization is noted by Cyan overlap of green/blue channels (K). **(D, H, L)** phospho-p42/p44 staining. (A, B, D, E, F, H, I, J, L, x400) (C, G, K, scale bars=50μm).

Figure 7. β-catenin acts as a gatekeeper of Kras induced reprogramming of acini into ductal PanINs.

Pattern of β-catenin signaling activity during acinar regeneration versus Kras induced ADM/PanIN. β-catenin levels are kept below a critical threshold during the initiation of Kras induced ductal reprogramming but increase as PanIN lesions form. Therefore, β-catenin antagonizes specification of a ductal state capable of forming PanINs, but likely contributes to PanIN progression and tumor growth.

Supplemental Figure 1. Failed acinar regeneration in mice possessing mutant Kras targeted to developing and adult acini.

(A, B) CK19/Alcian Blue staining in *Pdx1-Cre^{Early}; LSL-Kras^{G12D}* mice 7 and 21 days following caerulein. **(C-F)** H&E staining of pancreas from PBS and caerulein treated *Pdx1-Cre^{Late}; LSL-Kras^{G12D}* mice. Duct like cells develop 2 days following treatment (B), followed by persistent ADM/PanIN at 7 and 21 days (C, D) along a similar timeframe as *Pdx1-Cre^{Early}; LSL-Kras^{G12D}* mice. **(G-J)** CK19 (blue), amylase (red), YFP (green) immunfluorescent labeling in PBS and caerulein treated *Elastase-Cre^{ERT2}*; *R26R-EYFP* mice. Note that YFP, CK19 positive cells are observed 2 days following caerulein, but YFP is restricted from CK19 positive cells in PBS treated mice and following regeneration (7, 21 days after caerulein). Asterisks in G, I, and J denote auto fluorescent erythrocytes found in blood vessels frequently found near ducts. **(K-N)** H&E staining of pancreas from PBS and caerulein treated *Elastase-Cre^{ERT2}*; *LSL-Kras^{G12D};*

R26R-EYFP mice. As in *Pdx1-Cre^{Late}; LSL-Kras^{G12D}* and *Pdx1-Cre^{Early}; LSL-Kras^{G12D}* mice, duct like cells develop at day 2 (L) and persist as ADM/PanIN at 7 and 21 days (M, N) following caerulein. (A-F; K-N, x200 magnification, G-J, scale bar=50μM).

Supplemental Figure 2. Additional characterization of acinar regeneration versus Kras induced ADM/PanIN formation

(A-H) Pdx1 expression in caerulein treated *Pdx1-Cre^{Early}* (A-D) and *Pdx1-Cre^{Early}; LSL-Kras^{G12D}* (E-H) pancreata. (A-D) Pdx1 is strongly expressed in islets (arrowheads) in PBS treated (A) and post-regeneration pancreata (C, D). (B, inset) Pdx1 is reactivated in the regenerating exocrine compartment 2 days following caerulein treatment. (E-H) (E) Pdx1 is expressed in spontaneous PanIN lesions (asterisk) in *Pdx1-Cre^{Early}; LSL-Kras^{G12D}* pancreata. (F, inset) Pdx1 is found in duct like cells 2 days following caerulein and persists in metaplastic ducts and PanINs 7 and 21 days following caerulein (G, H). **(I-P)** Hes1 expression in caerulein treated *Pdx1-Cre^{Early}* (I-L) and *Pdx1-Cre^{Early}; LSL-Kras^{G12D}* (M-P) pancreata. (I-L) Hes1 is expressed in centroacinar cells (arrowheads) in PBS treated (I) and post-regeneration pancreata (K, L). (J, inset) Hes1 is reactivated in the regenerating exocrine compartment 2 days following caerulein treatment. (M-P) (M) Hes1 is expressed in spontaneous PanIN lesions (asterisk) in *Pdx1-Cre^{Early}; LSL-Kras^{G12D}* pancreata. (N, inset) Hes1 is expressed in duct like cells 2 days following caerulein and persists in

metaplastic ducts and PanINs 7 and 21 days following caerulein (O, P). (A-P, X400) (insets, original magnification X400).

Supplemental Figure 3. Mutant Kras blocks acinar regeneration in favor of persistently de-differentiated ADM/PanIN.

(A-H) Clusterin (blue) and YFP (green) immunofluoescent labeling in PBS and caerulein treated *Elastase-Cre^{ERT2}; R26R-EYFP and Elastase-Cre^{ERT2}*; *LSL-Kras^{G12D}; R26R-EYFP* mice. Co-expression is indicated by cyan. **(I-P)** Sox9 (blue) and YFP (green) immunofluoescent labeling in PBS and caerulein treated *Elastase-Cre^{ERT2}; R26R-EYFP and Elastase-Cre^{ERT2}*; *LSL-Kras^{G12D}; R26R-EYFP* mice. Co-expression is indicated by cyan. Strong Sox9 staining marks centroacinar and duct cells in I, K, L, M. (A-P, scale bar=50μM).

Supplemental Figure 4. phospho-p42/p44 is persistently active in Kras induced ADM/PanIN.

(A-H) phospho-p42/p44 staining in caerulein treated *Pdx1-Cre^{Early}* (A-D) and *Pdx1-Cre^{Early}; LSL-Kras^{G12D}* (E-H) pancreata. (A, C, D) phospho p42/44 staining above background levels is rare in PBS treated *Pdx1-Cre^{Early}* mice and pancreata following regeneration. (B, inset) phospho-p42/p44 is reactivated in some duct structures 2 days following caerulein treatment. (E) phospho-p42/p44 is found in spontaneous PanIN lesions (asterisk) in *Pdx1-Cre^{Early}; LSL-Kras^{G12D}* pancreata, but is mostly absent in morphologically normal acini. (F, inset) phospho-p42/p44 is strongly displayed in de-differentiated acini 2 days following caerulein and

persists in metaplastic ducts and PanINs 7 and 21 days following caerulein (G, H). (A-P), X400) (insets, original magnification X400).

Supplemental Figure 5. E-cadherin accumulates in response to pancreatitis in *Pdx1-Cre^{Early}* and *Pdx1-Cre^{Early}; LSL-Kras^{G12D}* mice.

(A-D) E-cadherin (green) and amylase (red) expression in caerulein treated *Pdx1-Cre^{Early}* mice. E-cadherin is weakly expressed at the acinar membrane in PBS treated (A) and post-regeneration animals (C, D). (B) E-cadherin accumulates in the regenerating exocrine compartment following caerulein. **(E-H)** E-cadherin (green) and amylase (red) expression in caerulein treated *Pdx1-Cre^{Early};LSL-Kras^{G12D}* mice. E-cadherin is strongly expressed at the membrane of spontaneous PanINs (E, asterisk) but weakly in morphologically normal acini. (F) Duct like cells display E-cadherin accumulation similar to such structures in WT mice (B). Strong E-cadherin expression persists in metaplastic ducts at day 7 (G) and in PanINs (H) at day 21 following caerulein treatment. (A-H, X400).

Supplemental Figure 6. Comparison of acinar regeneration following caerulein in *p48-Cre; LSL-Kras^{G12D}*, *p48-Cre; ß-catenin$^{exon3/+}$*, and *p48-Cre; ß-catenin$^{exon3/+}$; LSL-Kras^{G12D}* mice.

(A-C) PBS treated *p48-Cre; LSL-Kras^{G12D}* display rare spontaneous PanINs (asterisk). Acini assume a duct like state two days following caerulein (B), but undergo ADM and fail to regenerate seven days following treatment (C). **(D-F)** Acini assume a transient ductal state in *p48-Cre; ß-catenin$^{exon3/+}$* mice two days

following caerulein (E), but regenerate 7 days after treatment (F). **(G-I)** Yellow lines outline areas of cells with acinar morphology in PBS treated *p48-Cre; ß-catenin$^{exon3/+}$; LSL-Kras^{G12D}* mice (B) which are maintained at day two and 7 following caerulein treatment (H,I). (A-I, 200X)

Supplemental Figure 7. Additional characterization of antagonized Kras induced ADM by stabilized ß-catenin

(A, E) Hes1 is widely expressed in ADM seven days after caerulein treatment in *p48-Cre; LSL-Kras^{G12D}* mice, but is mainly restricted to abnormal ducts in caerulein treated *p48-Cre; ß-catenin$^{exon3/+}$; LSL-Kras^{G12D}* mice. **(B,F)** Similarly, phospho p42/p44 staining is displayed in ADM seven days after caerulein treatment in *p48-Cre; LSL-Kras^{G12D}* mice, but is mainly restricted to abnormal ducts in caerulein treated *p48-Cre; ß-catenin$^{exon3/+}$; LSL-Kras^{G12D}* mice. **(C, D; G, H)** (C) Merge of CK-19 (green) and amylase (red) indicating widespread ADM 7 days following caerulein treatment in *p48-Cre; LSL-Kras^{G12D}* mice. (D) ß-catenin (green) and DAPI (blue, marking nuclei) labeling of the same section shown in 'C'. (G) Merge of CK-19 (green) and amylase (red) indicating retained cells with acinar morphology and acinar marker expression 7 days following caerulein treatment in *p48-Cre; ß-catenin$^{exon3/+}$; LSL-Kras^{G12D}* mice. (H) ß-catenin (green) and DAPI (blue, marking nuclei) labeling of the field shown in (G), displaying ß-catenin accumulation throughout the transgenic exocrine compartment. Arrowheads mark areas of nuclear accumulation indicated by cyan (blue/green overlap). (A-H, 400X)

Figure 1

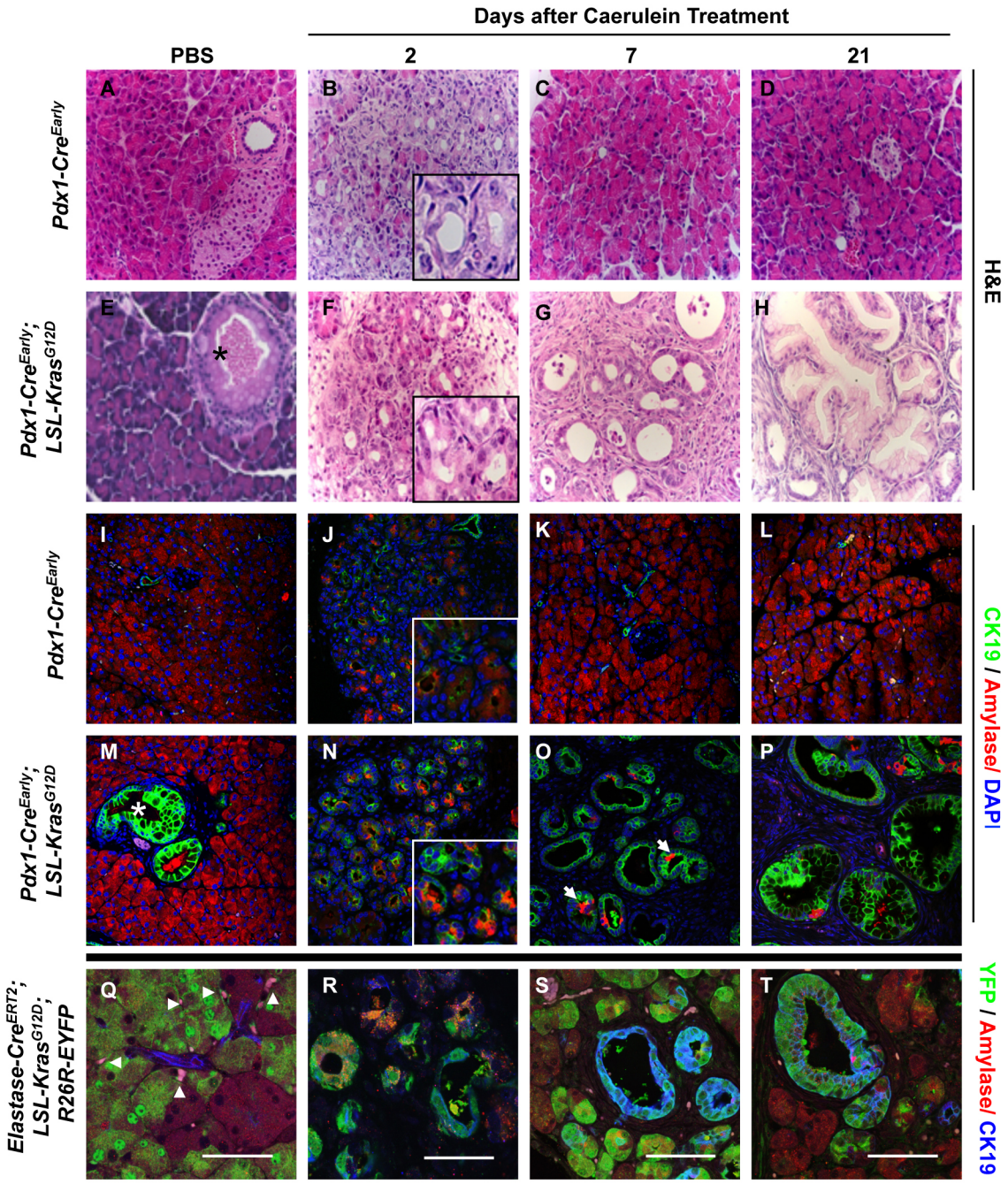
Days after Caerulein Treatment
PBS
2
7
21
Pdx1-Cre^Early
Pdx1-Cre^Early; LSL-Kras^G12D
Pdx1-Cre^Early
Pdx1-Cre^Early; LSL-Kras^G12D
Elastase-Cre^ERT2; LSL-Kras^G12D; R26R-EYFP
A
B
C
D
E
F
G
H
I
J
K
L
M
N
O
P
Q
R
S
T
H&E
CK19 / Amylase/ DAPI
YFP / Amylase/ CK19

Figure 2

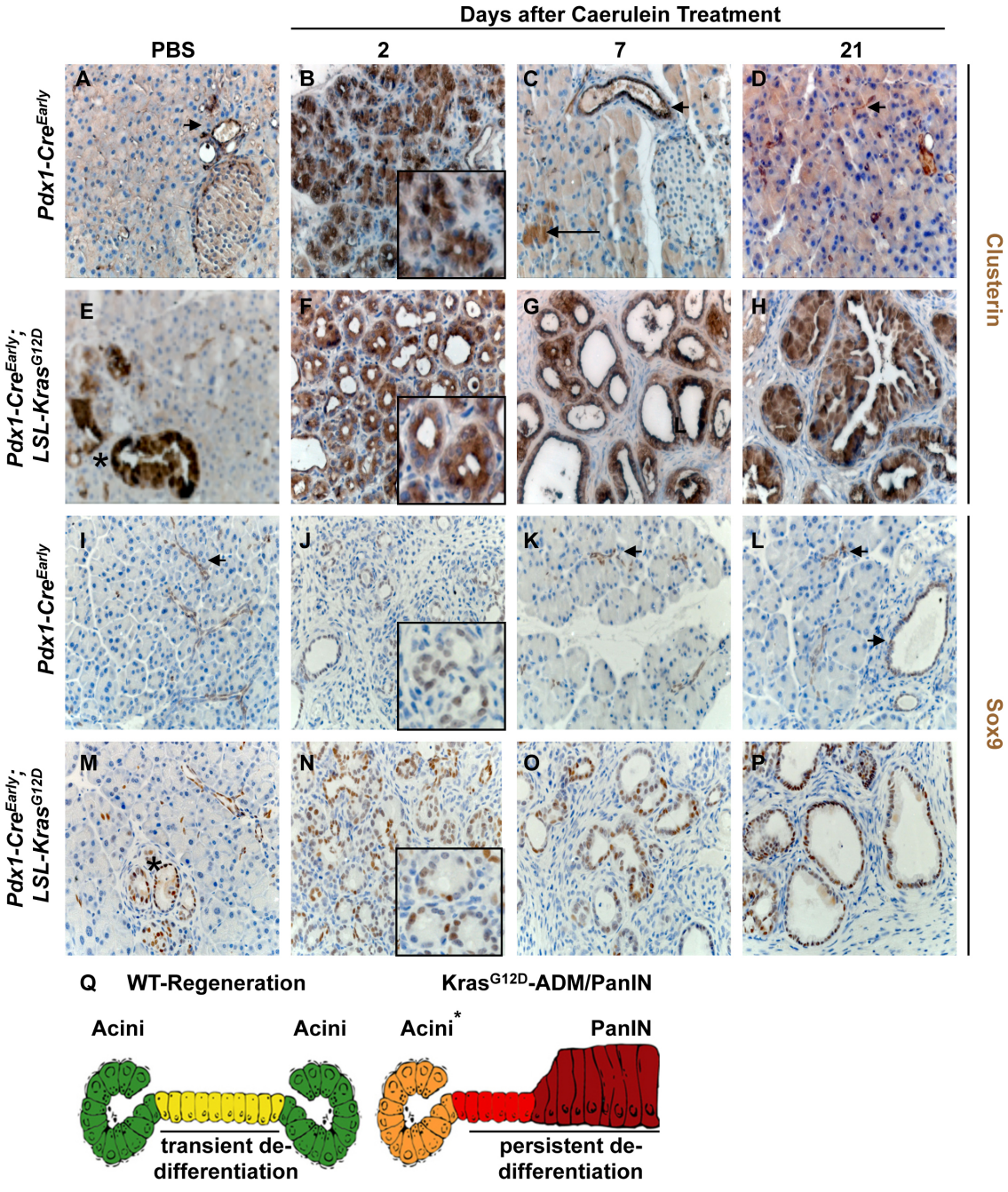
Days after Caerulein Treatment
PBS
2
7
21
Pdx1-Cre^Early
Pdx1-Cre^Early; LSL-Kras^G12D
Clusterin
Sox9
A
B
C
D
E
F
G
H
I
J
K
L
M
N
O
P
Q WT-Regeneration
Kras^G12D-ADM/PanIN
Acini
Acini
Acini*
PanIN
transient de-differentiation
persistent de-differentiation

Figure 3

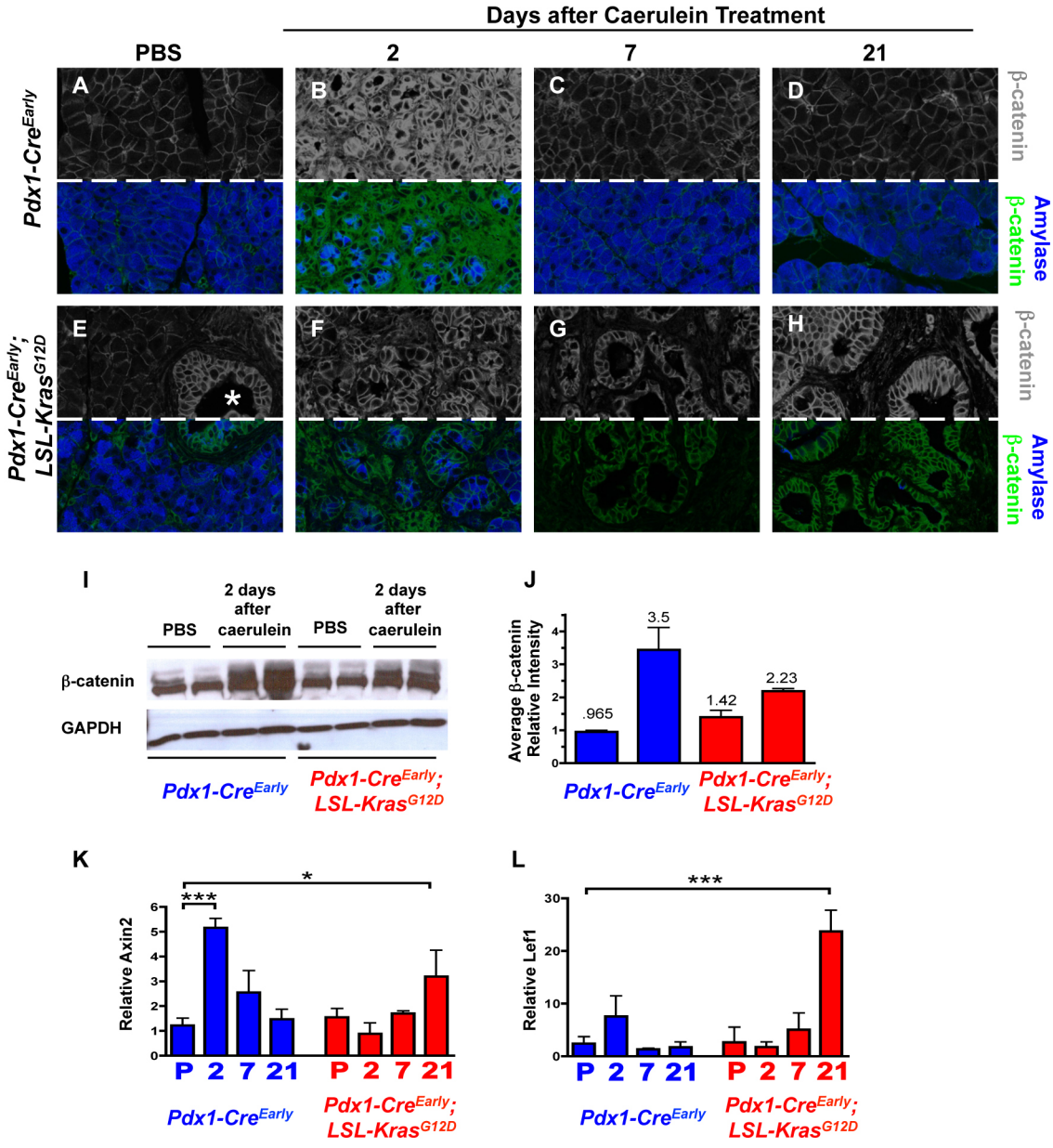
Days after Caerulein Treatment
PBS
2
7
21
A
B
C
D
E
F
G
H
Pdx1-Cre^Early
Pdx1-Cre^Early; LSL-Kras^G12D
β-catenin
Amylase
β-catenin
I
2 days after caerulein
PBS
2 days after caerulein
PBS
β-catenin
GAPDH
Pdx1-Cre^Early
Pdx1-Cre^Early; LSL-Kras^G12D
J
Average β-catenin Relative Intensity
.965
3.5
1.42
2.23
Pdx1-Cre^Early
Pdx1-Cre^Early; LSL-Kras^G12D
K
Relative Axin2
***
*
P 2 7 21 P 2 7 21
Pdx1-Cre^Early
Pdx1-Cre^Early; LSL-Kras^G12D
L
Relative Lef1
***
P 2 7 21 P 2 7 21
Pdx1-Cre^Early
Pdx1-Cre^Early; LSL-Kras^G12D

Figure 4

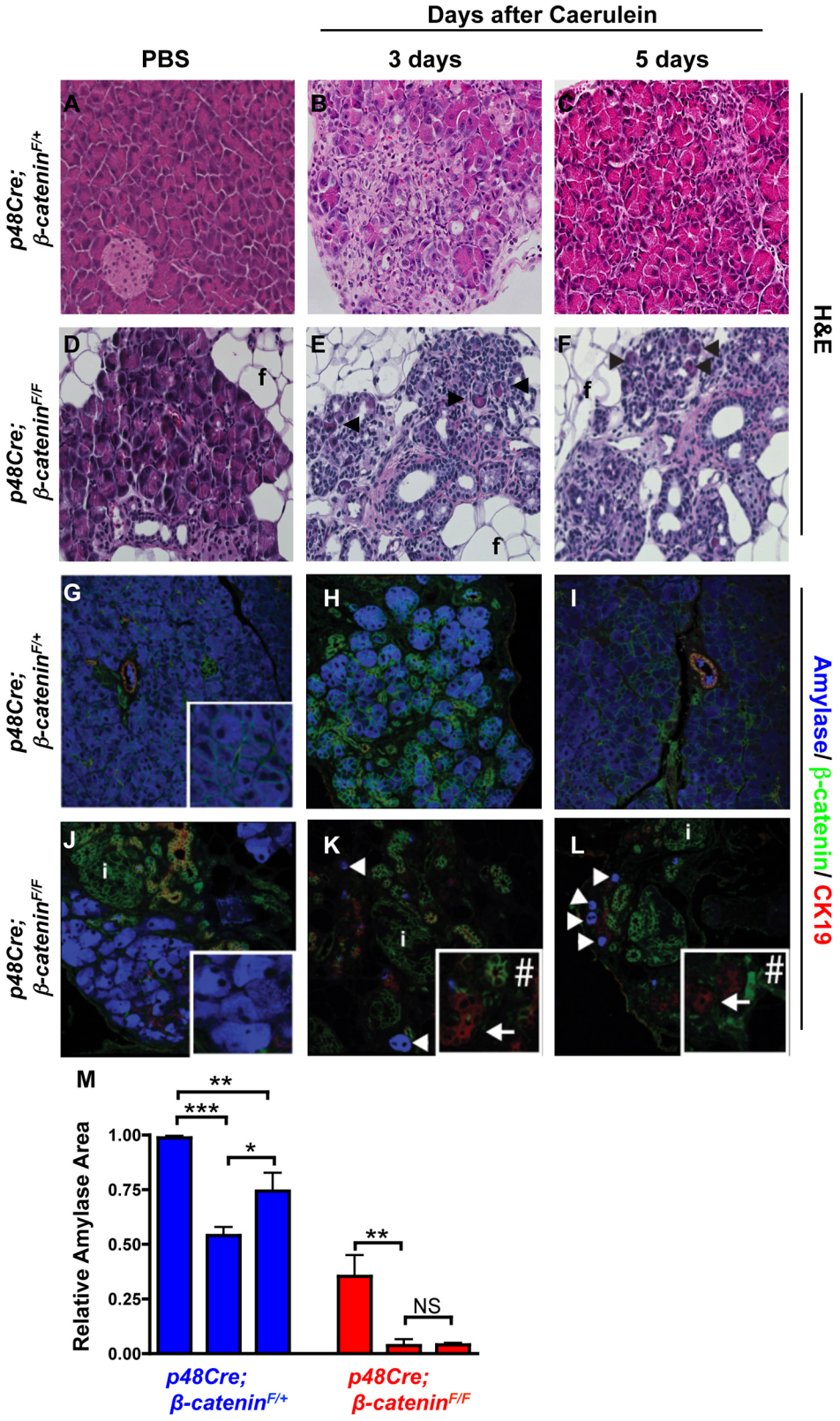
Days after Caerulein
PBS
3 days
5 days
A
B
C
D
E
F
G
H
I
J
K
L
M
p48Cre; β-catenin F/+
p48Cre; β-catenin F/F
H&E
Amylase/ β-catenin/ CK19
f
i
#
Relative Amylase Area
1.00
0.75
0.50
0.25
0.00
**
***
*
NS
p48Cre; β-catenin F/+
p48Cre; β-catenin F/F

Figure 5

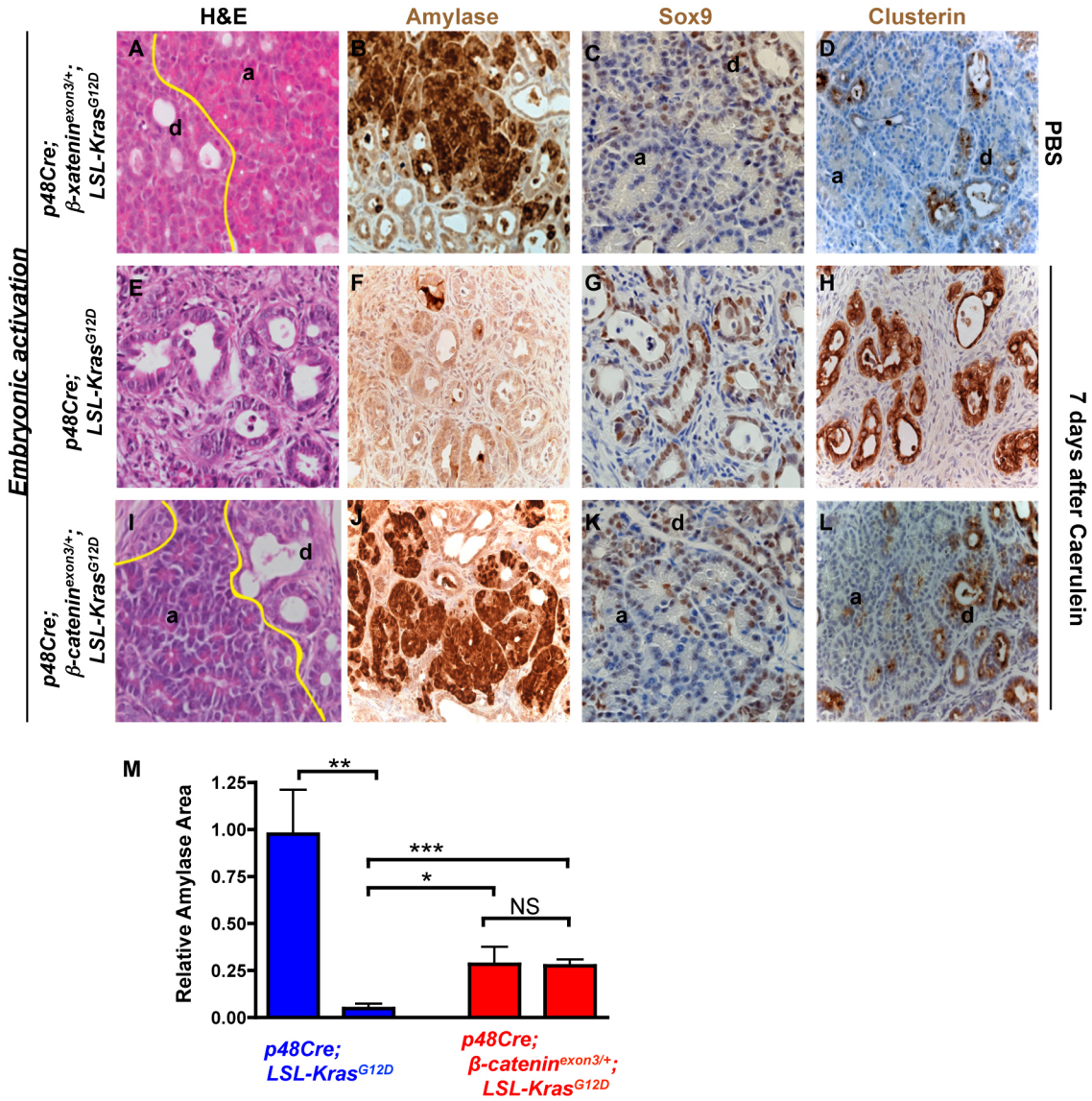
H&E
Amylase
Sox9
Clusterin
Embryonic activation
p48Cre; β-xatenin exon3/+; LSL-Kras G12D
p48Cre; LSL-Kras G12D
p48Cre; β-catenin exon3/+; LSL-Kras G12D
PBS
7 days after Caerulein
A
B
C
D
E
F
G
H
I
J
K
L
a
d
M
Relative Amylase Area
1.25
1.00
0.75
0.50
0.25
0.00
**
***
*
NS
p48Cre; LSL-Kras G12D
p48Cre; β-catenin exon3/+; LSL-Kras G12D

Figure 6

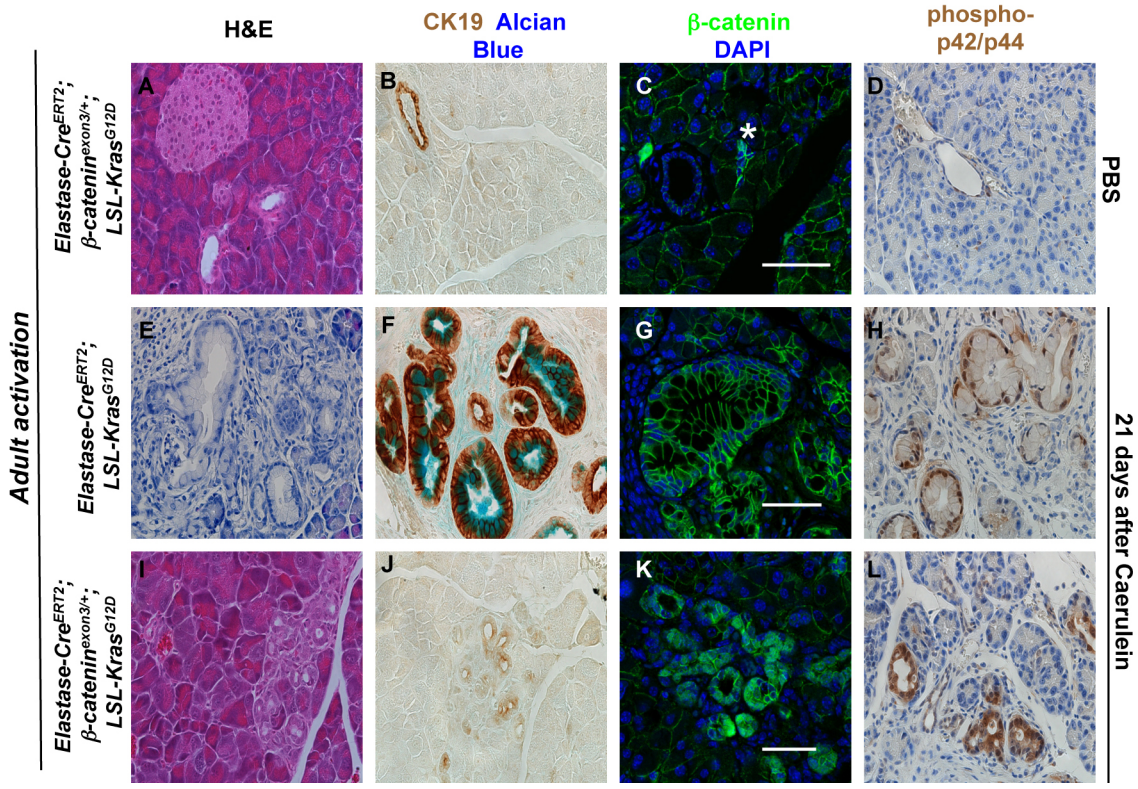
H&E
CK19 Alcian Blue
β-catenin DAPI
phospho-p42/p44
Adult activation
Elastase-Cre^ERT2; β-catenin^exon3/+; LSL-Kras^G12D
Elastase-Cre^ERT2; LSL-Kras^G12D
Elastase-Cre^ERT2; β-catenin^exon3/+; LSL-Kras^G12D
PBS
21 days after Caerulein
A
B
C
D
E
F
G
H
I
J
K
L
*

Figure 7

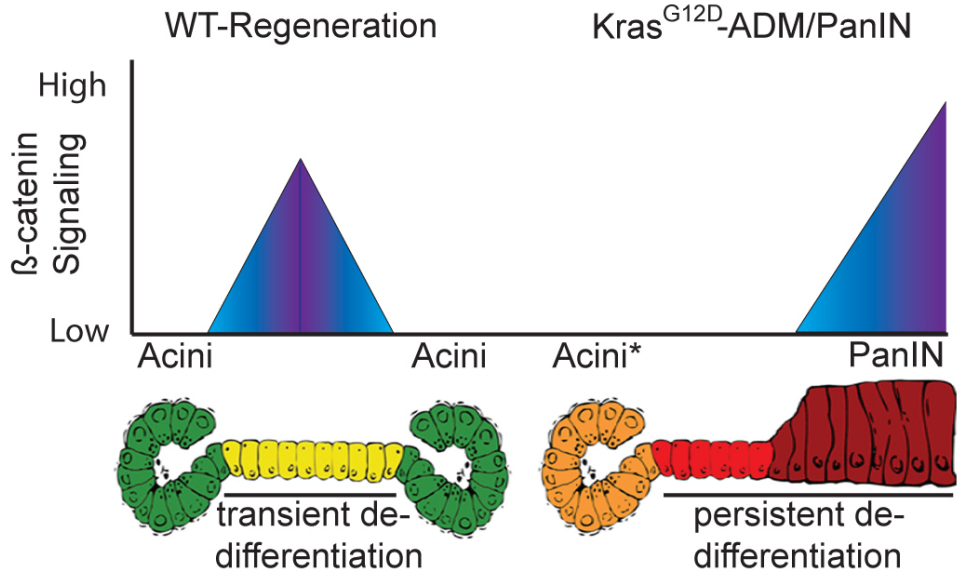
WT-Regeneration
Kras^{G12D}-ADM/PanIN
High
ß-catenin Signaling
Low
Acini
Acini
Acini*
PanIN
transient de-differentiation
persistent de-differentiation

Supplemental Figure 1

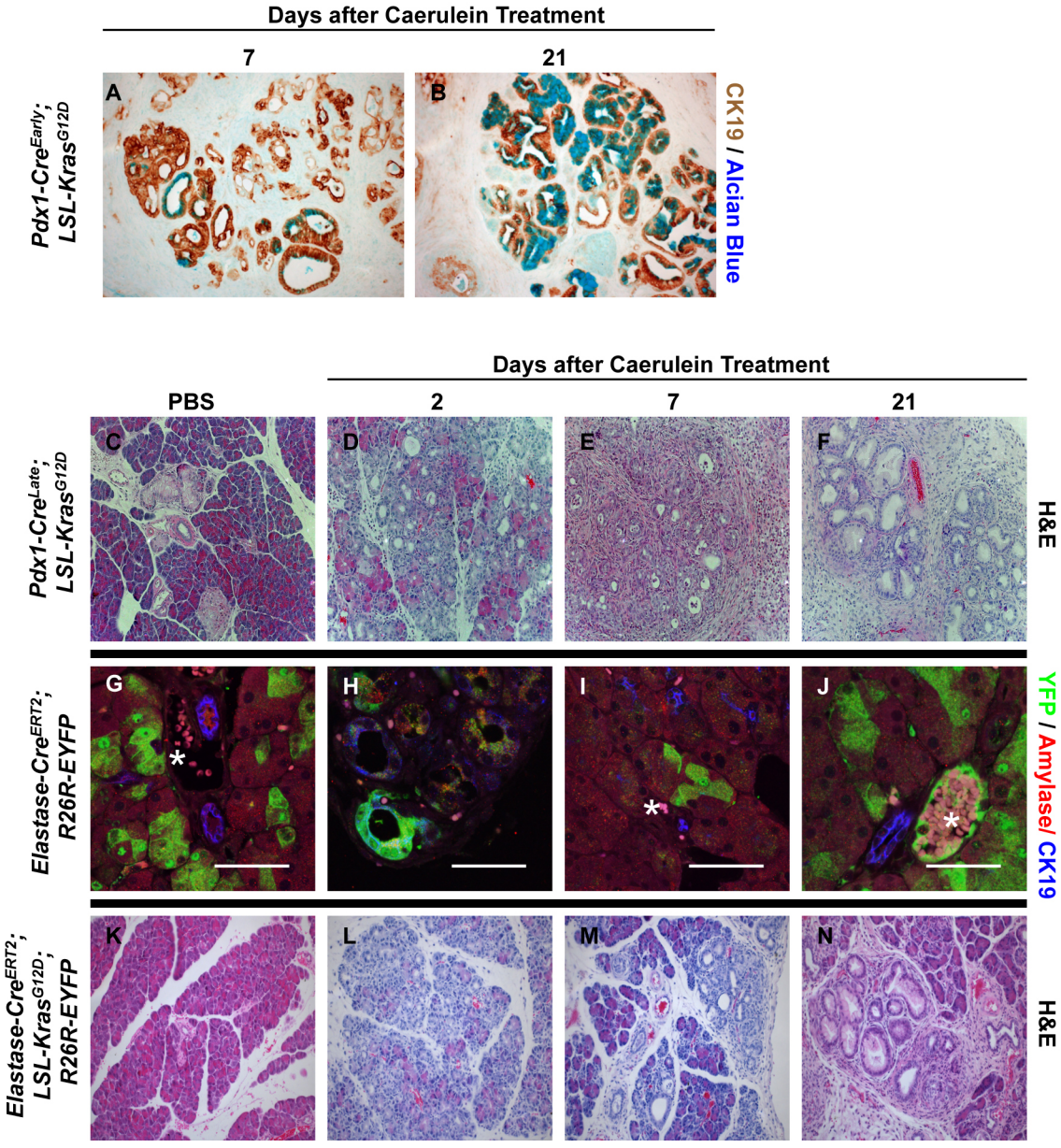

Supplemental Figure 2

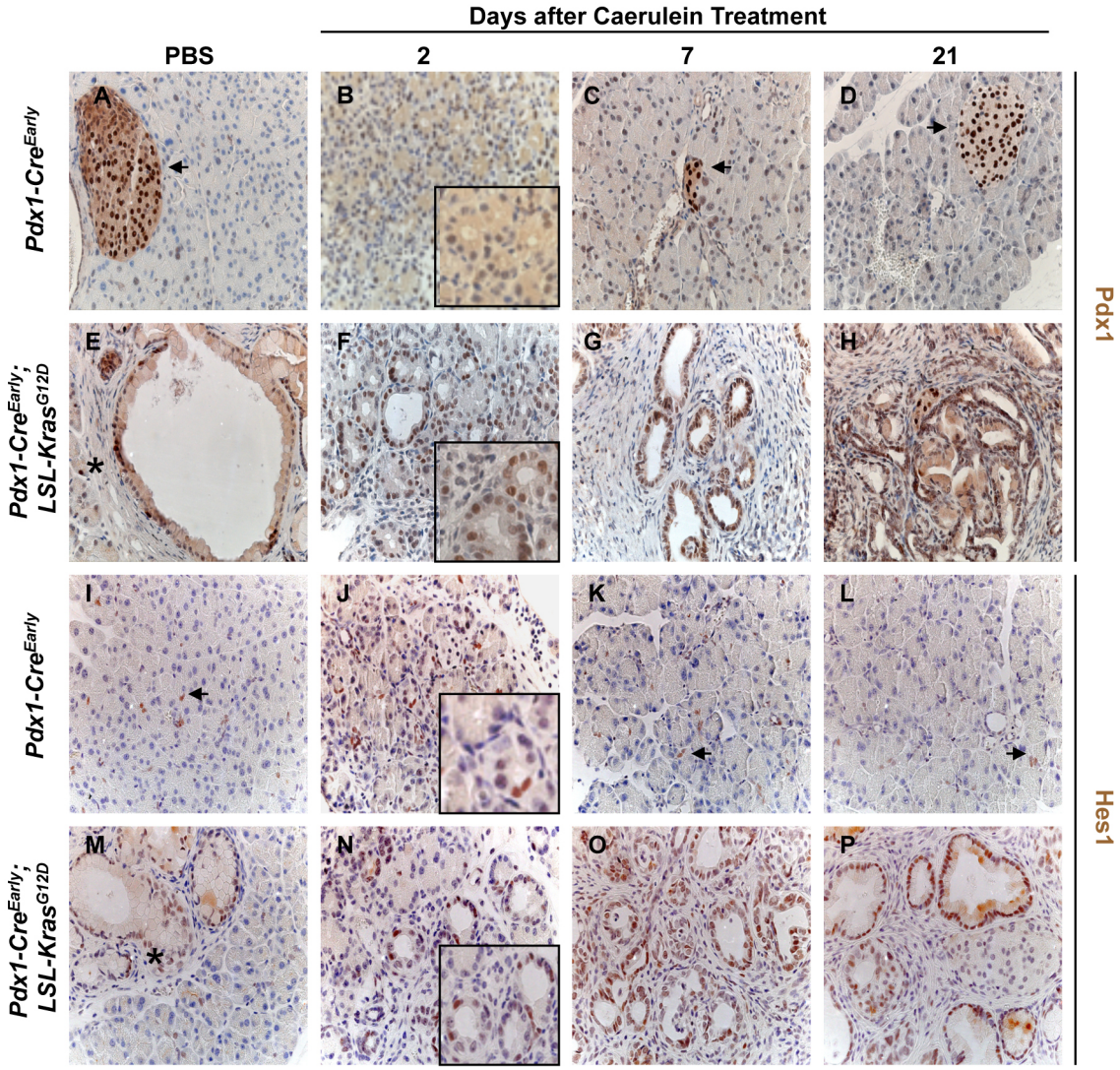

Supplemental Figure 3

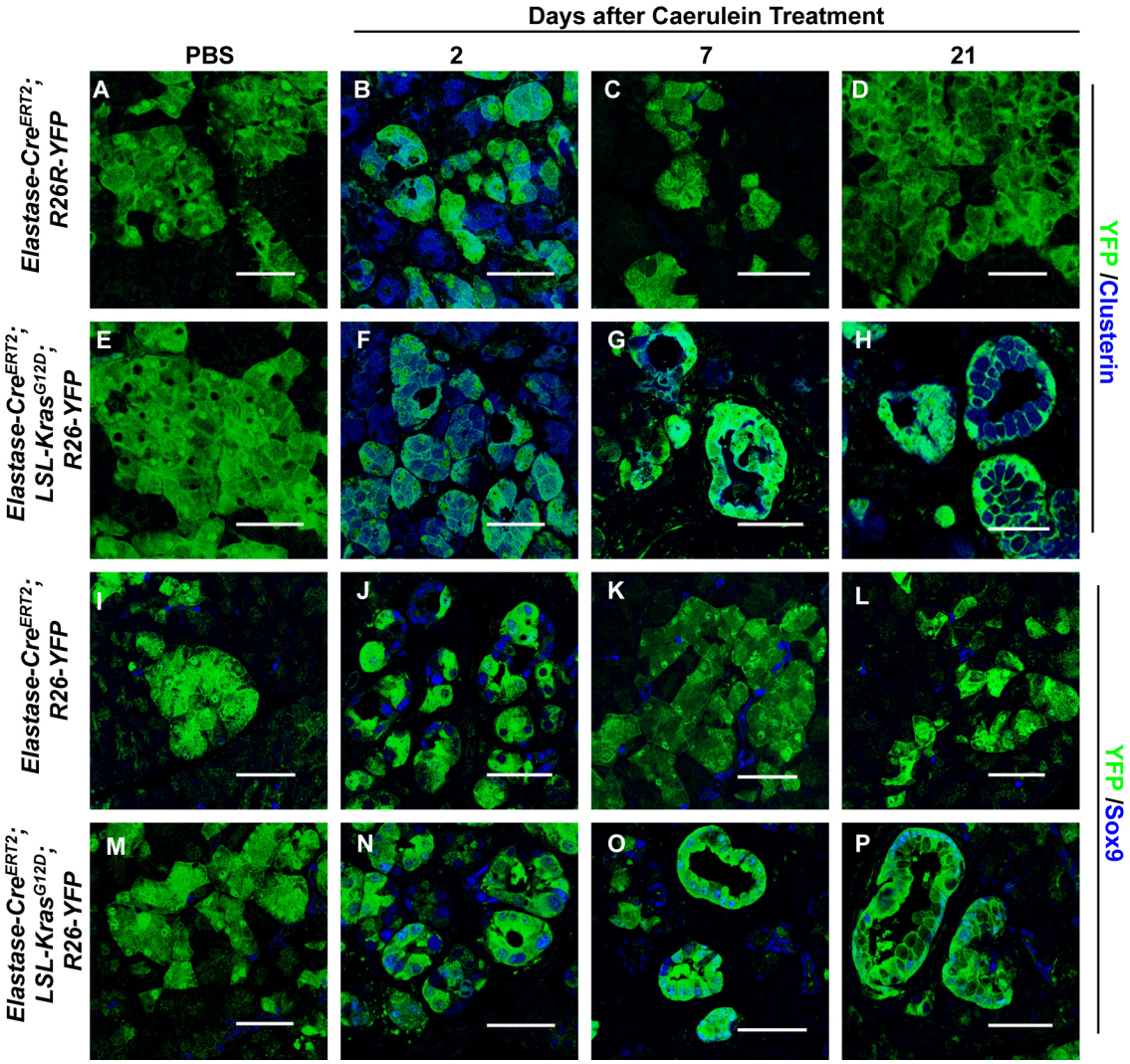

Supplemental Figure 4

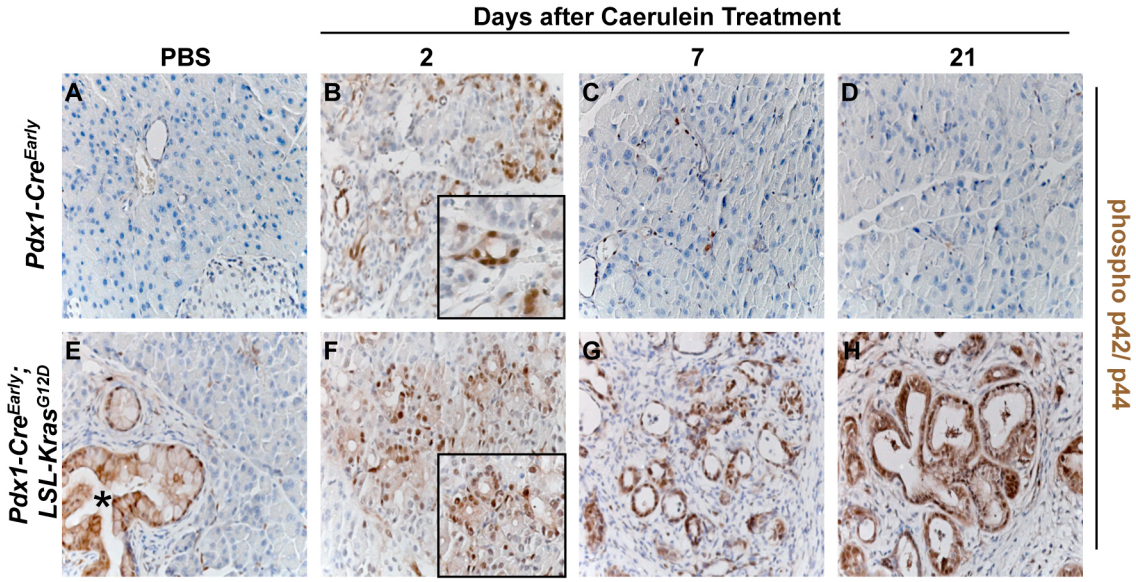

Supplemental Figure 5

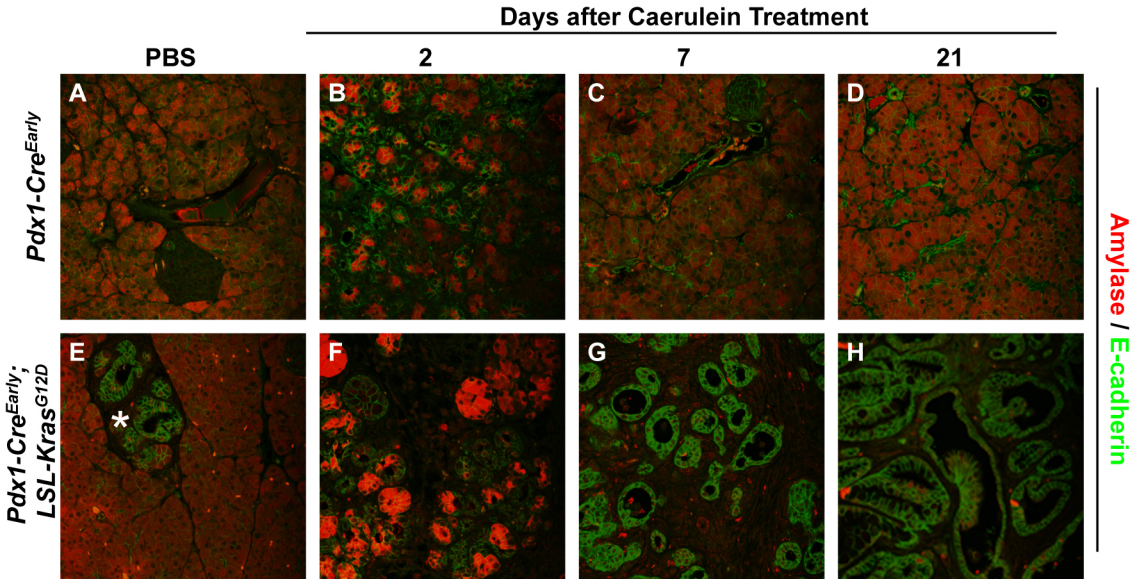

Supplemental Figure 6

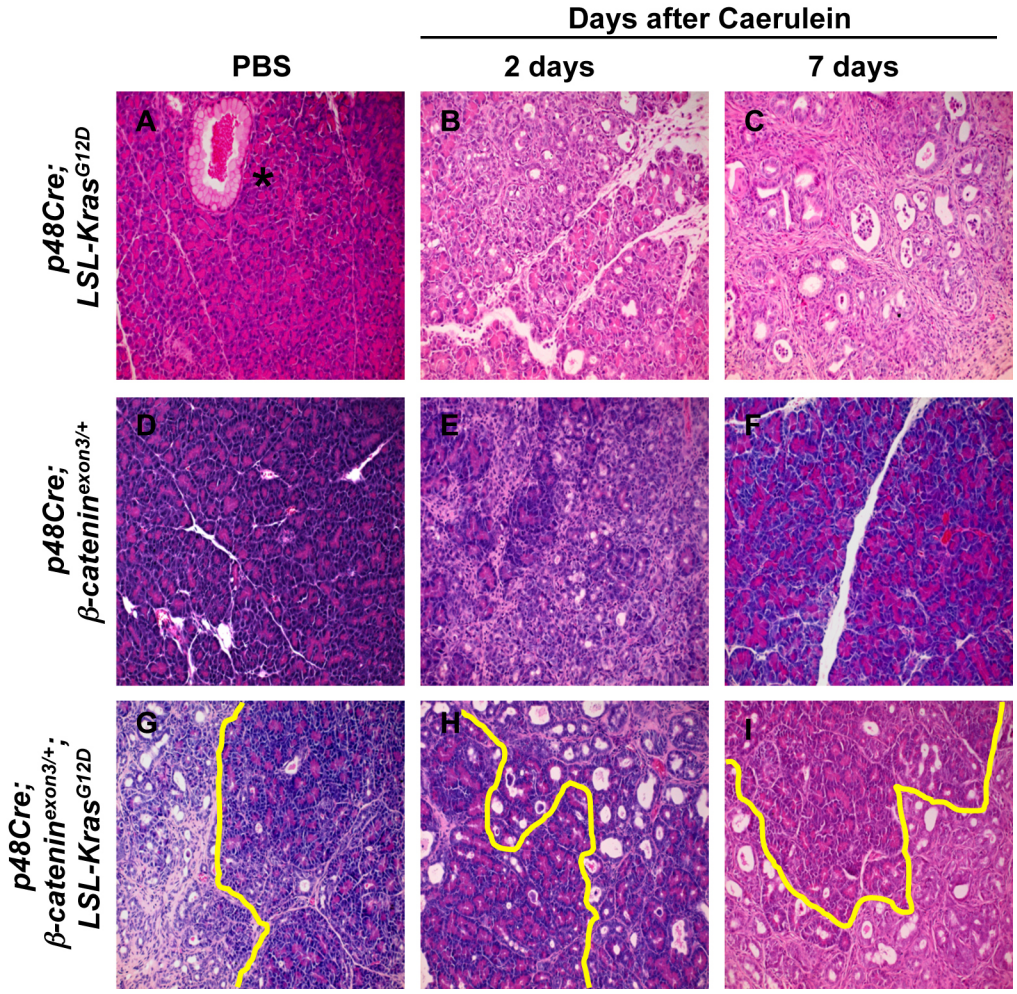

Supplemental Figure 7

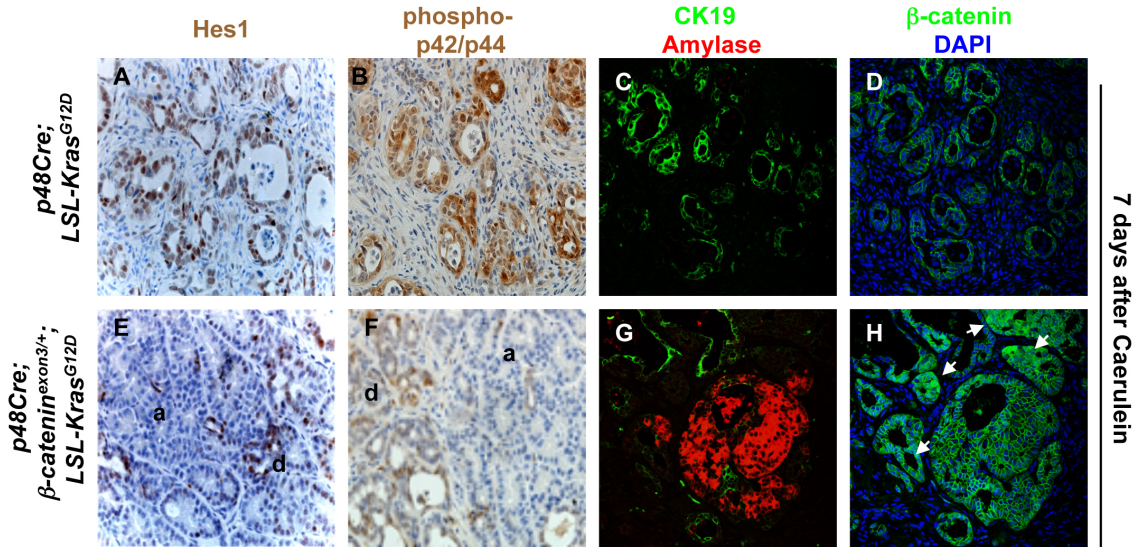

Chapter 3: miRNA processing constrains Kras driven acinar to ductal metaplasia, but is required for pancreatic ductal adenocarcinoma (PDA) formation in mice.

This work is currently being prepared for submission.

miRNA processing constrains Kras driven acinar to ductal metaplasia, but is required for pancreatic ductal adenocarcinoma (PDA) formation in mice.

Morris IV, J.P.[1], Vanderlaan, R.[1], Busch, A.[2], Hertel, K.[2], Kim, G.[3], Russ, H.[1],Hebrok., M[1].

[1] Diabetes Center, Department of Medicine, University of California, San Francisco, CA 94143, USA.

[2] Department of Microbiology and Molecular Genetics, University of California, Irvine, CA 92697, USA

[3] Department of Pathology, University of California, San Francisco, San Francisco, CA 94143, USA

Corresponding author: Matthias Hebrok, Diabetes Center, Department of Medicine, HSW1119, 513 Parnassus Avenue, University of California, San Francisco, CA 94143. Phone: 415-514-0820; Fax: 415-564-5813: Email: mhebrok@diabetes.ucsf.edu.

Abstract

Mutant Kras is sufficient to drive initiation and progression of pancreatic ductal adenocarcinoma (PDA). Unexpectedly, mutant Kras can promote PDA initiation by reprogramming pancreatic acinar cells into a duct like state, a dramatic alteration in pancreatic plasticity. The molecular events that constrain Kras driven acinar to ductal reprogramming are poorly understood. Here we study the role of miRNA processing in Kras driven pancreatic transformation by deleting the critical miRNA-processing enzyme Dicer in the context of targeted expression of mutant Kras. We find that loss of Dicer accelerates Kras driven acinar to ductal metaplasia. Acinar differentiation is compromised in the absence of Dicer, which appears to provide a permissive environment for Kras driven ductal differentiation. Despite precocious ductal metaplasia, Dicer loss in the context of mutant Kras does not accelerate development of PDA precursor lesions or invasive PDA, and PDA that develops in mice with conditional targeting of both Dicer alleles retains Dicer expression. Apoptosis is dramatically increased at the same time Dicer deficient mice display unconstrained ductal metaplasia, suggesting that intact miRNA processing is required for maintaining viability during Kras dependent transformation in the pancreas. Therefore, our data indicate that miRNA processing constrains the capacity of Kras to change acinar plasticity, but some Dicer dependent factors are required for the stabilization of a cell lineage that can give rise to PDA.

Introduction

Human Pancreatic Ductal Adenocarcinoma (PDA) development is characterized by a dramatic alteration in pancreatic differentiation, including reactivation of normally restricted embryonic signaling pathways as well as widespread metaplastic changes in the pancreatic parenchyma (1). Molecularly, PDA is characterized by near universal mutations in the Kras oncogene that render its signaling capacity constitutively active (2). In mice, targeting mutant Kras to multipotent pancreatic progenitors is sufficient to drive the initiation and progression of preneoplastic lesions and PDA that resemble the sequence of human pancreatic intraepithelial neoplasia (PanIN) believed to give rise to PDA in man (3). Therefore, mutant Kras represents a critical mediator of PDA specification and progression, and understanding the molecular environment required for Kras to drive and support cell fates that can give rise to PDA may help identify possible therapeutic or diagnostic tools.

While PanINs and PDA both express markers of ductal differentiation and display ductal morphology, mouse models targeting mutant Kras to other cell types have shown that mutant Kras can alter pancreatic plasticity to establish cell fates with duct like differentiation from non-ductal cells (reviewed in (1)). Considerable work has shown that acinar cells can be reprogrammed into a ductal lineage capable of giving rise to PanINs in a process termed acinar to ductal metaplasia (ADM) (4-8). Expression of mutant Kras in acini does not acute guarantee ductal reprogramming, as spontaneous, Kras dependent acinar derived PanIN

formation occurs very gradually (4, 5, 9). However, a number of studies have shown that the process can be accelerated by pancreatic damage, for example caerulein pancreatitis, that normally induces a transiently “de-differentiated” state in wild type acini, characterized by decreased expression of markers of acinar differentiation and re-activation of ductal markers and factors expressed during pancreatic development (6, 8-13). Unlike rapidly regenerating wildtype acinar cells, acinar cells expressing mutant Kras fail to re-establish acinar differentiation at the expense of a persistently duct like state that maintains expression of embryonic associated factors and can give rise to PanINs (9) (6, 10). Interestingly, Kras driven acinar to ductal reprogramming and PanIN formation can similarly be accelerated in the absence of pancreatic damage in genetic models in which elements of the persistent de-differentiated state are inappropriately activated (e.g. Notch signaling (4)) and when acinar differentiation is compromised (e.g. inactivation of the acinar transcription factor Mist1)(14). Therefore, mutant Kras appears to antagonize acinar homeostasis, gradually compromising acinar differentiation and blocking programs that permit acinar regeneration at the expense of ductal de-differentiation. Since erosion of acinar differentiation appears to be rate-limiting in Kras driven ductal reprogramming and PanIN formation, identifying mechanisms which modulate acinar differentiation in the context of mutant Kras could help elucidate requirements for Kras driven transformation in the pancreas.

MicroRNAs (miRNAs) are a class of small, non-coding RNAs that regulate gene expression post-transcriptionally (15). miRNAs are important both in development and tissue maintenance and are frequently deregulated in cancer where they regulate both tumor suppressors and oncogenes (16). As in other organs, miRNAs have been shown to play critical roles in pancreatic development and disease. Compromising miRNA biogenesis by targeting Dicer, the enzymatic node that processes precursor miRNAs into double stranded mature species, in early pancreatic progenitors results in stunted development of all pancreatic lineages, particularly endocrine cells (17). While specific miRNAs have been identified that contribute to the regeneration and maintenance of adult endocrine identity and function (reviewed in (18) less is known about the role of miRNAs in the development and maintenance of exocrine cells. However, the miRNA profile of predominantly exocrine, bulk normal pancreas tissue is significantly different than that of pancreatitis and pancreatic cancer tissues, suggesting that miRNAs may act as a marker of aberrant pancreatic differentiation (19-21). Furthermore, pancreatic development in the context of a hypomorphic allele of Dicer results in modest changes in acinar cells, including disrupted morphology and the appearance of multinucleated cells, as well as the misexpression of the transcription factor Pdx1, and the hormones insulin and glucagon in pancreatic ducts (22), suggesting that miRNAs may play a role in maintaining exocrine pancreatic differentiation and homeostasis.

Although specific misexpressed miRNAs have been identified that contribute to the biology of transformed PDA cells (for example, the Kras inhibited miRNAs miR-143 and miR-145(23)), the role of miRNAs in the Kras dependent specification of PDA precursors is not well understood. Since mutant Kras appears to occupy a central role in PDA initiation and progression, we set out to determine the general roles of miRNAs during Kras driven PDA initiation by eliminating Dicer expression in parallel with expression of mutant Kras. We find that acinar differentiation is compromised in the absence of Dicer, and this provides a permissive environment for Kras driven ductal de-differentiation. Despite this dramatic shift in differentiation, Dicer loss in the context of mutant Kras neither accelerates PanIN nor PDA development, and Dicer deficient cells do not appear to give rise to PDA. This occurs in part because of high levels of apoptosis that occurs in parallel with precocious ductal differentiation. Therefore, our work suggests that intact miRNA processing constrains the ability of mutant Kras to alter pancreatic plasticity, but some Dicer dependent signals are required to maintain the stability and progression of cell capable of giving rise to PDA.

Results and Discussion

Dicer deletion during pancreatic development results in decreased pancreatic weight, acinar disorganization, and apoptosis.

Dicer deletion in early pancreatic progenitors via recombination mediated by a *Pdx1-Cre* driver line (referred to as *Pdx1-Cre*^{Early} (24)) results in severe pancreatic agenesis, preventing mice from surviving longer than 3 days post partum(17). Therefore, we screened 2 additional Cre lines, *p48-Cre* and *Pdx1-Cre*^{Late}, to test if they can drive efficient conditional recombination of Dicer (*Dicer*^{flox}) while permitting pancreatic development. While all three Cre driver lines target multipotent pancreatic progenitors, *p48-Cre* and *Pdx1-Cre*^{Late} become active later in development than *Pdx1-Cre*^{Early} and lead to recombination in a more restricted set of adult cells(24, 25). Critically, this delayed Cre activity permits the manipulation of some signaling pathways that prevent pancreatic development when altered at earlier stages(24, 25). *p48-Cre; Dicer*$^{flox/flox}$ mice survived until p0, but displayed notable runting compared to littermates, and did not survive past p5. Similar to the observations of Lynn and colleagues, pancreata in *p48-Cre; Dicer*$^{flox/flox}$ were severely hypoplastic (Data not shown). However, *Pdx1-Cre*^{Late}*; Dicer*$^{flox/flox}$ mice thrived after birth and displayed grossly normal pancreatic development at p0 even in the context of significantly decreased Dicer expression compared to control *Pdx1-Cre*^{Late}*; Dicer*$^{flox/+}$ mice (Supplemental Figure 1).

To determine the effect of Dicer loss on postnatal pancreatic development, we audited pancreatic structure and differentiation at 3 weeks of age in *Pdx1-Cre*^{Late}*;*

Dicer$^{flox/flox}$ mice. Notably, Dicer expression remained significantly reduced (Figure 1E). Although *Pdx1-Cre*^{Late}*; Dicer*$^{flox/flox}$ mice displayed no gross differences in pancreatic morphology compared to controls, pancreatic mass was significantly reduced by ~25% (Figure 1E). However, this decrease in mass did not occur in the context of dramatic alterations in the structure of the pancreatic parenchyma. Acini, ducts, and islets remained morphologically recognizable in *Pdx1-Cre*^{Late}*; Dicer*$^{flox/flox}$ mice (Figure 1A, B), and immunofluorescence for the acinar marker amylase, duct marker CK19, and β-cell marker insulin revealed normal distribution and segregation in the expected exocrine and endocrine patterns (Figure 1C,D). Exocrine morphology was not entirely normal though, as we often observed disorganized acini that displayed small, fragmented cells not observed in controls (Inset Figure 1C,D). Despite the changes in morphology, we did not observe overlapping expression of amylase and CK19, suggesting that these disorganized cells were not taking on ductal characteristics.

Dicer loss has been shown to generate considerable cellular stress, including loss of viability in other endoderm-derived organs (e.g. the liver), which can result in the preferential outgrowth of cells that have escaped complete Dicer recombination (26). Therefore, we included a Cre inducible YFP allele expressed conditionally from the Rosa26 locus (*R26-EYFP*) to track the fate of recombined cells. Also, we employed *Pdx1-Cre*^{Late}*; Dicer*$^{flox/+}$ mice instead of *WT* mice as controls, to ensure that differences in Dicer expression in comparison to *Pdx1-Cre*^{Late}*; Dicer*$^{flox/flox}$ mice were more likely to represent loss of both Dicer

alleles rather than selection for hemizygously deleted cells. To determine if the disturbed acinar parenchyma was occurring in the context of acinar stress, we performed co-immunofluorescence for Clusterin, a marker of stressed and damaged acini(6, 27), and YFP in *Pdx1-Cre^{Late}; Dicer$^{flox/+}$; R26-EYFP* versus *Pdx1-Cre^{Late}; Dicer$^{flox/flox}$; R26-EYFP* animals. While acini from control mice displayed very limited overlap between YFP and Clusterin, we observed widespread co-expression in acini in *Pdx1-Cre^{Late}; Dicer$^{flox/flox}$; R26-EYFP* mice (Figure 1F,G). Since persistent acinar Clusterin expression often correlates with increased apoptosis(27), we audited cell death in recombined acini via co-staining for TUNEL and YFP. In contrast to the rare double positive acini in *Pdx1-Cre^{Late}; Dicer$^{flox/+}$; R26-EYFP* mice, *Pdx1-Cre^{Late}; Dicer$^{flox/flox}$; R26-EYFP* mice displayed an approximately ~30X higher relative rate of TUNEL+/YFP+ acini (Figure 1H,I quantified in J). Therefore, while the exocrine compartment can develop efficiently in the absence of Dicer processing, it appears important for maintaining acinar homeostasis and viability.

Dicer loss accelerates Kras driven ductal metaplasia

To test the effect of compromised miRNA processing on Kras driven transformation in the pancreas, we generated compound *Pdx1-Cre^{Late}; LSL-Kras^{G12D}; Dicer$^{flox/flox}$; R26-EYFP* mice as a tool to track cells with targeted expression of constitutively active Kras and Dicer deletion. Like other mouse models in which mutant Kras is targeted to the developing pancreas, *Pdx1-Cre^{Late}; LSL-Kras^{G12D}* mice gradually develop ADM and PanINs that can progress

to PDA over time(28). As expected, the exocrine compartment of 3 week old control *Pdx1-Cre^{Late}; LSL-Kras^{G12D}; Dicer$^{flox/+}$; R26-EYFP* mice appeared nearly completely normal and was predominantly composed of amylase positive acinar cells, with rare areas of amylase negative ADM and low grade PanINs expressing moderate to high levels of both CK19 and Sox9 (Figure 2A, C, E, G), characteristic of early stages of Kras driven transformation in the pancreas(4-6). In contrast to controls, *Pdx1-Cre^{Late}; LSL-Kras^{G12D}; Dicer$^{flox/flox}$; R26-EYFP* mice displayed widespread ductal metaplasia. Although some morphologically normal acini were present, large areas of the pancreatic parenchyma were replaced with duct like structures that resembled the rare ADM in controls (Figure 2B). Ductal metaplasia in *Pdx1-Cre^{Late}; LSL-Kras^{G12D}; Dicer$^{flox/flox}$; R26-EYFP* mice displayed decreased expression of amylase, low to moderate expression of CK19, strong expression of Sox9, and accumulation of the Notch effector Hes1 (Figure 2D, F, H, data not shown). Sox9 accumulation was also observed in structures retaining some acinar morphology (Figure 2H). YFP staining revealed that the ductal metaplasia in *Pdx1-Cre^{Late}; LSL-Kras^{G12D}; Dicer$^{flox/flox}$; R26-EYFP* mice derived from cells in which Cre was active, and not from expansion of an un-recombined population (Figure 2J). Clusterin, which marks damaged acini as well as cells undergoing Kras driven metaplasia(6), was widely expressed in YFP+ cells in *Pdx1-Cre^{Late}; LSL-Kras^{G12D}; Dicer$^{flox/flox}$; R26-EYFP,* while it remained mainly limited to rare areas of YFP+ ADM or PanIN in *Pdx1-Cre^{Late}; LSL-Kras^{G12D}; Dicer$^{flox/+}$; R26-EYFP* mice (Figure 2I,J). Similarly, YFP+ metaplasia in *Pdx1-Cre^{Late}; LSL-Kras^{G12D}; Dicer$^{flox/flox}$; R26-EYFP* mice appeared

to be highly proliferative, displaying widespread expression of the proliferation antigen Ki67, which again was mainly observed in rare areas of ADM or PanIN in controls (Figure 2K,L). Therefore, Dicer loss in the context of mutant Kras dramatically accelerates ductal metaplasia, a process that has been shown to precede Kras driven PanIN formation(4-6, 29). However, while ductal metaplasia was considerably increased in *Pdx1-Cre^{Late}; LSL-Kras^{G12D}; Dicer$^{flox/flox}$; R26-EYFP* mice at 3 weeks compared to *Pdx1-Cre^{Late}; LSL-Kras^{G12D}; Dicer$^{flox/+}$; R26-EYFP* mice, we did not note increased PanIN formation at this stage.

Dicer loss compromises acinar differentiation and provides a permissive environment for Kras driven acinar to ductal reprogramming

Since Kras driven acinar to ductal metaplasia and PanIN formation normally occurs gradually unless accelerated by damage or genetic events that compromise acinar differentiation(1), we asked if Dicer loss compromises acinar differentiation. To specifically isolate acinar cells and minimize contamination from other pancreatic and non-pancreatic cell types, we modified a sorting protocol developed by Sugiyama and colleagues (2007) for isolation of pancreatic progenitors (30) to specifically separate differentiated acinar and ductal cells. We found that while adult acini and ducts both express the epithelial marker CD49f, differentiated ducts also express CD133 (Supplemental Figure 2B, C). Single cell pancreatic suspensions were generated as described in the Methods, and viable (DAPI-), non-hematopoietic (CD45-), cells were sorted

based on expression of CD49f and CD133 (Suppplementary Figure 2A). RT-PCR for Amylase and Mist1, and CK19 and Sox9, enriched in acinar and duct cells, respectively, revealed that this sorting protocol allowed for efficient separation of these populations (Supplemental Figure 2D). Interestingly, expression of Notch pathway members, restricted to centroacinar and terminal duct cells in the adult pancreas (31, 32), appeared to segregate with the CD49f+CD133+ duct population. Endocrine cells did not appear to express CD49f or CD133, and Insulin was not detected by RT-PCR in either of the sorted acinar or ductal populations (Supplemental Figure 2B,C, data not shown), suggesting that they were excluded by this sorting technique.

We next applied this sorting protocol to isolate cells with acinar surface markers from 3 week old *Pdx1-Cre^{Late}; Dicer$^{flox/flox}$; R26-EYFP, Pdx1-Cre^{Late}; LSL-Kras^{G12D}; Dicer$^{flox/flox}$; R26-EYFP*, and control *Pdx1-Cre^{Late}; Dicer$^{flox/+}$; R26-EYFP* and *Pdx1-Cre^{Late}; LSL-Kras^{G12D}; Dicer$^{flox/+}$; R26-EYFP* mice. To further enrich for pancreatic exocrine cells in which Cre recombination had taken place, CD49f+CD133- cells were separated from viable, CD45-, YFP+ cells (Figure 3A). Critically, YFP expression correlated with Dicer deletion at 3 weeks of age, as Dicer expression was significantly reduced in cells sorted from *Pdx1-Cre^{Late}; Dicer$^{flox/flox}$; R26-EYFP* and *Pdx1-Cre^{Late}; LSL-Kras^{G12D}; Dicer$^{flox/flox}$; R26-EYFP* mice compared to controls with and without Kras (Figure 3B). Due to the high rate of acinar apoptosis in *Pdx1-Cre^{Late}; Dicer$^{flox/flox}$* mice, we suspect that the incomplete loss of Dicer expression represents selection for cells that have not

fully recombined the conditional locus, a noted phenomenon in other models of targeted Dicer deletion(26, 33, 34). We performed RT-PCR for the acinar enriched genes Amylase and Mist1 and duct enriched genes CK19 and Sox9 in sorted cells with an acinar surface profile from all 4 genotypes. Interestingly CD49f+CD133- cells from *Pdx1-Cre^{Late}; Dicer$^{flox/flox}$; R26-EYFP* mice displayed significantly decreased expression of Amylase and Mist1 compared to cells in control *Pdx1-Cre^{Late}; Dicer$^{flox/+}$; R26-EYFP* mice (Figure 3B). Although expression of markers of acinar differentiation were reduced, we did not observe an increase in the ductal markers CK19 or Sox9 in these cells (Figure 3B), similar to the lack of CK19 misexpression in acinar cells as gauged by immunofluorescent staining (Figure 1D). Therefore Dicer loss appears to compromise acinar differentiation, but is not sufficient to drive a ductal program in acinar cells.

In contrast, loss of Dicer appeared to accelerate ductal reprogramming of acinar cells in the context of mutant Kras. Amylase and Mist1 expression was significantly decreased, and CK19 and Sox9 were significantly increased, in cells with an acinar surface profile in *Pdx1-Cre^{Late}; LSL-Kras^{G12D}; Dicer$^{flox/flox}$; R26-EYFP* mice compared to such cells in *Pdx1-Cre^{Late}; Dicer$^{flox/+}$; R26-EYFP* and *Pdx1-Cre^{Late}; LSL-Kras^{G12D}; Dicer$^{flox/+}$; R26-EYFP* animals (Figure 3B). Also, acinar makers were further decreased, and duct markers were increased in these cells compared to cells from *Pdx1-Cre^{Late}; Dicer$^{flox/flox}$; R26-EYFP* mice. Therefore, Dicer loss and mutant Kras synergize to drive acinar to ductal

reprogramming. Our data further suggest that the erosion of acinar differentiation is a rate-limiting step for mutant Kras to drive a ductal phenotype in acinar cells, and that intact miRNA processing represents one factor that constrains acinar to ductal differentiation in the context of mutant Kras. Interestingly, while we observed neither decrease in amylase nor increase in CK19 or Sox9 due to the activation of mutant Kras alone in acinar cells sorted from *Pdx1-Cre^{Late}; LSL-Kras^{G12D}; Dicer$^{flox/+}$; R26-EYFP* compared to *Pdx1-Cre^{Late}; Dicer$^{flox/+}$; R26-EYFP* mice, we did observe significant decrease in Mist1. Loss of Mist1 has been shown to synergize with mutant Kras to drive acinar to ductal reprogramming and PanIN development(14). This data suggests that even at 3 weeks of age, mutant Kras actively erodes acinar differentiation, although Kras dependent effects on differentiation have not reached a point where ductal differentiation is activated.

Dicer loss does not accelerate PanIN or PDA development, and Dicer deficient cells do not give rise to PDA

Since the accelerated ductal metaplasia in *Pdx1-Cre^{Late}; LSL-Kras^{G12D}; Dicer$^{flox/flox}$* mice resembles a state that precedes PanIN development in the context of mutant Kras(4-6), we asked if PanIN development was increased in *Pdx1-Cre^{Late}; LSL-Kras^{G12D}; Dicer$^{flox/flox}$* compared to control *Pdx1-Cre^{Late}; LSL-Kras^{G12D}; Dicer$^{flox/+}$* mice at 9 weeks of age. Despite the considerable metaplasia observed at 3 weeks in *Pdx1-Cre^{Late}; LSL-Kras^{G12D}; Dicer$^{flox/flox}$* mice, we found no difference in the number of ductal lesions that were positive for Alcian Blue (a

marker of intestinal mucins that characterize human and mouse PanINs(3)) compared to *Pdx1-Cre^{Late}; LSL-Kras^{G12D}; Dicer$^{flox/+}$* mice (Figure 4A,B,C). Similarly, in contrast to the 3 week timepoint when structural differences in *Pdx1-Cre^{Late}; LSL-Kras^{G12D}; Dicer$^{flox/flox}$* versus *Pdx1-Cre^{Late}; LSL-Kras^{G12D}; Dicer$^{flox/+}$* mice were grossly apparent, *Pdx1-Cre^{Late}; LSL-Kras^{G12D}; Dicer$^{flox/flox}$* mice at 9 weeks displayed considerable normal acinar tissue (Figure 4B). One remaining notable difference between the 2 genotypes was fatty replacement of pancreas tissue observed in some *Pdx1-Cre^{Late}; LSL-Kras^{G12D}; Dicer$^{flox/flox}$* animals (Figure 4B).

Next, we tracked the long-term disease progression of *Pdx1-Cre^{Late}; LSL-Kras^{G12D}; Dicer$^{flox/flox}$* and *Pdx1-Cre^{Late}; LSL-Kras^{G12D}; Dicer$^{flox/+}$* mice to determine if Dicer loss affected PDA development. Similar to indistinguishable PanIN development, *Pdx1-Cre^{Late}; LSL-Kras^{G12D}; Dicer$^{flox/flox}$ and Pdx1-Cre^{Late}; LSL-Kras^{G12D}; Dicer$^{flox/+}$* mice showed no difference in survival (Median survival 336 versus 338.5 days, n=7, n=6, respectively) (Figure 4F). 4/7 (57%) of *Pdx1-Cre^{Late}; LSL-Kras^{G12D}; Dicer$^{flox/+}$* compared to 3/6 (50%) *Pdx1-Cre^{Late}; LSL-Kras^{G12D}; Dicer$^{flox/flox}$* developed PDA or suspicious invasive disease by 1 year of age (Figure 4D,E, Table 1). To determine if Dicer deficient cells expressing mutant Kras in fact contributed to mPDA with the same frequency as cells heterozygous for Dicer, we tested the status of Dicer expression and recombination at the Dicer conditional locus from 2 PDA cell lines generated from mice of each genotype. By RT-PCR we observed no evidence of decreased

Dicer expression in cells derived from PDA from *Pdx1-Cre^{Late}; LSL-Kras^{G12D}; Dicer$^{flox/flox}$* mice (Figure 4H). Indeed, PDA cells from *Pdx1-Cre^{Late}; LSL-Kras^{G12D}; Dicer$^{flox/flox}$* mice appeared to retain at least one copy of an unrecombined, lox-p flanked allele (Figure 4G). To ensure mPDA cell lines were not contaminated with non-tumor cells, we audited recombination at the LSL-Kras^{G12D} locus, and found no evidence for cells that had not recombined the LSL cassette (Figure 4G). Therefore while Dicer loss considerably accelerates Kras driven acinar to ductal reprogramming, Dicer processing must be intact for cells to be stably specified into a lineage that can give rise to PDA. Interestingly, obligate maintenance of Dicer expression has also been demonstrated in a Kras driven model of lung cancer(33) and an Rb deficient model of retinoblastoma(34), suggesting that mutant Kras generally depends on some miRNA processing to maintain cell states competent for malignancy.

To determine if a defect in viability might explain the loss of Dicer deficient cells during PDA initiation and progression, we audited TUNEL+/YFP+ cells at 3 weeks in *Pdx1-Cre^{Late}; LSL-Kras^{G12D}; Dicer$^{flox/flox}$; R26-EYFP* and *Pdx1-Cre^{Late}; LSL-Kras^{G12D}; Dicer$^{flox/+}$; R26-EYFP* animals. We found a dramatic increase in double positive cells, ~100X higher than the rare double positive cells found in *Pdx1-Cre^{Late}; LSL-Kras^{G12D}; Dicer$^{flox/+}$; R26-EYFP* controls (Figure 2M, N, O). Interestingly, Dicer loss appeared to synergize with mutant Kras to promote cell death, as *Pdx1-Cre^{Late}; LSL-Kras^{G12D}; Dicer$^{flox/flox}$; R26-EYFP* mice exhibited a trend of ~2.5 fold more apoptosis than *Pdx1-Cre^{Late}; Dicer$^{flox/flox}$; R26-EYFP* cells

(Figure 2O). Therefore, while intact Dicer processing constrains Kras driven acinar to ductal reprogramming, some Dicer dependent signals are required for stabilizing a ductal lineage capable of becoming PDA.

Future Directions

This work implicates miRNA processing as both an inhibitor of Kras driven acinar to ductal reprogramming and a critical mediator of the stability of a ductal lineage capable of giving rise to PDA. Compromised acinar differentiation, either due to damage such as acute or chronic pancreatitis (6, 8-11), or genetic modifications which promote acinar de-differentiation (4, 14) has been shown to accelerate Kras dependent ductal reprogramming and PanIN formation. Therefore, *Pdx1-Cre^{Late}; LSL-Kras^{G12D}; Dicer$^{flox/flox}$;* mice represent a unique example where unconstrained ADM does *not* give rise to accelerated PanIN development. A critical future direction is molecular analysis of precocious metaplasia at the 3 week timepoint in *Pdx1-Cre^{Late}; LSL-Kras^{G12D}; Dicer$^{flox/flox}$* mice compared to control cells at early stages of Kras dependent metaplasia. This synchronized control condition could be achieved by collecting metaplastic acinar cells expressing mutant Kras shortly after acute caerulein pancreatitis. Performing this comparison could yield Dicer dependent factors that either synergize with mutant Kras to drive ductal reprogramming, or factors required by Kras to maintain ductal differentiation capable of giving rise to PDA.

We have initiated a collaboration with the Hertel Group at UC Irvine to perform this analysis by performing RNA deep sequencing on YFP+ cells with acinar surface markers from 3 week old *Pdx1-Cre^{Late}; LSL-Kras^{G12D}; Dicer$^{flox/flox}$; R26-EYFP and Pdx1-Cre^{Late}; LSL-Kras^{G12D}; Dicer$^{flox/+}$; R26-EYFP* mice 2 days after acute caerulein pancreatitis. At present, we are analyzing the resulting

expression data. Our preliminary analysis indicates that Dicer deficient acinar cells undergoing Kras dependent ductal reprogramming fail to activate a number of genes involved in maintaining acinar viability during normal regeneration that appear enriched in control, Kras expressing, Dicer competent cells. Furthermore, Dicer deficient cells also appear to overexpress a number of factors involved in establishing epigenetic control of gene expression that have been shown to cooperate with Kras in other cellular contexts. We are currently performing functional analysis on these candidates to determine if they contribute to the simultaneously permissive and destabilizing effect on Kras transformation that compromised miRNA processing plays in the pancreas. We are also extending our analysis to gauge the expression of these candidates in PanINs and PDA, to determine if they might be able to alter the function of mutant Kras at later stages of the disease. Finally, we are determining which miRNAs regulate these candidates as another possible route to altering Kras function at early and late stages of PDA development.

Methods:

Mouse lines:

Experimental animals were generated by crossing *Pdx-Cre*^{Late} (generous gift from Pedro Herrera, University of Geneva Medical School, Geneva, Switzerland) and *p48-Cre* mice (generous gift from Chris Wright, Vanderbilt University, Nashville, TN, USA) with *LSL-Kras*^{G12D} (generous gift from Dave Tuveson, Cancer Research UK Cambridge Research Institute, Cambridge, UK), *Dicer*^{flox} (35) (generous gift from Michael Mcmanus, UCSF Diabetes Center, San Francisco, CA, USA), and R26R-EYFP (36). All mouse experiments were performed under the approval of the UCSF Institutional Care and Use of Animals Committee (IACUC).

Immunohistochemistry and Immunofluorescence

Pancreata were fixed overnight in zinc-containing neutral-buffered formalin (Anatech LTD), embedded in paraffin, cut into 5-μm-thick sections, and mounted on Superfrost Plus slides (Fisher Scientific). Sections were subjected to hematoxylin and eosin (H&E), immunohistochemical, and immunofluorescent staining as described (22, 35). The following primary antibodies were used: rabbit anti-amylase (1:300; Sigma), rat anti-CK19 (TROMAIII, 1:200 dilution; developed by Dr. Rolf Kemler [Max-Planck Institute of Immunobiology, Freiburg, Germany] and obtained from the Hybridoma Bank at the University of Iowa), rabbit anti-Hes1 (1:500 dilution; generous gift from Dr. Tetsuo Sudo, Toray Industries, Inc., Kamakura, Japan), goat anti-clusterin (1:200; Santa Cruz), rabbit

anti-Sox9 (1:1000; Chemicon), chicken anti-GFP (1:200; Abcam). For immunohistochemistry, biotinylated secondary antibodies were used at a 1:200 dilution. 3-3′-Diaminobenzidine tetrahydrochloride (Vector Labs) was used as a chromogen. Bright-field images were acquired using a Zeiss Axio Imager D1 scope. For immunofluorescence detection of primary antibodies, appropriate Alexafluor conjugated secondary antibodies were used at a 1:200 dilution. Confocal images were collected on a Leica SP5 microscope. Alcian blue staining was performed as described (6), and quantified by collecting 100X images encompassing 2 complete tissue sections of each mouse and scoring the number of Alcian Blue positive lesions per mm^2 of pancreatic area (measured by outlining pancreatic tissue with the Axiovision software package (Zeiss)).

TUNEL assay

TUNEL staining was performed with the Apoptag Fluorescein in situ Apoptosis Detection Kit (Chemicon) according to manufacturer's instructions. The number of TUNEL+ cells per unit YFP+ area were quantified by imaging at least 1 entire tissue section at 100X on an InCell image automated microscope (GE).

Cell sorting

Single cell suspensions of 3 week old pancreata were generated with a modified version of a protocol established by Sugiyama and colleagues, 2007 (30). Briefly, pancreatic lymph nodes were removed, and pancreata were minced and sequentially incubated with collagenase D, trypsin, and dispase. Suspensions

were then filtered, subjected to FC block, and incubated with PE-conjugated anti-Cd49f, PE-CY7-conjugated anti-CD45, and biotin conjugated anti-CD133 antibodies. Streptavidin conjugated to APC was then applied to detect CD133 positive cells. Cell sorting was performed on a FacsARIAII (Becton Dickinson).

RT-PCR

RNA was extracted from sorted cells using the RNAqueous RNA extraction kit (Ambion) according to manufacturer's instructions, including the optional DNAse treatment to eliminate contaminating genomic material. cDNA was synthesized using Superscript II Reverse Transcriptase (Invitrogen). Taqman RT-PCR was performed using inventoried probes for mouse *Amylase2, Mist1, CK19, Sox9, Insulin, Hes1, Hey1, Hey2, and HeyL* (Applied Biosystems). Expression levels were normalized using a custom primer/probe set for *Gus* (generously provided by the Genome Analysis Core at the UCSF Helen Diller Family Comprehensive Cancer Center). RT-PCR for Dicer was performed using SYBR GREEN master mix (Applied Biosystems) with primers specifically designed to detect deletion of the conditional Dicer allele (26). Dicer expression was normalized to Gus levels detected by RT-PCR with SYBR GREEN using primers designed by Heiser and colleagues (2008)(24)

Statistical methods:

Comparison of means was performed using unpaired T-Tests, calculated using Prism for Macintosh version 4. Statistical significance was assumed when $P<0.0$. Results are represented as mean ± SD.

References

1. Morris, J.P.t., Wang, S.C., and Hebrok, M. 2010. KRAS, Hedgehog, Wnt and the twisted developmental biology of pancreatic ductal adenocarcinoma. *Nature reviews. Cancer* 10:683-695.
2. Hezel, A.F., Kimmelman, A.C., Stanger, B.Z., Bardeesy, N., and Depinho, R.A. 2006. Genetics and biology of pancreatic ductal adenocarcinoma. *Genes Dev* 20:1218-1249.
3. Hingorani, S.R., Petricoin, E.F., Maitra, A., Rajapakse, V., King, C., Jacobetz, M.A., Ross, S., Conrads, T.P., Veenstra, T.D., Hitt, B.A., et al. 2003. Preinvasive and invasive ductal pancreatic cancer and its early detection in the mouse. *Cancer Cell* 4:437-450.
4. De La, O.J., Emerson, L.L., Goodman, J.L., Froebe, S.C., Illum, B.E., Curtis, A.B., and Murtaugh, L.C. 2008. Notch and Kras reprogram pancreatic acinar cells to ductal intraepithelial neoplasia. *Proc Natl Acad Sci U S A*.
5. Habbe, N., Shi, G., Meguid, R.A., Fendrich, V., Esni, F., Chen, H., Feldmann, G., Stoffers, D.A., Konieczny, S.F., Leach, S.D., et al. 2008. Spontaneous induction of murine pancreatic intraepithelial neoplasia (mPanIN) by acinar cell targeting of oncogenic Kras in adult mice. *Proc Natl Acad Sci U S A* 105:18913-18918.
6. Morris, J.P.t., Cano, D.A., Sekine, S., Wang, S.C., and Hebrok, M. 2010. Beta-catenin blocks Kras-dependent reprogramming of acini into pancreatic cancer precursor lesions in mice. *J Clin Invest* 120:508-520.
7. Ji, B., Tsou, L., Wang, H., Gaiser, S., Chang, D.Z., Daniluk, J., Bi, Y., Grote, T., Longnecker, D.S., and Logsdon, C.D. 2009. Ras activity levels control the development of pancreatic diseases. *Gastroenterology* 137:1072-1082, 1082 e1071-1076.
8. Guerra, C., Schuhmacher, A.J., Canamero, M., Grippo, P.J., Verdaguer, L., Perez-Gallego, L., Dubus, P., Sandgren, E.P., and Barbacid, M. 2007. Chronic pancreatitis is essential for induction of pancreatic ductal adenocarcinoma by K-Ras oncogenes in adult mice. *Cancer Cell* 11:291-302.
9. De La, O.J., and Murtaugh, L.C. 2009. Notch and Kras in pancreatic cancer: at the crossroads of mutation, differentiation and signaling. *Cell Cycle* 8:1860-1864.
10. Carrière C, Y.A., Gunn JR, Longnecker DS, Korc M. 2011. Acute pancreatitis accelerates initiation and progression to pancreatic cancer in mice expressing oncogenic kras in the nestin cell lineage. *PLoS One* 6:e27725.
11. Carriere, C., Young, A.L., Gunn, J.R., Longnecker, D.S., and Korc, M. 2009. Acute pancreatitis markedly accelerates pancreatic cancer progression in mice expressing oncogenic Kras. *Biochemical and biophysical research communications* 382:561-565.

12. Jensen, J.N., Cameron, E., Garay, M.V., Starkey, T.W., Gianani, R., and Jensen, J. 2005. Recapitulation of elements of embryonic development in adult mouse pancreatic regeneration. *Gastroenterology* 128:728-741.
13. Fendrich, V., Esni, F., Garay, M.V., Feldmann, G., Habbe, N., Jensen, J.N., Dor, Y., Stoffers, D., Jensen, J., Leach, S.D., et al. 2008. Hedgehog Signaling Is Required for Effective Regeneration of Exocrine Pancreas. *Gastroenterology* 135:621-631.
14. Shi, G., Zhu, L., Sun, Y., Bettencourt, R., Damsz, B., Hruban, R.H., and Konieczny, S.F. 2009. Loss of the acinar-restricted transcription factor Mist1 accelerates Kras-induced pancreatic intraepithelial neoplasia. *Gastroenterology* 136:1368-1378.
15. Bartel, D.P., and Chen, C.Z. 2004. Micromanagers of gene expression: the potentially widespread influence of metazoan microRNAs. *Nat Rev Genet* 5:396-400.
16. Ventura, A., and Jacks, T. 2009. MicroRNAs and cancer: short RNAs go a long way. *Cell* 136:586-591.
17. Lynn, F.C., Skewes-Cox, P., Kosaka, Y., McManus, M.T., Harfe, B.D., and German, M.S. 2007. MicroRNA expression is required for pancreatic islet cell genesis in the mouse. *Diabetes* 56:2938-2945.
18. Fernandez-Valverde, S.L., Taft, R.J., and Mattick, J.S. 2011. MicroRNAs in beta-cell biology, insulin resistance, diabetes and its complications. *Diabetes* 60:1825-1831.
19. Bloomston, M., Frankel, W.L., Petrocca, F., Volinia, S., Alder, H., Hagan, J.P., Liu, C.G., Bhatt, D., Taccioli, C., and Croce, C.M. 2007. MicroRNA expression patterns to differentiate pancreatic adenocarcinoma from normal pancreas and chronic pancreatitis. *Jama* 297:1901-1908.
20. Lee, E.J., Gusev, Y., Jiang, J., Nuovo, G.J., Lerner, M.R., Frankel, W.L., Morgan, D.L., Postier, R.G., Brackett, D.J., and Schmittgen, T.D. 2007. Expression profiling identifies microRNA signature in pancreatic cancer. *Int J Cancer* 120:1046-1054.
21. Szafranska, A.E., Davison, T.S., John, J., Cannon, T., Sipos, B., Maghnouj, A., Labourier, E., and Hahn, S.A. 2007. MicroRNA expression alterations are linked to tumorigenesis and non-neoplastic processes in pancreatic ductal adenocarcinoma. *Oncogene* 26:4442-4452.
22. Morita, S., Hara, A., Kojima, I., Horii, T., Kimura, M., Kitamura, T., Ochiya, T., Nakanishi, K., Matoba, R., Matsubara, K., et al. 2009. Dicer is required for maintaining adult pancreas. *PLoS One* 4:e4212.
23. Kent, O.A., Chivukula, R.R., Mullendore, M., Wentzel, E.A., Feldmann, G., Lee, K.H., Liu, S., Leach, S.D., Maitra, A., and Mendell, J.T. 2010. Repression of the miR-143/145 cluster by oncogenic Ras initiates a tumor-promoting feed-forward pathway. *Genes & development* 24:2754-2759.
24. Heiser, P.W., Cano, D.A., Kim, G., Kench, J.G., Taketo, M.M., Biankin, A.V., and Hebrok, M. 2008. Stabilization of beta-catenin induces pancreas tumor formation. *Gastroenterology* in press.

25. Heiser, P.W., Lau, J., Taketo, M.M., Herrera, P.L., and Hebrok, M. 2006. Stabilization of beta-catenin impacts pancreas growth. *Development* 133:2023-2032.
26. Sekine, S., Ogawa, R., Ito, R., Hiraoka, N., McManus, M.T., Kanai, Y., and Hebrok, M. 2009. Disruption of Dicer1 induces dysregulated fetal gene expression and promotes hepatocarcinogenesis. *Gastroenterology* 136:2304-2315 e2301-2304.
27. Siveke, J.T., Lubeseder-Martellato, C., Lee, M., Mazur, P.K., Nakhai, H., Radtke, F., and Schmid, R.M. 2008. Notch signaling is required for exocrine regeneration after acute pancreatitis. *Gastroenterology* 134:544-555.
28. Fukuda, A., Wang, S.C., Morris, J.P.t., Folias, A.E., Liou, A., Kim, G.E., Akira, S., Boucher, K.M., Firpo, M.A., Mulvihill, S.J., et al. 2011. Stat3 and MMP7 contribute to pancreatic ductal adenocarcinoma initiation and progression. *Cancer cell* 19:441-455.
29. Zhu, L., Shi, G., Schmidt, C.M., Hruban, R.H., and Konieczny, S.F. 2007. Acinar cells contribute to the molecular heterogeneity of pancreatic intraepithelial neoplasia. *Am J Pathol* 171:263-273.
30. Sugiyama, T., Rodriguez, R.T., McLean, G.W., and Kim, S.K. 2007. Conserved markers of fetal pancreatic epithelium permit prospective isolation of islet progenitor cells by FACS. *Proceedings of the National Academy of Sciences of the United States of America* 104:175-180.
31. Rovira, M., Scott, S.G., Liss, A.S., Jensen, J., Thayer, S.P., and Leach, S.D. 2010. Isolation and characterization of centroacinar/terminal ductal progenitor cells in adult mouse pancreas. *Proceedings of the National Academy of Sciences of the United States of America* 107:75-80.
32. Kopinke, D., Brailsford, M., Shea, J.E., Leavitt, R., Scaife, C.L., and Murtaugh, L.C. 2011. Lineage tracing reveals the dynamic contribution of Hes1+ cells to the developing and adult pancreas. *Development* 138:431-441.
33. Kumar, M.S., Pester, R.E., Chen, C.Y., Lane, K., Chin, C., Lu, J., Kirsch, D.G., Golub, T.R., and Jacks, T. 2009. Dicer1 functions as a haploinsufficient tumor suppressor. *Genes Dev* 23:2700-2704.
34. Lambertz, I., Nittner, D., Mestdagh, P., Denecker, G., Vandesompele, J., Dyer, M.A., and Marine, J.C. 2010. Monoallelic but not biallelic loss of Dicer1 promotes tumorigenesis in vivo. *Cell death and differentiation* 17:633-641.
35. Harfe, B.D., McManus, M.T., Mansfield, J.H., Hornstein, E., and Tabin, C.J. 2005. The RNaseIII enzyme Dicer is required for morphogenesis but not patterning of the vertebrate limb. *Proceedings of the National Academy of Sciences of the United States of America* 102:10898-10903.
36. Srinivas, S., Watanabe, T., Lin, C.S., William, C.M., Tanabe, Y., Jessell, T.M., and Costantini, F. 2001. Cre reporter strains produced by targeted insertion of EYFP and ECFP into the ROSA26 locus. *BMC Dev Biol* 1:4.

Figure Legends

Figure 1. Pancreas Development at 3 weeks in *PdxCre^{Late}; Dicer$^{flox/flox}$* mice. **(A,B).** H&E staining of pancreata from *PdxCre^{Late}; Dicer$^{flox/+}$* and *PdxCre^{Late}; Dicer$^{flox/flox}$* reveals development of acinar (A), duct (D), and islet cells (I) in both genotypes despite significant reduction in Dicer expression and modest, yet significant reduction in pancreas mass:body mass. A, B 100X **(E)** (Upper panel: *Pdx1-Cre^{Late}; Dicer$^{flox/+}$* n=4. *PdxCre^{Late}; Dicer$^{flox/flox}$* n=3, **<0.01; Lower panel: n=7, *<0.05)**.** **(C,D)** Immunofluorescence for amylase (red), CK19 (green), and Insulin (blue) displays normal restricted distribution of acinar, duct, and beta cell markers, respectively. However, disorganized acini containing unevenly distributed, small cells are observed in *PdxCre^{Late}; Dicer$^{flox/flox}$* mice (arrowheads, inset, D). C,D 400X **(F, G)** Widspread Clusterin expression (blue) is observed in recombined cells (YFP+, green) in *PdxCre^{Late}; Dicer$^{flox/flox}$; R26^{-}EYFP* mice compared to *PdxCre^{Late}; Dicer$^{flox/+}$; R26^{-}EYFP* mice. F,G 400X **(H-J)** TUNEL staining (blue) reveals a significant (~30X) increase in apoptosis in YFP+ recombined cells (green) in *PdxCre^{Late}; Dicer$^{flox/flox}$; R26^{-}EYFP* mice (H), in contrast to rare double positive cells (arrowhead) in *PdxCre^{Late}; Dicer$^{flox/+}$; R26^{-}EYFP* mice (I). Quantified in J, n=3, *<0.05. H,I 400X

Figure 2. Dicer loss accelerates Kras driven ductal metaplasia at 3 weeks in *PdxCre^{Late}; LSL-Kras^{G12D}; Dicer$^{flox/flox}$* mice.

(A,B). H&E staining shows widespread ductal metaplasia (magnified in inset,B) in *PdxCre^{Late}; LSL-Kras^{G12D} Dicer$^{flox/flox}$*; *R26-EYFP* mice compared to *PdxCre^{Late}; LSL-Kras^{G12D}; Dicer$^{flox/+}$*; *R26-EYFP* mice. Rare focus of metaplasia and PanIN lesion is shown in *PdxCre^{Late}; LSL-Kras^{G12D}; Dicer$^{flox/+}$*; *R26-EYFP* mice (inset, A). A,B 100X **(C-H)** Immunohistochemistry reveals widespread loss of Amylase, weak to moderate expression of CK19, and strong Sox9 expression in metaplastic epithelium of *PdxCre^{Late}; LSL-Kras^{G12D}; Dicer$^{flox/flox}$*; *R26-EYFP* mice. This pattern is limited to rare ADM and PanIN in *PdxCre^{Late}; LSL-Kras^{G12D}; Dicer$^{flox/+}$*; *R26-EYFP* mice. C-H 400X **(I-L)** Metaplastic epithelium in *PdxCre^{Late}; LSL-Kras^{G12D}; Dicer$^{flox/flox}$*; *R26-EYFP* mice results from recombined cells (YFP, green), expresses high levels of Clusterin, and is frequently positive for the proliferative antigen Ki67. Clusterin and Ki67 positive cells are mainly found in rare ADM and PanIN in *PdxCre^{Late}; LSL-Kras^{G12D}; Dicer$^{flox/+}$*; *R26-EYFP* mice. I, J 400x K,L originally 630X **(M,N,O)** TUNEL staining reveals a significant increase in apoptosis in recombined cells in *PdxCre^{Late}; LSL-Kras^{G12D}; Dicer$^{flox/flox}$*; *R26-EYFP* compared to rare double positive cells (arrowhead) in *PdxCre^{Late}; LSL-Kras^{G12D}; Dicer$^{flox/+}$*; *R26-EYFP* mice. Quantification (O) reveals a trend of cooperative apoptosis between Dicer loss and mutant Kras. n=3, *<0.05. M,N 400X

Figure 3. Dicer loss compromises acinar differentiation and accelerates Kras dependent ductal reprogramming

A. Representative flow cytometry strategy for isolating recombined (YFP positive) acinar cells from 3 week old mice. Live CD45-, YFP+ cells (upper plots) were gated and sorted for CD49f and CD133 expression (lower plots). **B. RT-PCR analysis of Dicer and markers of acinar and ductal differentiation in CD49f+CD133- from** *PdxCre^{Late}; Dicer$^{flox/+}$; R26^{-}EYFP* (n=5)*, PdxCre^{Late}; Dicer$^{flox/flox}$; R26^{-}EYFP* (n=5)*, PdxCre^{Late}; LSL-Kras^{G12D}; Dicer$^{flox/+}$*; *R26-EYFP* (n=3)*, and PdxCre^{Late}; LSL-Kras^{G12D}; Dicer$^{flox/flox}$*; *R26-EYFP* (n=5) mice. *, **, ***<0.05, 0.01, 0.0001, respectively.

Figure 4. Dicer is required for PDA development in mice

(A-C) Representative Alcian Blue staining at 9 weeks in *PdxCre^{Late}; LSL-Kras^{G12D}; Dicer$^{flox/+}$* (A) compared to *PdxCre^{Late}; LSL-Kras^{G12D}; Dicer$^{flox/flox}$* mice (B). f marks fat replacement. Quantified in C, n=4, p=0.45. A, B 100X **(D,E)** Representative histology of PDA from 9 month old *PdxCre^{Late}; LSL-Kras^{G12D}; Dicer$^{flox/+}$* (D) and *PdxCre^{Late}; LSL-Kras^{G12D}; Dicer$^{flox/flox}$* mice (E). D,E 200X **(F)** Survival curve of *PdxCre^{Late}; LSL-Kras^{G12D}; Dicer$^{flox/+}$* (n=7) and *PdxCre^{Late}; LSL-Kras^{G12D}; Dicer$^{flox/flox}$* (n=6) mice. **(G)** Recombination of the LSL-Kras^{G12D} and Dicer conditional loci in PDA cell lines from *PdxCre^{Late}; LSL-Kras^{G12D}; Dicer$^{flox/+}$* (4041 and 4283) and *PdxCre^{Late}; LSL-Kras^{G12D}; Dicer$^{flox/flox}$* (4130, 4279) mice. M-Cre and M+Cre represent positive control LSL-Kras^{G12D} mouse embryonic fibroblasts (MEFs) with or without Adenoviral Cre treatment. Note loss of the unrecombined “LSL” band and appearance of recombined “I loxp” band in Cre treated MEFs and all PDA cell lines. Het tail DNA represents positive control for

the WT and unrecombined "2loxp" band. While the conditional Dicer allele is recombined in *PdxCre^{Late}; LSL-Kras^{G12D}; Dicer$^{flox/+}$* derived lines, it is present in cells from *PdxCre^{Late}; LSL-Kras^{G12D}; Dicer$^{flox/flox}$* mice. **(H)** RT-PCR for Dicer in PDA cell lines from both genotypes reveal no evidence of loss of Dicer expression in cell lines derived from PDA in *PdxCre^{Late}; LSL-Kras^{G12D}; Dicer$^{flox/flox}$* mice.

Supplemental Figure 1. Deletion of Dicer with *Pdx1-Cre^{Late}* permits pancreatic development.

(A,B) Grossly normal pancreas histology in *Pdx1-Cre^{Late}; Dicer$^{flox/flox}$* compared to control *Pdx1-Cre^{Late}; Dicer$^{flox/+}$* mice at p0. A,B 100X **C.** QPCR reveals efficient pancreatic Dicer deletion in *Pdx1-Cre^{Late}; Dicer$^{flox/flox}$* versus *Pdx1-Cre^{Late}; Dicer$^{flox/+}$* mice at p0.

Supplemental Figure 2. FACS enrichment of pancreatic acinar and ductal compartments.

(A) Representative flow cytometry plot of a pancreas from an adult, 6 week old mouse, dissociated into a single cell suspension. Viable, non-hematopoietic cells (DAPI-CD45-, left panel) were gated and further analyzed for expression of CD49f and CD133 (right panel). **(B, C)** CD49f and CD133 staining in 6 week old mice. 400x **(D,E)** RT-PCR analysis of acinar and ductal markers from CD49f+CD133- and double positive CD49f+CD133+ cells (D). Analysis of Notch effectors in CD49f+CD133- and double positive CD49f+CD133+ cells. n=3.

Figure 1

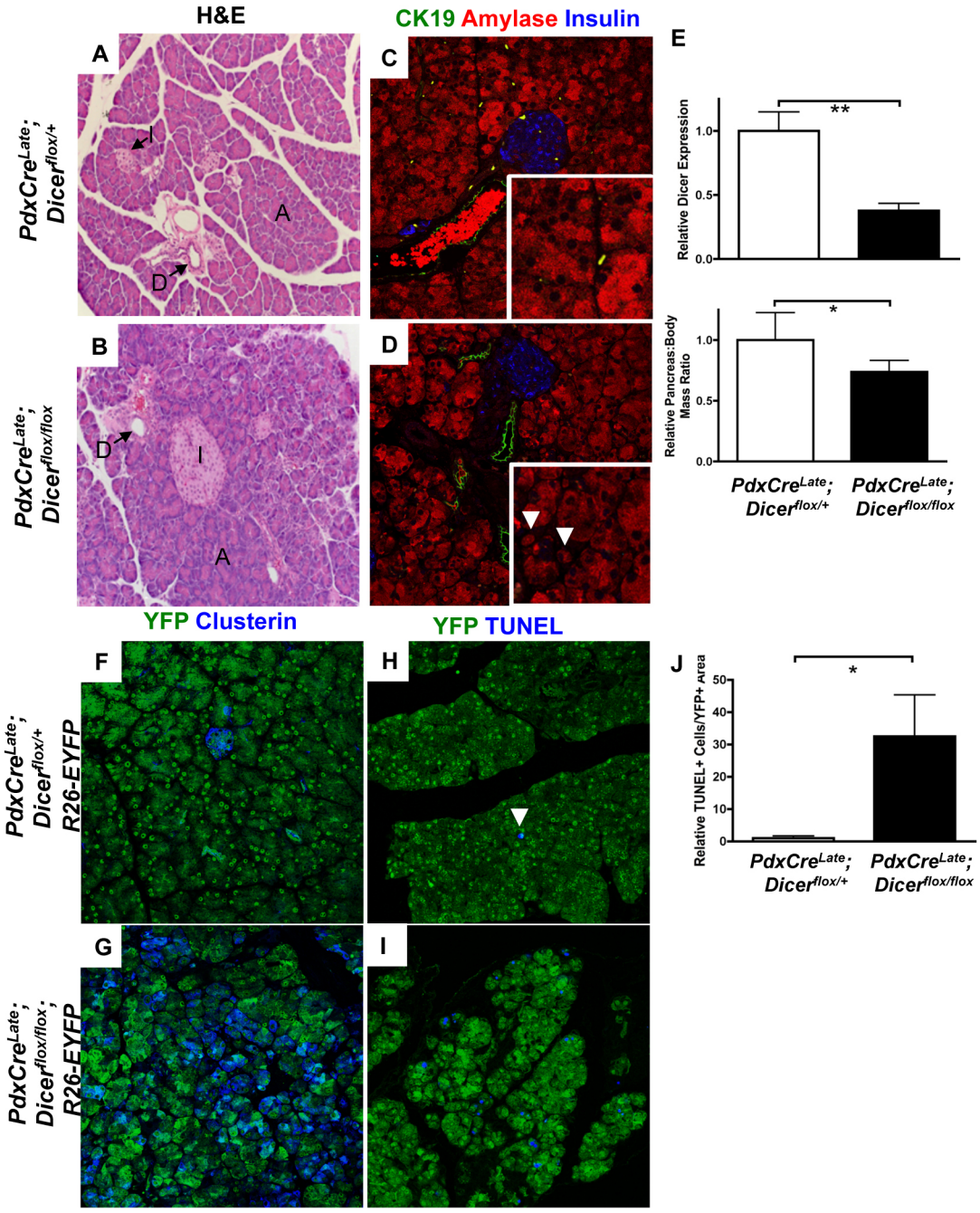
H&E
CK19 Amylase Insulin
A
B
C
D
E
F
G
H
I
J
PdxCreLate; Dicerflox/+
PdxCreLate; Dicerflox/flox
PdxCreLate; Dicerflox/+ R26-EYFP
PdxCreLate; Dicerflox/flox; R26-EYFP
YFP Clusterin
YFP TUNEL
Relative Dicer Expression
Relative Pancreas:Body Mass Ratio
Relative TUNEL+ Cells/YFP+ Area
**
*
*
PdxCreLate; Dicerflox/+
PdxCreLate; Dicerflox/flox

Figure 2

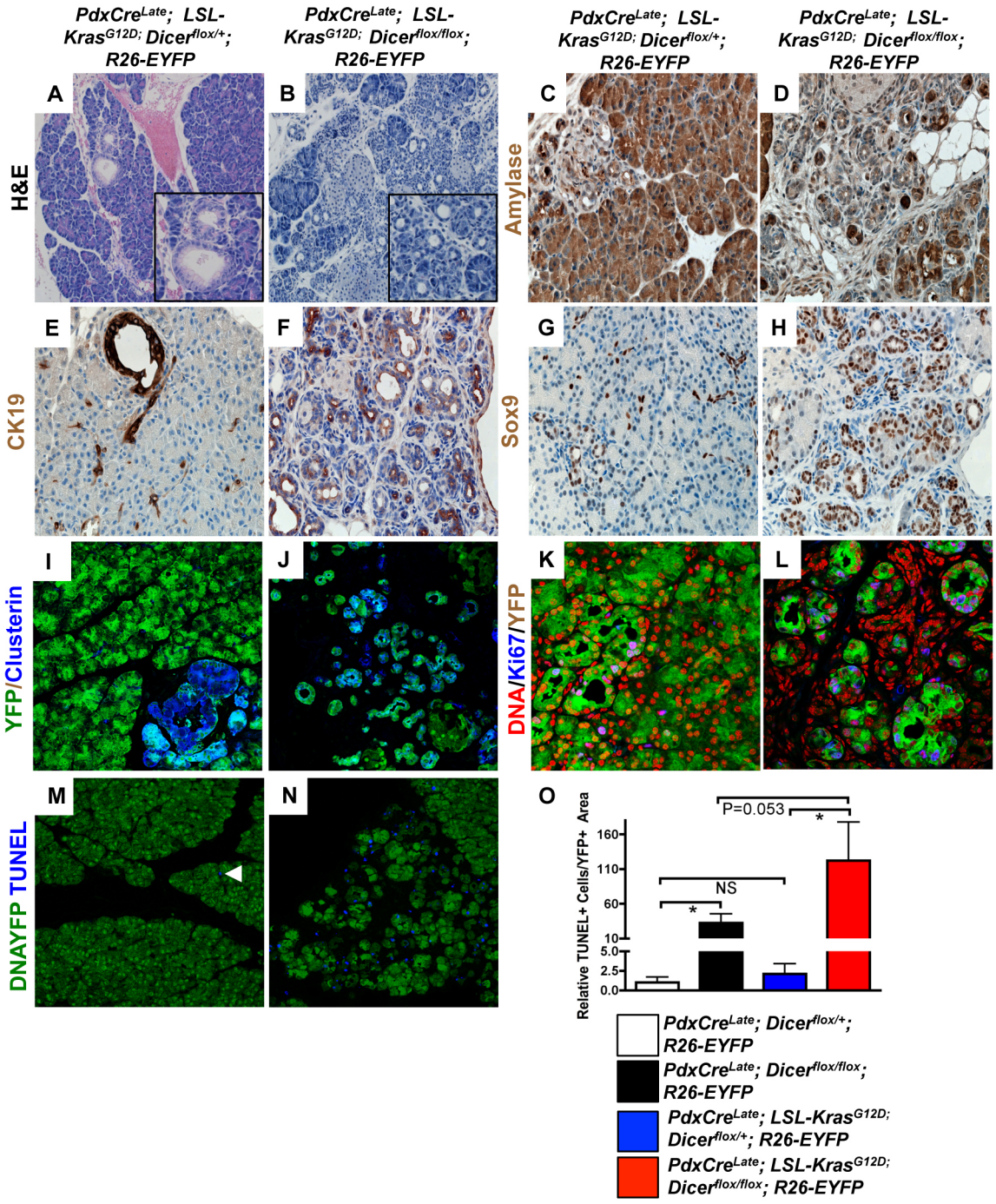
PdxCre^Late; LSL-Kras^G12D; Dicer^flox/+; R26-EYFP
PdxCre^Late; LSL-Kras^G12D; Dicer^flox/flox; R26-EYFP
PdxCre^Late; LSL-Kras^G12D; Dicer^flox/+; R26-EYFP
PdxCre^Late; LSL-Kras^G12D; Dicer^flox/flox; R26-EYFP
A
B
C
D
H&E
Amylase
E
F
G
H
CK19
Sox9
I
J
K
L
YFP/Clusterin
DNA/Ki67/YFP
M
N
O
DNAYFP TUNEL
Relative TUNEL+ Cells/YFP+ Area
P=0.053
NS
*
*
160
110
60
10
5.0
2.5
0.0
PdxCre^Late; Dicer^flox/+; R26-EYFP
PdxCre^Late; Dicer^flox/flox; R26-EYFP
PdxCre^Late; LSL-Kras^G12D; Dicer^flox/+; R26-EYFP
PdxCre^Late; LSL-Kras^G12D; Dicer^flox/flox; R26-EYFP

Figure 3

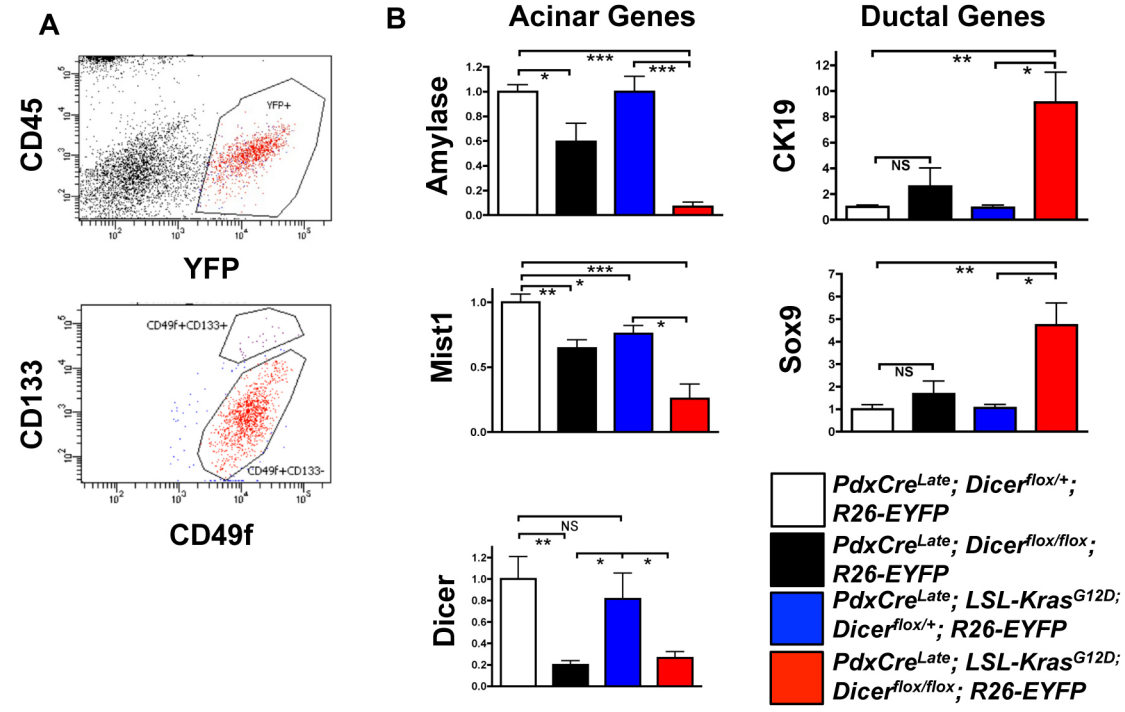
A
CD45
YFP+
YFP
CD133
CD49f+CD133+
CD49f+CD133-
CD49f
B
Acinar Genes
Ductal Genes
Amylase
CK19
Mist1
Sox9
Dicer
NS
PdxCre^Late; Dicer^flox/+; R26-EYFP
PdxCre^Late; Dicer^flox/flox; R26-EYFP
PdxCre^Late; LSL-Kras^G12D; Dicer^flox/+; R26-EYFP
PdxCre^Late; LSL-Kras^G12D; Dicer^flox/flox; R26-EYFP

Figure 4

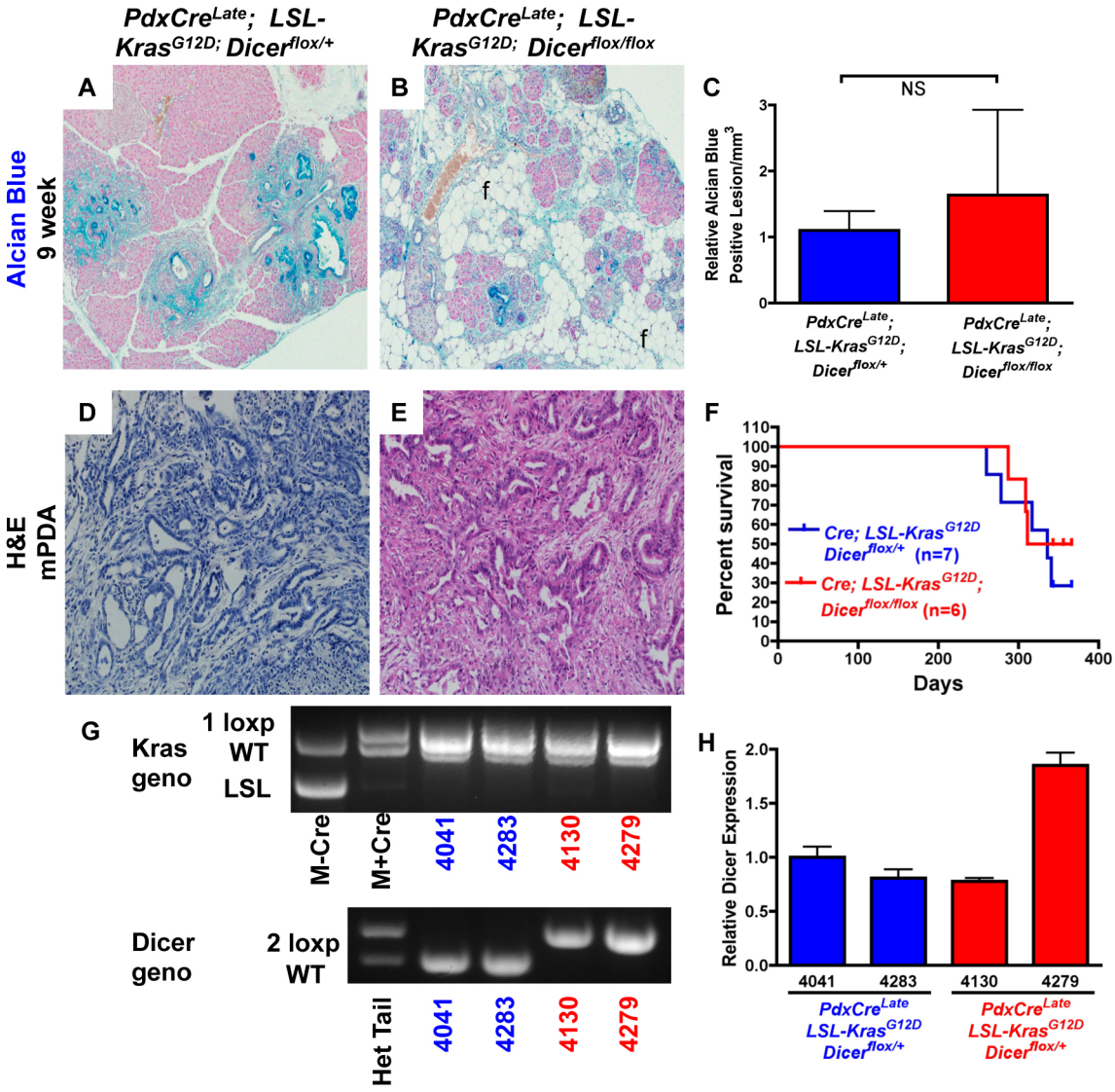
PdxCre^Late; LSL-Kras^G12D; Dicer^flox/+
PdxCre^Late; LSL-Kras^G12D; Dicer^flox/flox
A
B
C
Alcian Blue 9 week
NS
Relative Alcian Blue Positive Lesion/mm3
PdxCre^Late; LSL-Kras^G12D; Dicer^flox/+
PdxCre^Late; LSL-Kras^G12D; Dicer^flox/flox
D
E
F
H&E mPDA
Percent survival
Cre; LSL-Kras^G12D Dicer^flox/+ (n=7)
Cre; LSL-Kras^G12D; Dicer^flox/flox (n=6)
Days
G
Kras geno
1 loxp
WT
LSL
M-Cre
M+Cre
4041
4283
4130
4279
Dicer geno
2 loxp
WT
Het Tail
4041
4283
4130
4279
H
Relative Dicer Expression
4041
4283
4130
4279
PdxCre^Late LSL-Kras^G12D Dicer^flox/+
PdxCre^Late LSL-Kras^G12D Dicer^flox/+

Table 1

Dicer genotype	Mouse	Days until sacrifice	Pathology	Cell line
Het	4041	317	mPDA	
Het	4046	278	mPDA	Yes
Het	4180	Alive (359 days)	NA	
Het	4267	336	mPDA	
Het	4283	261	Local invasion	Yes
Het	4288	Alive (335 days)	NA	
Het	4294	Alive (335 days)	NA	
Homo	4130	308	mPDA	Yes
Homo	4170	310	Local invasion	
Homo	4176	Alive (390)		
Homo	4268	Alive (380)		
Homo	4279	286	mPDA	Yes
Homo	4291	Alive (335 days)		

Table 1: Survival and mPDA development in Dicer heterozygous and homozygous conditional mice

Supplemental Figure 1

H&E

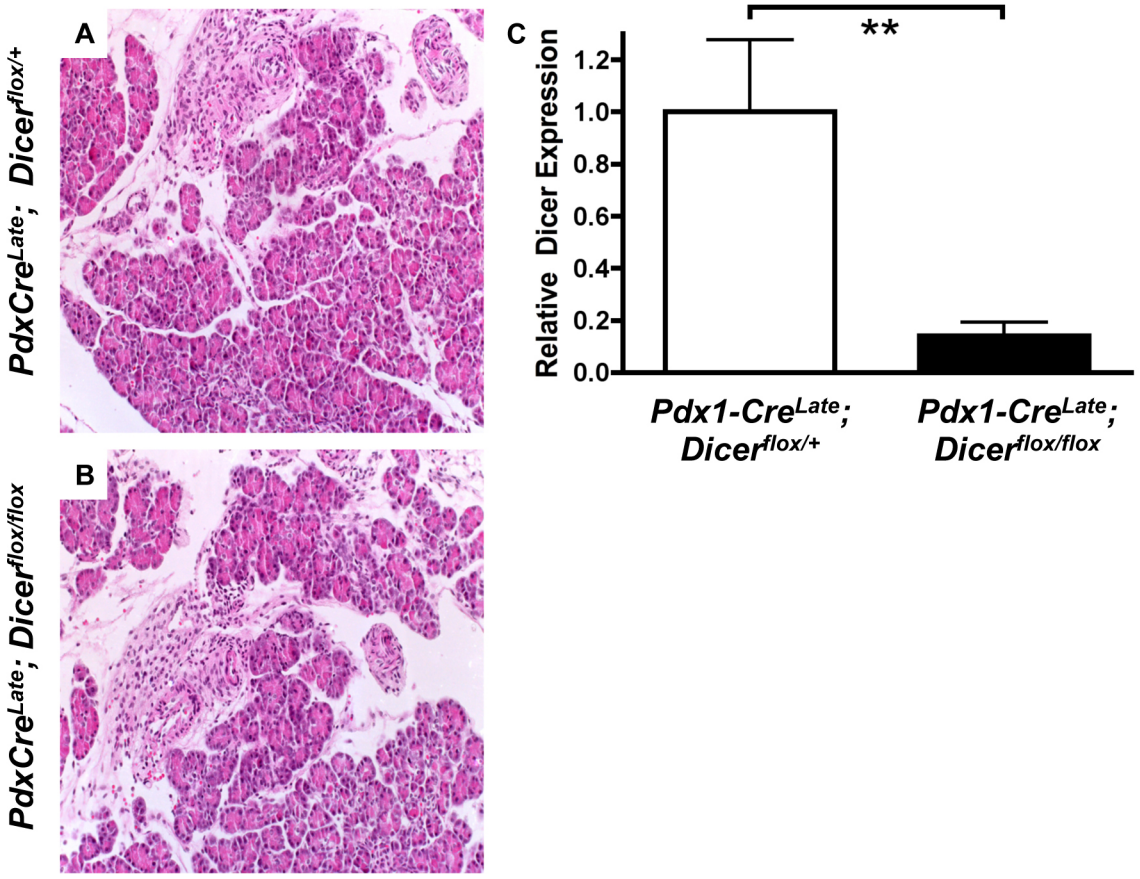

Supplemental Figure 2

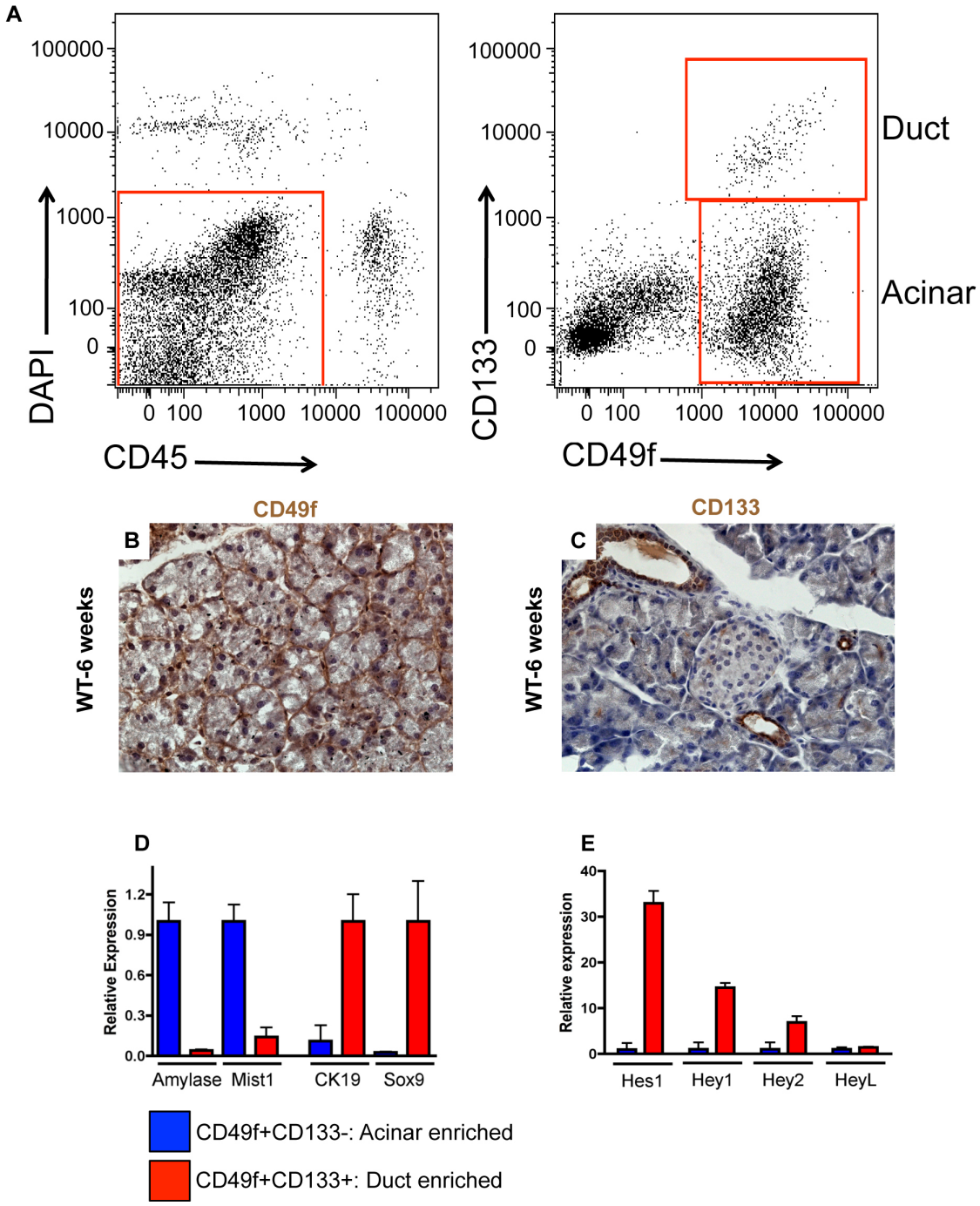

Library Release

Publishing Agreement

It is the policy of the University to encourage the distribution of all theses, dissertations, and manuscripts. Copies of all UCSF theses, dissertations, and manuscripts will be routed to the library via the Graduate Division. The library will make all theses, dissertations, and manuscripts accessible to the public and will preserve these to the best of their abilities, in perpetuity.

Please sign the following statement:

I hereby grant permission to the Graduate Division of the University of California, San Francisco to release copies of my thesis, dissertation, or manuscript to the Campus Library to provide access and preservation, in whole or in part, in perpetuity.

Author Signature

1-6-12

Date